

# **Dissertation**

submitted to the

Combined Faculties for the Natural Sciences and for Mathematics

of the Ruperto-Carola University of Heidelberg, Germany

for the degree of

## **Doctor of Natural Science**

Presented by

**Gennaro Ruggiero M.Sc.**

born in: Naples, Italy

Oral examination: 22th of May 2019

The function of clock input and output pathways in zebrafish

**Referees: Prof. Dr. Nicholas S. Foulkes**

**Prof. Dr. Uwe Strähle**



## **Acknowledgements**

First of all, I would like to thank to my supervisor Prof. Dr. Nicholas S. Foulkes for giving me the opportunity to do my Ph.D. in his laboratory and to work on several intriguing projects. During my Ph.D., I shared with him several great scientific and helpful discussions about my project, that have contributed to increase my scientific knowledge. Subsequently, I would like to thank Dr. Daniela Vallone for scientific and technical supporting. Moreover, a special thanks to my thesis advisory committee, Prof. Dr. Bastian Rapp and Dr. Olivier Kassel, that helped me a lot with their advice and feedback about my projects. I want to express my gratitude to all the present and former lab members that shared with me funny and relaxing moments: Giuseppe Di Mauro, Felicia Sangermano, Rosa Ceinos, Cristina Pagano, Rima Siauciunaite, Natalie Gayer, Zhao Haiyu, Li Ying, Andrea Maria Guarino and Bilge GÜNGÖR. I would like to acknowledge our collaborators Prof. Viola Calabrò, Dr. Ravindra Peravali, Prof. Yohav Gothilf and all the staff in ITG institute. I wish to thank my examiners Prof. Dr. Uwe Strähle, Prof. Dr. Ingrid Lohmann and Prof. Dr. Steffen Lemke for reading my thesis and conducting my PhD exam. Last but not least, I want to thank, from the bottom of my heart, my mother, my father and my brother. During these three years, that I spent in Germany, I am missed my family all the time. During my life, they supported me each moment and I want to dedicate all the goals that I achieved until now to them.

# Table of contents

<b>Publications</b> .....	<b>6</b>
<b>Abbreviations</b> .....	<b>7</b>
<b>Abstract</b> .....	<b>11</b>
<b>Zusammenfassung</b> .....	<b>13</b>
<b>1 Introduction</b> .....	<b>16</b>
<b>1.1 Overview of the circadian timing system</b> .....	<b>16</b>
<b>1.2 Evolution of the circadian timing system in vertebrates</b> .....	<b>17</b>
<b>1.3 The core molecular clock components</b> .....	<b>18</b>
<b>1.4 Light-entrainable oscillator (LEO)</b> .....	<b>19</b>
<b>1.5 Food-entrainable oscillator (FEO)</b> .....	<b>22</b>
<b>1.6 Clock output pathways in vertebrates</b> .....	<b>25</b>
<b>1.7 Clock output regulation of the cell cycle</b> .....	<b>26</b>
<b>1.8 The circadian clock in fish</b> .....	<b>29</b>
1.8.1 Zebrafish ( <i>Danio rerio</i> ): a powerful model organism for circadian rhythm studies ...	30
1.8.1.1 Zebrafish-derived cell cultures as tools to investigate circadian rhythms in vertebrates.....	32
1.8.2 Light entrainable oscillator (LEO) in zebrafish .....	33
1.8.3 Food entrainable oscillator (FEO) in zebrafish.....	34
<b>1.9 <i>Period2 (Per2)</i>: a multifunctional gene</b> .....	<b>35</b>
1.9.1 <i>Per2</i> a regulator of the FEO? .....	38
1.9.2 <i>Per2</i> involvement in the regulation of the cell cycle.....	38
<b>1.10 TGF-<math>\beta</math> signaling pathways</b> .....	<b>40</b>
1.10.1 Clock output regulation of the TGF- $\beta$ signaling pathway .....	41
1.10.2 Clock output regulation of the TGF- $\beta$ signaling pathway in zebrafish.....	42

<b>Aim of the thesis project .....</b>	<b>43</b>
<b>2 Materials and Methods .....</b>	<b>44</b>
<b>2.1 Animal experiments .....</b>	<b>44</b>
2.1.1 Ethics statement .....	44
2.1.2 Animals .....	44
2.1.3 Feeding entrainment.....	44
2.1.4 Locomotor activity recording of zebrafish adult fish.....	45
2.1.5 Locomotor activity monitoring of zebrafish larvae .....	45
2.1.6 Fin regeneration measurements .....	46
<b>2.2 Cell culture methods .....</b>	<b>46</b>
2.2.1 Zebrafish cell culture establishment and maintenance .....	46
<b>2.3 Molecular experiments.....</b>	<b>47</b>
2.3.1 RNA extraction .....	47
2.3.2 RT and Real-time PCR .....	48
2.3.3 Whole mount ISH .....	49
2.3.4 TGF- $\beta$ inhibitors and indirect activator .....	50
2.3.5 Constructs and real-time bioluminescence assays .....	50
2.3.6 Cell cycle analysis.....	51
2.3.7 Western blotting.....	51
<b>2.4 Transcriptome data mining.....</b>	<b>51</b>
<b>2.5 Statistical analysis.....</b>	<b>52</b>
<b>3 Results.....</b>	<b>53</b>
<b>3.1 Characterization of the <i>per2</i> KO zebrafish line and the derived cell lines. ....</b>	<b>53</b>
3.1.1 Unaffected expression of circadian clock genes in <i>per2</i> mutant larvae.....	53
3.1.2 Tissue-specific regulatory roles of <i>per2</i> in zebrafish peripheral tissues/organs. ....	54

3.1.3	Disrupted expression of circadian clock genes in <i>per2</i> mutant embryonic and adult fin primary fibroblast cell lines. ....	56
3.1.4	Unaffected peripheral light entrainment mechanism in cultured <i>per2</i> KO adult tissues.....	58
3.1.5	<i>Per2</i> role in clock outputs: Clock-controlled gene (CCGs) expression in <i>per2</i> mutant heart, liver and muscle. ....	60
3.1.6	<i>Per2</i> role in clock outputs: Locomotor activity .....	67
3.1.7	Role of <i>Per2</i> in clock outputs: food anticipatory activity (FAA) in zebrafish. ....	68
3.1.8	<i>Per2</i> function in clock outputs: circadian regulation of the cell cycle in zebrafish. ....	71
3.1.8.1	Affected cell cycle clock-controlled gene expression <i>per2</i> KO adult fin tissues.....	71
3.1.8.2	Clock-controlled cell cycle gene expression in <i>per2</i> KO adult fin and embryonic fibroblast cell lines. ....	73
3.1.8.3	Circadian pattern of M phase progression in <i>per2</i> KO adult fin tissues. ....	75
3.1.8.4	Abnormal cell cycle progression in the <i>per2</i> KO embryonic fibroblast cell lines ...	76
3.1.8.5	The regenerative capacity of the zebrafish caudal fin is not affected in the <i>per2</i> KO line.....	77
<b>3.2</b>	<b>TGF-<math>\beta</math> signaling pathway affects the circadian clock in zebrafish.....</b>	<b>78</b>
3.2.1	Disruption of TGF- $\beta$ signaling interferes with the molecular circadian clock in zebrafish PAC-2 cells.....	78
3.2.2	TGF- $\beta$ inhibition leads to phase delay of <i>per1b</i> mRNA rhythms in zebrafish larvae. ....	82
3.2.3	TGF- $\beta$ inhibition reversibly disrupts clock-controlled rhythmic locomotor activity in zebrafish larvae. ....	84
<b>4</b>	<b>Discussion .....</b>	<b>90</b>
4.1	Contribution of the <i>per2</i> gene to light input pathways in zebrafish .....	90
4.2	Characterization of <i>per2</i> gene function in a zebrafish <i>in vitro</i> system.....	92
4.3	<i>Per2</i> gene function affects clock-controlled gene expression.....	92
4.4	<i>Per2</i> gene function influences circadian output systems in zebrafish .....	94
4.4.1	Does <i>per2</i> gene function play a role in the regulation of the FEO in zebrafish?.....	96
4.5	Interactions between the circadian clock and TGF- $\beta$ signaling pathway in zebrafish....	97

<b>5</b>	<b>Supplementary Information.....</b>	<b>100</b>
<b>6</b>	<b>References .....</b>	<b>113</b>

## **Publications**

C. Pagano\*, O. di Martino\*, **G. Ruggiero**, A. M. Guarino, N. Mueller, R. Siauciunaite, M. Reischl, N. S. Foulkes, D. Vallone, V. Calabrò. “The tumor-associated YB-1 protein: new player in the circadian control of cell proliferation.,” *Oncotarget*, vol. 8, no. 4, pp. 6193–6205, Jan. 2017.

C. Pagano, R. Siauciunaite, M. L. Idda, **G. Ruggiero**, R. M. Ceinos, M. Pagano, E. Frigato, C. Bertolucci, N. S. Foulkes and D. Vallone. “Evolution shapes the responsiveness of the D-box enhancer element to light and reactive oxygen species in vertebrates” *Scientific Reports*, vol. 8, no. 1, pp. 1–17, 2018.

H. E. Sloin, **G. Ruggiero**, A. Rubinstein, S. S. Storz, N. S. Foulkes, Y. Gothilf. “Interactions between the circadian clock and TGF- $\beta$  signaling pathway in zebrafish” *PLoS One*, vol. 13, no. 6, pp. 1–23, 2018.

## Abbreviations

<b>Aanat2</b>	Arylalkylamine-Nacetyltransferase 2
<b>Agrp</b>	Agouti-related protein
<b>Asns</b>	Asparagine synthetase
<b>BMAL</b>	Brain and muscle Arnt-like protein-1
<b>ATM</b>	ATM serine/threonine kinase
<b>bp</b>	Base pair
<b>Ca</b>	Calcium
<b>cAMP</b>	Cyclic adenosine monophosphate
<b>CCGs</b>	Clock-controlled genes
<b>CDC25A</b>	Cell division cycle 25 homolog A
<b>CDK</b>	Cyclin-dependent kinases
<b>cDNA</b>	Complementary DNA
<b>CKI</b>	Cyclin-dependent kinase inhibitor
<b>CLD</b>	Cytoplasmic localization domain
<b>CLOCK1</b>	Circadian Locomotor Output Cycles Kaput 1
<b>c-MYC</b>	C-MYC proto-oncogene
<b>CNNb1</b>	Catenin Beta 1
<b>CRE</b>	cAMP responsive element modulator
<b>CREB</b>	cAMP responsive element-binding protein
<b>Cry1a</b>	Cryptochrome-1
<b>Cyp1a</b>	Cytochrome P450, family 1, subfamily A
<b>Dbp</b>	D site of albumin promoter (albumin D-box) binding protein
<b>DD</b>	Constant dark
<b>Dec1</b>	Deleted In Esophageal Cancer 1
<b>DL</b>	Dark/Light
<b>DNA</b>	Deoxyribonucleic acid
<b>dpf</b>	Days post fertilization
<b>E4bp4</b>	E4-binding protein 4
<b>ERK</b>	extracellular signal–regulated kinase
<b>FAA</b>	Food anticipatory activity
<b>FAD</b>	Flavin adenine dinucleotide

<b>FBXL3</b>	F-box/LRR-repeat protein 3
<b>FFA</b>	Free fatty acid
<b>FEO</b>	Food-entrainable oscillator
<b>Glu</b>	Glutamate
<b>Glu1a</b>	Glutamine synthetase 1a
<b>Glud1b</b>	Glutamate dehydrogenase 1b
<b>Got1</b>	Glutamic-oxaloacetic transaminase 1
<b>Gpt2l</b>	Glutamic pyruvate transaminase 2
<b>GSK3β</b>	Glycogen synthase kinase-3β
<b>HAUSP</b>	Herpesvirus-associated ubiquitin-specific protease
<b>HLH</b>	Helix-loop-helix motif
<b>Hnf1a</b>	Hepatocyte Nuclear Factor 1-Alpha
<b>Hsf2</b>	Heat Shock Transcription Factor 2
<b>H<sub>2</sub>O<sub>2</sub></b>	Hydrogen peroxide
<b>IEGs</b>	Immediate early genes
<b>Impdh2</b>	Inosine Monophosphate Dehydrogenase 2
<b>INK4a</b>	Inhibitor of CDK4
<b>ipRGCs</b>	Intrinsically photosensitive retinal ganglion cells
<b>JNK</b>	C-Jun N-terminal kinase
<b>LD</b>	Light/Dark
<b>LEO</b>	Light-entrainment oscillator
<b>LL</b>	Constant light
<b>LXXLL</b>	Leu-Xaa-Xaa-Leu-Leu
<b>ml</b>	Milliliter
<b>mM</b>	Millimolar
<b>mRNA</b>	Messenger RNA
<b>Myf6</b>	Myogenic Factor 6
<b>NAD<sup>+</sup></b>	Nicotinamide adenine dinucleotide
<b>NES</b>	Nuclear export signal
<b>NLS</b>	Nuclear localization sequence
<b>NPY</b>	Neuropeptide Y
<b>Opn4m2</b>	Opsin 4 mammalian-like 2
<b>OXM</b>	Oxyntomodulin

<b>P21</b>	Cyclin-dependent kinase inhibitor 1
<b>P38 MAPK</b>	P38 mitogen-activated protein kinase
<b>P53</b>	Cellular tumor antigen p53
<b>PACAP</b>	pituitary adenylate cyclase-activating polypeptide
<b>PARP-1</b>	Poly [ADP-ribose] polymerase 1
<b>PAS</b>	Per-Arnt-Sim
<b>PBS</b>	Phosphate-buffered saline
<b>Per2</b>	Period 2
<b>phospho-H3</b>	Phosphohistone H3
<b>PLC-PKC</b>	Phospholipase C - Protein kinase C
<b>Pparg1b</b>	Peroxisome Proliferator-Activated Receptor Gamma, Coactivator 1 Beta
<b>PPAR<math>\alpha</math></b>	Peroxisome proliferator-activated receptor alpha
<b>PTU</b>	Phenylthiourea
<b>qRT-PCR</b>	Quantitative reverse transcription PCR
<b>REV-ERB<math>\alpha</math></b>	Nuclear receptor subfamily 1, group D, member 1
<b>RGCs</b>	Retinal ganglion cells
<b>RNA</b>	Ribonucleic acid
<b>RHT</b>	Retinohypothalamic tract
<b>ROR<math>\alpha</math></b>	RAR-related orphan receptor alpha
<b>RORE</b>	retinoic acid-related orphan receptor response element
<b>Rory</b>	RAR-related orphan receptor gamma
<b>ROS</b>	Reactive oxygen species
<b>RXR</b>	Retinoid X receptor
<b>SCN</b>	Suprachiasmatic nucleus
<b>Sirt1</b>	NAD-Dependent Protein Deacetylase Sirtuin-1
<b>SMAD</b>	Mothers against decapentaplegic homolog
<b>Tef</b>	Thyrotrophic Embryonic Factor
<b>TGF-<math>\beta</math></b>	Transforming growth factor beta
<b>TGIF1</b>	TGFB Induced Factor Homeobox 1
<b>TFRE</b>	Transcription factor response element
<b>TIM</b>	Timeless
<b>TMT</b>	Teleost Multiple Tissue (TMT) Opsin
<b>UV</b>	Ultraviolet

<b>WGD</b>	Whole-genome duplication
<b>WT</b>	Wild type
<b>YFP</b>	Yellow fluorescent protein
<b>ZT</b>	Zietgeber
<b>μg</b>	Microgram
<b>μl</b>	Microliter
<b>6-4 Phr</b>	(6-4) DNA photolyase

## Abstract

This project focuses attention on the input and output pathways of the circadian clock using zebrafish as a genetic model system. In particular, by establishing a new *per2* loss of function (KO) zebrafish line we have revealed that the *per2* gene plays a tissue-specific function in setting the phase of rhythmic expression of certain core clock genes under light dark cycle (LD) conditions. Specifically, we have observed rhythmic expression patterns with 6 hours phase delay for both the *clock1* and *cry1a* core clock genes in *per2* KO adult heart, liver, gut and muscle, all internal organs that experience a reduced light exposure. In contrast, no differences were detected in the core clock gene expression patterns in brain, eyes and fin tissues as well as in embryos, that all represent superficial organs/tissues and so are exposed to higher light intensities. Interestingly, we also observed an absence or strongly reduced amplitude of rhythmic core clock gene expression in embryonic and adult fin fibroblast cell lines that we generated from the *per2* KO line, possibly suggesting that systemic signals might override local Per2 function in the entrainment of peripheral tissue clocks during light exposure. However, in explanted fin and heart tissue cultures prepared from the *per2* KO fish and maintained under LD conditions, rhythmic clock gene expression was equivalent to that in cultures derived from wild type (WT) fish, thus demonstrating that the *per2* gene function is not essential for the direct light entrainment mechanism of peripheral clocks, even in the absence of systemic signals in zebrafish. Subsequently, we have demonstrated that the rhythmic expression of several tissue-specific, clock-controlled genes, involved in the regulation of various aspects of heart, liver and muscle physiology shows a reduction of the amplitude or a phase shift of the rhythmic pattern in *per2* KO adult fish thus implicating *per2* in the circadian regulation of clock outputs and tissue-specific physiology in zebrafish. Therefore, we analyzed rhythmic locomotor activity of *per2* KO larvae under different light conditions and revealed an alteration of the robustness and precision of rhythmic locomotor output in free running conditions. However, we also showed that under time restricted feeding regimes, food anticipatory activity (FAA) is equivalent to that of wild type fish in the *per2* KO line suggesting that *per2* function is linked with the light rather than the food entrainable clock. Importantly, we have also demonstrated that the *per2* gene mutation has a strong effect on the circadian regulation of the cell cycle *in vivo* and *in vitro* in zebrafish, although it does not appear to impact on the rate of tissue regeneration following fin amputation. Together these results imply that the *per2* clock gene plays multiple roles in both clock input and output pathways in zebrafish. In parallel, we have revealed the existence of a functional interaction between the circadian clock and the TGF- $\beta$  signaling pathway in zebrafish. In particular, we have demonstrated that pharmacological

alteration of TGF- $\beta$  signaling interferes with the molecular circadian clock in zebrafish PAC-2 cells. Subsequently, we showed that TGF- $\beta$  inhibition generates a phase delay of *per1b* mRNA rhythms in zebrafish larvae. Finally, we demonstrated that the inhibition of the TGF- $\beta$  signaling pathway reversibly disrupts clock-controlled rhythmic locomotor activity in zebrafish larvae maintained under different lighting conditions. Therefore, we reveal complexity and overlap of the clock input and output mechanisms in zebrafish.

## Zusammenfassung

Dieses Projekt konzentriert sich auf die Eingabe- und Ausgabemechanismen der zirkadischen Uhr, wobei der Zebrafisch als genetisches Modellsystem verwendet wird. Durch die Etablierung einer neuen Zebrafischlinie mit Per2-Funktionsverlust (KO) haben wir gezeigt, dass das Per2-Gen eine gewebespezifische Funktion bei der Festlegung der Phase der rhythmischen Expression bestimmter Core-Clock-Gene unter Licht-Dunkelzyklus-Bedingungen (LD) erfüllt. Wir haben insbesondere rhythmische Expressionsmuster mit einer Phasenverzögerung von 6 Stunden sowohl für die Clock1- als auch für die cry1a-Core-Clock-Gene in per2 KO-Herz, Leber, Darm und Muskel, d.h. allen inneren Organen, die eine reduzierte Lichtexposition ausgesetzt sind, beobachtet. Im Gegensatz dazu wurden keine Unterschiede in den Genexpressionsmustern der Core-Clock-Gene in Gehirn, Augen und Flossengewebe festgestellt, die alle oberflächliche Organe / Gewebe sind und daher höheren Lichtintensitäten ausgesetzt sind. Interessanterweise beobachteten wir auch eine Abwesenheit oder stark verminderte Amplitude der rhythmischen Core-Clock-Genexpression in embryonalen und adulten Flossenfibroblasten-Zelllinien, die wir aus der per2-KO-Linie generierten. Dies deutet darauf hin, dass systemische Signale die lokale Per2-Funktion bei der Einstellung peripherer Gewebetakte während der Belichtung überschreiben könnten. In explantierten Flossen- und Herzgewebekulturen, die aus per2-KO-Fischen hergestellt wurden und unter LD-Bedingungen gehalten wurden, entsprach die Genexpression der rhythmischen Uhr derjenigen von Kulturen, die von Wildtyp (WT)-Fischen abstammen. Dies zeigt, dass die Funktion des per2-Gens für den Lichtaufnahmemechanismus peripherer Uhren selbst in Abwesenheit systemischer Signale im Zebrafisch nicht wesentlich ist. Anschließend haben wir erwiesen, dass die rhythmische Expression mehrerer gewebespezifischer, uhrgesteuerter Gene, die an der Regulierung verschiedener Aspekte der Herz-, Leber- und Muskelphysiologie beteiligt sind, eine Verringerung der Amplitude und eine Phasenverschiebung des rhythmischen Musters zeigt. In adulten per2-KO-Fischen impliziert Per2 somit die zirkadiane Regulierung der Taktleistung und die gewebespezifische Physiologie im Zebrafisch. Daher untersuchten wir die rhythmische Bewegungsaktivität von Per2-KO-Larven unter verschiedenen Lichtbedingungen und zeigten eine Veränderung der Robustheit und Präzision der rhythmischen Bewegungsleistung bei Freilaufbedingungen. Wir haben jedoch auch gezeigt, dass unter zeitbeschränkten Fütterungsbedingungen die antizipatorische Aktivität (FAA) der von Wildtyp-Fischen äquivalent zur KO-Linie von Per2 ist. Dies deutet darauf hin, dass die per2-Funktion eher mit der lichtgesteuerten als mit der fütterungsgesteuerten Uhr verbunden ist. Wir haben maßgeblich gezeigt, dass die Mutation des per2-Gens in vivo und in vitro in Zebrafischen eine starke Wirkung

auf die zirkadiane Regulation des Zellzykluses ausübt, obwohl sie offenbar keinen Einfluss auf die Geweberegeneration nach der Flossen-Amputation hat. Zusammenfassend bedeuten diese Ergebnisse, dass das *per2*-Clock-Gen sowohl im Clock-Input- als auch im Output-Pfad im Zebrafisch eine Rolle spielt. Parallel dazu haben wir die Existenz einer funktionellen Wechselwirkung zwischen der zirkadianen Uhr und dem TGF- $\beta$ -Signalweg im Zebrafisch dargelegt. Insbesondere beeinflusst die pharmakologische Veränderung der TGF- $\beta$ -Signalgebung die molekulare zirkadiane Uhr in Zebrafisch-PAC-2-Zellen. Zudem wurde erwiesen, dass die TGF- $\beta$ -Hemmung eine Phasenverzögerung der *per1b*-mRNA-Rhythmen in Zebrafischlarven bewirkt. Die Hemmung der TGF- $\beta$ -Signalwege stört außerdem reversibel die uhrgesteuerte rhythmische Bewegungsaktivität in Zebrafischlarven unter verschiedenen Lichtbedingungen. Die Takteingangs- und -ausgabemechanismen im Zebrafisch weisen erwiesenermaßen eine hohe Komplexität und Überlappung auf.



# 1 Introduction

## 1.1 Overview of the circadian timing system

The circadian clock is an endogenous and self-sustained timing mechanism shared by most organisms, which evolved to anticipate daily environmental changes and thereby to coordinate physiological and behavioral adaptations required for survival [1], [2]. The circadian clock generates rhythms with a period of around 24 hours (circadian comes from the Latin *circa*, meaning "around" (or "approximately"), and *diem*, meaning "day") determining rhythmicity in various physiological processes, including nervous system activity and hormone production, which influences sleeping and feeding patterns. Therefore, the disruption of the circadian timing system is associated with several pathological conditions [3]. Since, the period of circadian oscillations is not precisely 24h, the internal clock needs to be synchronized by external environmental timing signals (defined as *zeitgebers*, such as light, food, temperature), by adjusting the phase of the circadian system to match that of the environmental day-night cycle.

Generally, the vertebrate circadian system consists of three major components (figure 1) [4]:

- The input pathways which can detect the environmental signals, and relay these to the core clock.
- The core pacemaker that generates the circadian rhythms.
- The output pathways which relay timing information from the core clock to various physiological and behavioral control systems.

# The Circadian Timing System

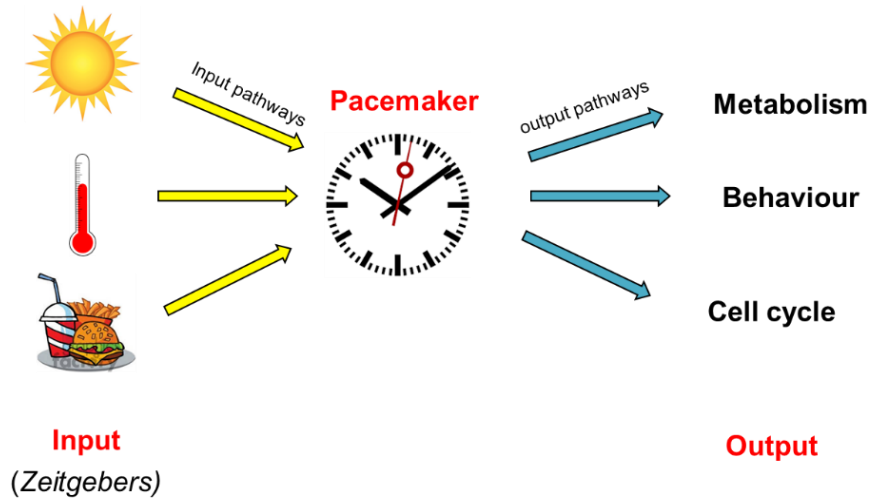


**Figure 1: Schematic representation of the circadian timekeeping system.**

It is composed of three major components: A pacemaker, that drives the oscillations with a period of around 24h. The pacemaker can be synchronized via input pathways with the local environment by external cues (*zeitgebers*) such as light, food and temperature. Based on this environmental synchronization, physiological mechanisms (such as metabolism, cell cycle and behavior) are controlled by the pacemaker via output pathways.

## 1.2 Evolution of the circadian timing system in vertebrates

Over the course of vertebrate evolution, the regulatory mechanisms, as well as the anatomical organization which underlie the circadian timing system, have undergone significant changes. At the anatomical level, in mammals, the circadian timing system is characterized by a ‘master’ clock located in the suprachiasmatic nucleus (SCN) of the hypothalamus and multiple independent peripheral clocks distributed in most tissues, organs and cells. This ‘master’ clock receives light input indirectly from the retina and is thereby synchronized with the external solar day. It subsequently relays this timing information to peripheral clocks via a variety of endocrine and systemic cues [5].

In contrast, in non-mammalian vertebrates, the central oscillator is distributed in multiple tissues such as the pineal gland, retina, and various brain nuclei, which are anatomically and functionally associated with photoreception [6]. For example, in teleosts that represent the largest vertebrate group, the “master” clock is located in the pineal gland, that contains all elements required for photic entrainment and circadian rhythm generation at the whole animal level [7].

The view of a “decentralized” circadian timing system in lower vertebrates emerged in part from the discovery that direct exposure of tissues and cells to light leads to entrainment of the local peripheral clocks in zebrafish [8]. Over the course of vertebrate evolution, the nature of the selective pressures shaping the transition from directly light regulated peripheral clocks in groups such as fish, to the centralized, retina-based photoreception system observed in modern mammals remains unclear. However, a hypothesis termed the “Nocturnal Bottleneck” hypothesis proposes that some features of mammalian sensory systems, such as the centralized light-entrainable circadian system, loss of visual pigments compared with non-mammalian species, and certain features of eye anatomy, support the hypothesis that the ancestors of extant mammals evolved within nocturnal niches, during the Mesozoic Era, in order to avoid diurnal saurian predators [9].

### **1.3 The core molecular clock components**

In vertebrates, the core clock is composed of a series of interlocking transcription translation feedback loops (figure 2). The positive limb of the clock is characterized of the transcription factors CLOCK and BMAL, which heterodimerize and bind to E-box enhancer promoter elements to activate the transcription of downstream clock target genes, including the *period* (*Per*) and *cryptochrome* (*Cry*) genes, *Rev-erb $\alpha$* , *Rora*, and other clock-controlled genes. Following translation, the PER and CRY proteins heterodimerize, translocate back to the nucleus, and inhibit transcriptional activation directed by CLOCK/BMAL. This core feedback loop is stabilized through another loop involving the transcriptional regulation of *Bmal1*. Transactivation of *Bmal1* is mediated by the ROR/REV-ERB Response Element (RORE) in the *Bmal1* promoter, to which ROR $\alpha$  and REV-ERB $\alpha$  bind. REVERB $\alpha$  repress the expression of *bmal1*, whereas ROR $\alpha$  acts as a transcriptional activator. This loop is thought to stabilize the core clock mechanism, and confers robustness by “protecting” the core clock-generated rhythm from the effect of irregular environmental perturbations and thereby helping to maintain accurate circadian timing. [10].

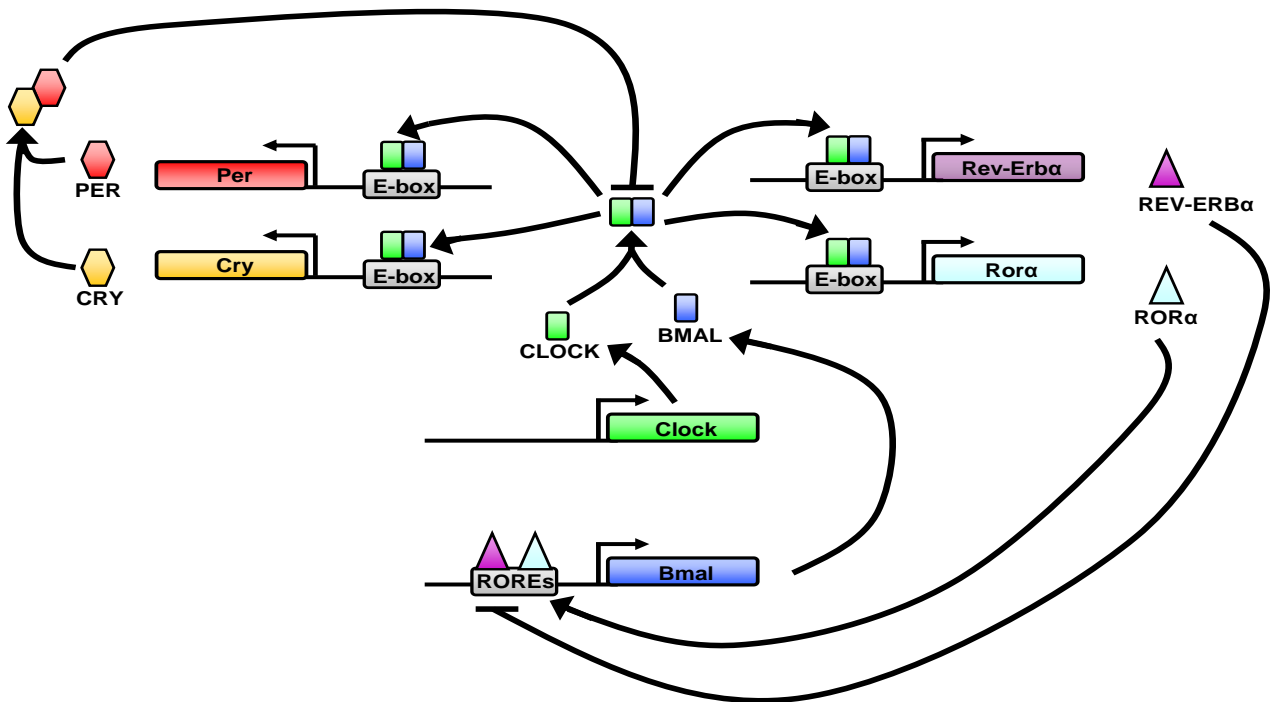


**Figure 2: Schematic representation of the organization of the circadian core clock in vertebrates.**

It is characterized by two transcription translation feedback loops: A core clock loop, in which the positive elements CLOCK and BMAL heterodimerize and bind the E-box enhancer element in order to activate the transcription of *per* and *cry* genes. After translation, the negative elements PER and CRY can heterodimerize and translocate back to the nucleus to repress their own transcription by inhibiting the CLOCK and BMAL complex. This core loop is stabilized by another loop (the stabilizing loop), that relies on the concerted action of two transcription factors, ROR $\alpha$  and REV-ERB $\alpha$ .

#### 1.4 Light-entrainable oscillator (LEO)

The transcription translation feedback loop, previously described, represents the molecular structure of a self-sustaining, light-entrainable circadian oscillator (LEO). In mammals, the LEO system is characterized by a “master” pacemaker that consists of a small nucleus within the hypothalamus that is constituted by around 20.000 neurons, called the suprachiasmatic nucleus (SCN). Each neuron of this region can independently generate self-sustained rhythmicity, thereby indicating that the SCN is characterized by a collection of cell-autonomous oscillators that are coupled to each other, through a variety of paracrine signals such as neuropeptides, vasoactive intestinal polypeptide (VIP), arginine vasopressin (AVP) and astrin-releasing peptide (GRP) [11], to form the complete pacemaker. In turn, the SCN is responsible for the control of overt circadian rhythms in physiology and behavior throughout the organism [12]. Indeed, the ablation or the malfunctioning of the SCN in mammals the

alters the circadian patterns of the levels of brain neurotransmitters, eliminates circadian rhythmicity of body temperature and locomotor activity and is also associated with altered energy metabolism and development of insulin resistance [13]–[16]. Photic input to the clock, in mammals, is detected exclusively through the retina, via a small population of intrinsically photosensitive retinal ganglion cells (ipRGCs) which express the non-visual photoreceptor, melanopsin [17]–[19]. In melanopsin knockout mice, the intrinsic photosensitivity of the RGCs is eliminated, indicating the key role played by melanopsin in detecting cellular irradiance information [20]. However interestingly, the behavioral rhythms of the knockout mice are still entrained in response to environmental light-dark cycles, although they do display attenuated phase resetting in response to brief pulses of monochromatic light [21], [22]. This observation reveals that the visual rod and cone photoreceptors also play a role in photic entrainment. This contribution has been studied by generating and testing mice lacking both the functional rod-cone system and melanopsin [17], [23]. These double mutant mice exhibit complete loss of photic resetting, therefore emphasizing the complementary function of the visual rod-cone photoreceptors and non-visual melanopsin in the transmission of the photoentrainment signal to the mammalian SCN.

The photic signal is conveyed from the RHT to the SCN via glutamate (Glu) and pituitary adenylate cyclase-activating polypeptide (PACAP) neurotransmitters that are released from the presynaptic retinal ganglion cells (RGCs) by synaptic vesicles and then bind to their cognate receptors on the post synaptic membranes of SCN neurons [24], [25]. The synaptic transmission triggers signaling cascades, including a  $Ca^{2+}$  influx and increased cAMP levels that induce the activation of multiple kinases and the consequent phosphorylation of CREB (cAMP response element binding protein) which finally regulates circadian oscillation in SCN neurons by binding to *cis*-regulatory elements (cAMP response elements (CREs)) in the promoters of target genes [26]. The transcriptional induction of a subset of core clock genes in response to light exposure appears to serve as a key step in entrainment of the clock by the day-night cycle; in particular, the *Per* and *Cry* genes seem to play an important role in regulation of the core clock by light. For this reason, in the last few years, the light induced expression of *Per1* and *Per2* in the SCN via the function of CRE elements has been widely studied in the mammals [27], [28]. In turn, the synchronized SCN, through its neuronal projections, can directly adjust the oscillators in extra-SCN brain regions, such as the raphe nucleus, locus coeruleus, hypocretin or orexin neurons, and pars tuberalis [29], as well as indirectly synchronizes the peripheral oscillators by extracellular systemic cues, such as hormones. In particular, has been shown that glucocorticoids can shifts the phase of peripheral tissues in mammals, through

the transcriptional regulation of core clock genes, such as *Bmal1*, *Cry1*, *Per1* and *Per2*, mediated by the *cis*-regulatory sequence Glucocorticoid-Response Elements (GREs) [30]–[32] (figure 3).

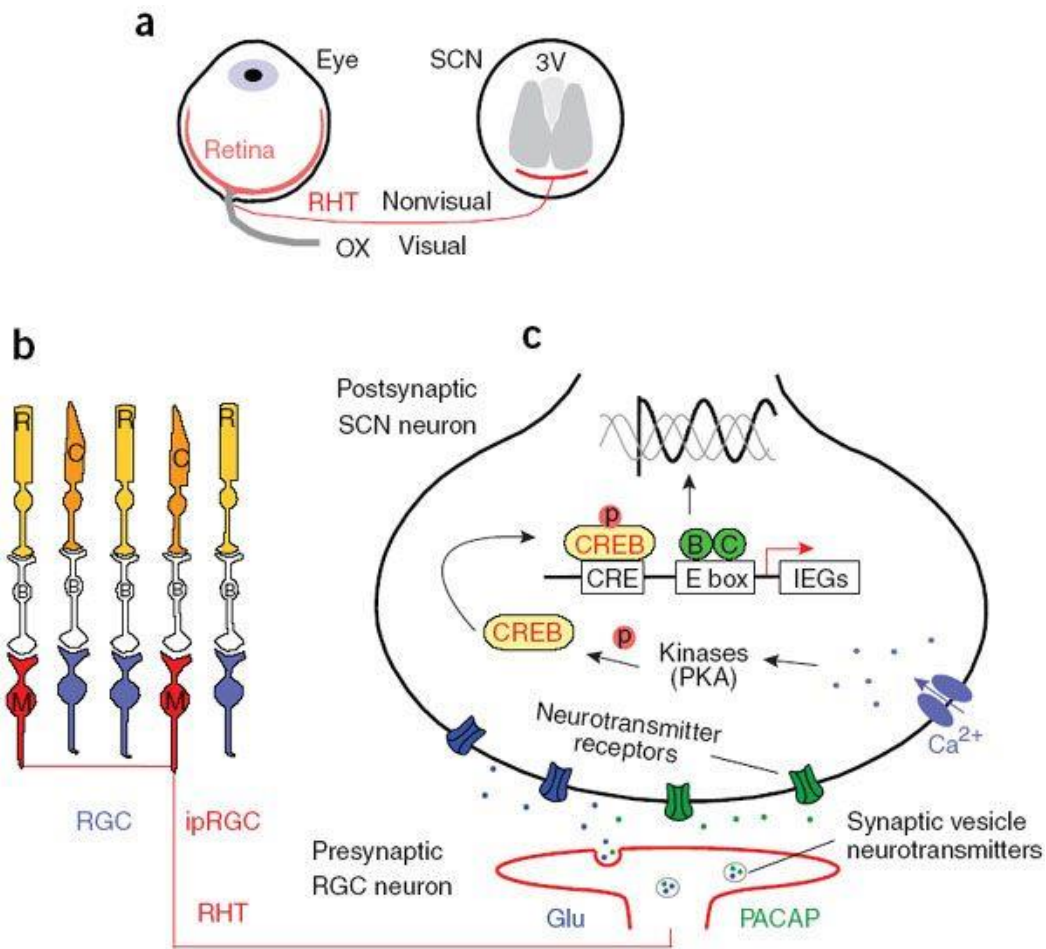


**Figure 3: Synchronization of the SCN by light-dark cycles.**

(a) Photic inputs from the retina to the ventral SCN. The SCN is situated in the hypothalamus immediately above the optic chiasm (OX) on either side of the third ventricle (3V). A small population of retinal ganglion cells (RGCs; red) form the retinohypothalamic tract (RHT) in the OX, which projects to the neurons in the ventral SCN. (b) Retinal photoreception. Melanopsin (M)-containing RGCs are intrinsically photosensitive, and these ipRGCs also receive light input from the rods (R) and cones (C) of the retina through bipolar (B) and amacrine cells (not shown). Their axons form the RHT and project to the SCN. (c) Photic transmission to the SCN and intracellular signal transduction. Glutamate (Glu) and PACAP are the main neurotransmitters released from the presynaptic RGCs. The glutamate and PACAP bind to their respective receptors, resulting in membrane depolarization and an influx of  $\text{Ca}^{2+}$  in targeted SCN neurons. Within postsynaptic SCN neurons, changes in intracellular  $\text{Ca}^{2+}$  and cAMP levels lead to activation of multiple kinases and ultimately phosphorylation of CREB; phospho-CREB (P-CREB) acutely activates immediate early genes (IEGs) such as

*Per1* and *Per2* via CRE elements, leading to establishment of a new circadian phase (depicted in black). Schematic from: Liu AC et al. *Nat Chem Biol.* 2007 [33].

### **1.5 Food-entrainable oscillator (FEO)**

It has been known for decades that regular food availability can function as a powerful synchronizer of the circadian clock in many species, e.g. bees [34], fish [35], birds [36] and mammals [37], [38]. The food-entrainable oscillator (FEO) is a circadian pacemaker, distinct from the light-entrainable oscillator (LEO), that is entrained by temporally restricted food availability. Regular feeding activity can act as a potent synchronizer of circadian rhythms in vertebrates, resulting in an increase in locomotor activity several hours before mealtime, which is known as food anticipatory activity (FAA) [39]. The self-sustained nature of the FEO is revealed by the persistence of FAA during fasting subsequent to restricted feeding. While much work has focused on the function of the LEO, very little is known about the function and organization of the FEO. In mammals, this circadian oscillator has been shown to be located outside of the hypothalamic SCN [40], the site of the master circadian LEO. Moreover, in mammals temporal feeding restriction, under different lighting conditions, can change the phase of rhythmic expression of some core clock and clock-controlled genes in peripheral tissues, while leaving the phase of cyclic gene expression in the SCN unaffected; therefore, reinforcing the notion that the FEO is an SCN-independent clock. [41]–[46]. Moreover, lesioning experiments have demonstrated that other sites within the central nervous, such as hypothalamus (ventromedial, paraventricular and lateral parts), hippocampus, amygdale and nucleus accumbens, area postrema and olfactory bulb are not necessary to established the FAA [40], [47]–[49], therefore the precise location of the FEO still remains elusive. While the phase of rhythmic clock gene expression in the SCN seems unaffected by the time of restricted feeding, it can still affect the entrainment of the rhythms in peripheral tissues via systemic signals, such as glucocorticoids, according to local environmental conditions [42]. In particular, it has been revealed, by studying the effect of ablation of the glucocorticoid receptor (GR) in the liver in the response to the inversion of feeding time, that GR function plays a rule in the phase resetting of liver clocks [50]. The relationship between the SCN and feeding behavior is shown in figure 4.

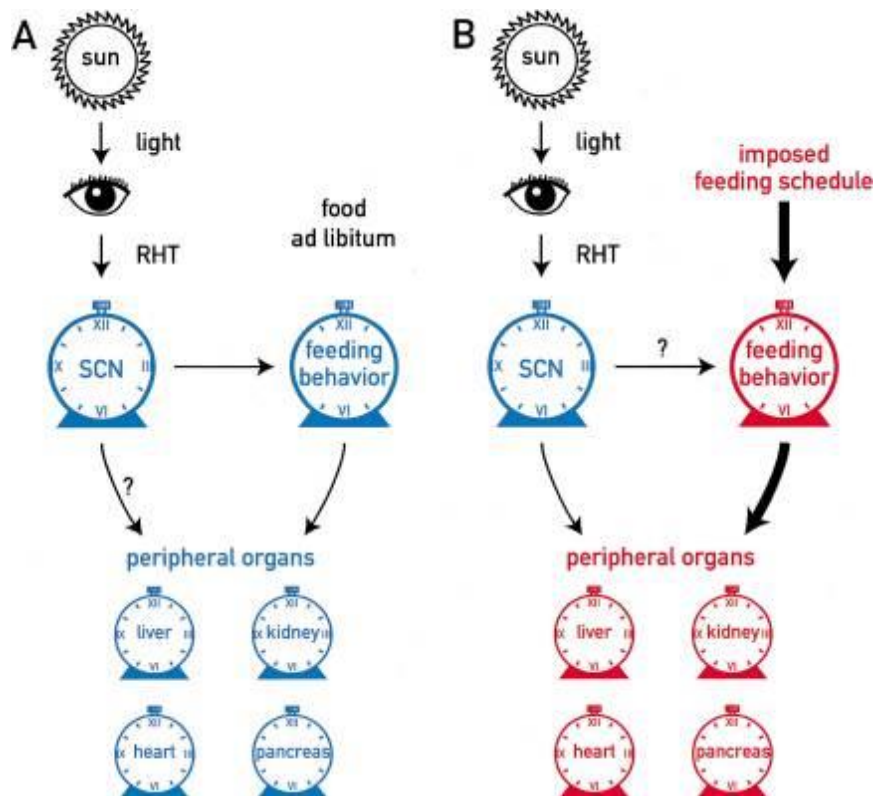


**Figure 4: Hypothetical model for the effect of feeding entrainment on peripheral organ clocks.**

(A) When food availability is under ad libitum conditions, the SCN regulates the feeding behavior and then synchronizes peripheral clocks through daily secretion of systemic factors (e.g., hormones) or rhythms of body temperature (B). When the feeding is time-restricted, signals arising from feeding and/or fasting act as dominant zeitgebers for the oscillators in peripheral tissues. Damiola F. et al. *Genes Dev.* 2000 [47].

The molecular mechanism underlying synchronization of peripheral oscillators by periodic feeding still remains poorly understood. The circadian and self-sustained nature of the FEO has led some to hypothesize the involvement of the classical core clock genes in the regulation and synchronization of the FEO. However, *Clock* $\Delta$ 19 mutant mice, that has arrhythmic SCN-controlled nocturnal activity, exhibits normal FEO-controlled food anticipatory activity [51]. Similarly, studies performed on mice lacking both functional Cryptochromes (*Cry1* and *Cry2*), or both *Period (Per)1* and *Per2*, or *Per1*, *Per2*, and *Per3* show that the function of these core clock genes is not necessary for FAA. Indeed, FAA persisted during restricted feeding and subsequent fasting in constant darkness in all these loss of function mutants (when SCN synchronizing activity is affected) [52]–[54]; in contrast, other studies have indicated that eliminating the function of one or two clock genes results in altered circadian meal anticipation [55], [56].

Many studies have focused on understanding how feeding time can impact on the phase of peripheral clocks. These works have implicated redox cycles, feeding-dependent hormone signaling as well as metabolites as key signals in the response to food and feeding activity. For example, the NAD<sup>+</sup>-dependent PARP-1 (poly (ADP-ribose) polymerase 1) poly(ADP-ribosyl)ation activity displays a circadian pattern in the mouse liver in synchrony with feeding signals rather than with the phase of the circadian clock in the SCN. [44]. Furthermore, it has been revealed that the circadian modulation of mitochondrial protein acetylation generates cycles of nicotinamide adenine dinucleotide (NAD<sup>(+)</sup>) biosynthesis, adenosine triphosphate production, and mitochondrial respiration thus allowing the synchronization of the oxidative metabolic pathways with the 24-hour fasting and feeding cycle [57]. In addition to the circadian regulation of redox metabolism, food intake can also modulate the secretion of certain hormones, which may contribute to peripheral FEO synchronization. For example, it has been shown that food intake in mice, induces OXM (oxyntomodulin) secretion in the gut that modulates the resetting of transcriptional rhythms via the induction of the core clock genes *Per1* and *Per2* in liver [58]. Moreover, inverted feeding cycles induce corresponding phase shifts in the daily oscillation of insulin levels. This resulting reversed insulin signaling induces the reset of clock gene rhythms by affecting hepatic BMAL1 nuclear translocation in mouse [59]. Furthermore, in the pineal gland of arrhythmic SCN-lesioned rats, melatonin shows a rhythmic pattern where the phase is set by the restricted feeding cycle [60].

Just as the circadian timing system is able to confer rhythmicity on several metabolic processes, even metabolic pathways and signals can feed back on the circadian system, strengthening and adapting the circadian clock oscillations according to the organism's metabolic needs. Indeed, it has been reported how several metabolites can affect the phase resetting of circadian genes according to the daily time-restricted feeding. For example, in mice, a restricted feeding regime imposed during the “rest” phase (light period) generates a hypoinsulinemia condition during the active phase (dark period) which triggers a metabolic remodulation by increasing free fatty acid (FFA) and glucagon levels. These changes activate peroxisome proliferator-activated receptor alpha (PPAR $\alpha$ ) and cAMP response element-binding protein (CREB) signaling pathways respectively, resulting in anti-phase rhythmic expression of *Reverba*, *Per1* and *Per2* in the liver [45]. Moreover, it has been reported that the activation of expression of the *Sirt1* gene in *Agrp*/*NPY* neurons may trigger food anticipatory behavior in mice [61], [62].

## 1.6 Clock output pathways in vertebrates

In vertebrates, local, tissue-specific circadian clocks direct rhythmic activity of gene regulatory networks, thereby conferring tissue-specific rhythmicity on various aspects of physiology [63]. Among the broad range of biological processes that exhibit daily rhythmicity in a tissue specific fashion in vertebrates are cell cycle [64], metabolism [65], and feeding behavior [41], [66], [67] (figure 5). In mammals, it has been shown that the SCN plays a crucial role in the regulation and synchronization of the peripheral clocks according to environmental changes. However, the peripheral clocks have the ability to adapt to their own local environmental signals, such as feeding cues for the liver and pancreas, and internal tissue-specific signals, that generates a subsequent feedback of tissue-specific information to the SCN. However, the global phase of circadian rhythmicity at the whole organismal level is guided by the light-dark cues sensed by the central clock [68]–[71].

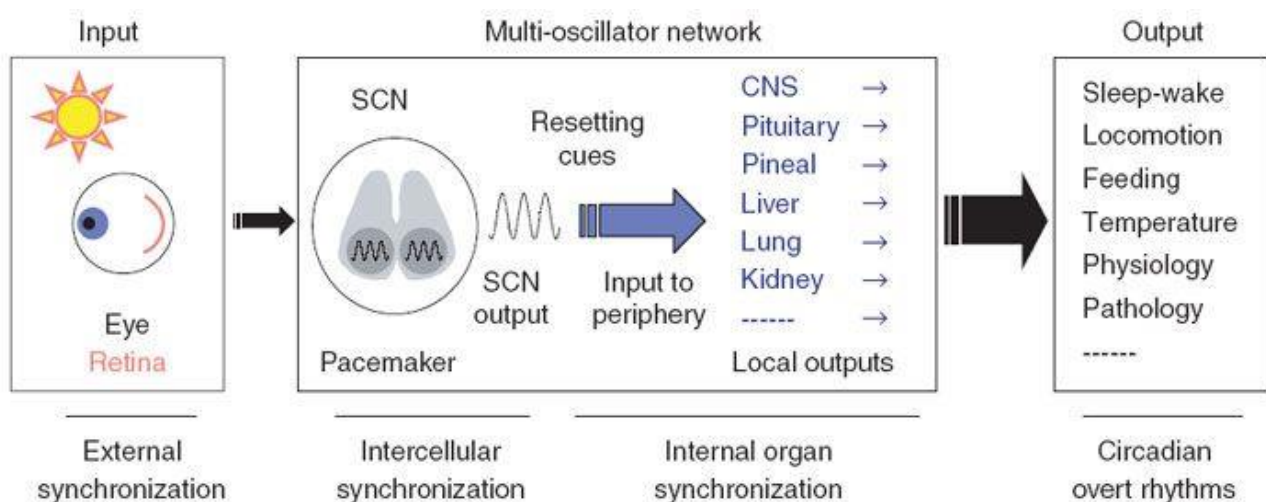


**Figure 5: The mammalian circadian timekeeping system.**

The mammalian circadian clock is organized as a hierarchy of multiple oscillators, in which the SCN is the central pacemaker at the top of the hierarchy. The SCN is synchronized by the external 24-h cycle and in turn coordinates physiological outputs. Peripheral oscillators are reset by timing cues emanating from the SCN, which regulate tissue-specific circadian physiology (local outputs). Internal organ synchronization is critically important for the robust operation of the entire body clock, which regulates overt circadian rhythms. Schematic from: Liu AC et al. *Nat Chem Biol.* 2007 [33]

The molecular mechanism underlying the daily oscillation of several physiological functions is based upon the transcriptional regulation of thousands of tissue specific clock-controlled genes (CCGs). For example at least 10% of all mRNAs exhibit circadian oscillations in abundance in mammalian liver, including many genes involved in metabolic processes [72]. The rhythmic expression of these genes is generated by the same intracellular transcriptional feedback loops involving *cis*-regulatory elements such as E-boxes, D-boxes, and ROR-elements (RREs) previously described for the core circadian clock mechanism (figure 2) [73], [74]. Therefore, unravelling the role of peripheral clocks in each tissue, and their relationship with other tissue-specific clocks is crucial in order to better clarify the role of the peripheral clocks in circadian physiology. Here again, many questions remain concerning the molecular output mechanisms underpinning of the clock-controlled tissue specific function in vertebrates.

### **1.7 Clock output regulation of the cell cycle**

Cells are exposed to multiple environmental stimuli that ultimately influence their fate. Many of these stimuli also regulate the circadian clock. Therefore, one may speculate that a coupling between the circadian clock and cell cycle would confer a selective advantage whereby basic cellular processes such as the cell cycle are synchronized with optimal environmental conditions.

The process of clock-regulated cell division is observed in different vertebrates, in highly proliferative tissues and cell lines, as well as during embryonic development [75]–[77]. In mice, ablation or loss-of-function mutations of core clock genes is associated with altered mitotic rhythmicity and cell cycle progression in high proliferative cell lines and tissues [78]–[81]. The circadian clock plays an important role in the synchronization of regeneration processes after induction of damage in different tissues, such as the skin [82] liver [75] and intestinal epithelium [83]. However, mice in which circadian clock genes are mutated do show normal development [84]. Therefore, the circadian clock is clearly not essential for all cell cycle progression, but rather seems to be an instrument for temporally coordinating key cellular events so that they occur in an optimally timed sequence or coincide with certain parts of the day night cycle.

An interplay between the circadian clock and cell cycle control machineries has been revealed by many different investigations. For example, in human oral mucosa some cell cycle proteins display clear circadian variations in their abundance [85], [86]. In turn, relative RNA expression of some clock genes in human oral mucosa and skin, is coupled with specific phases of the cell cycle.

Specifically, *cyclin B1* and *Cnnb1* show a peak of expression that coincides with *Bmal1*'s peak expression, and *Per1* gene expression parallels that of *p53* levels in late G1 phase [85]. Several molecular studies have reported that circadian clock components can interact with and thereby regulate the cell cycle at different levels (figure 6).

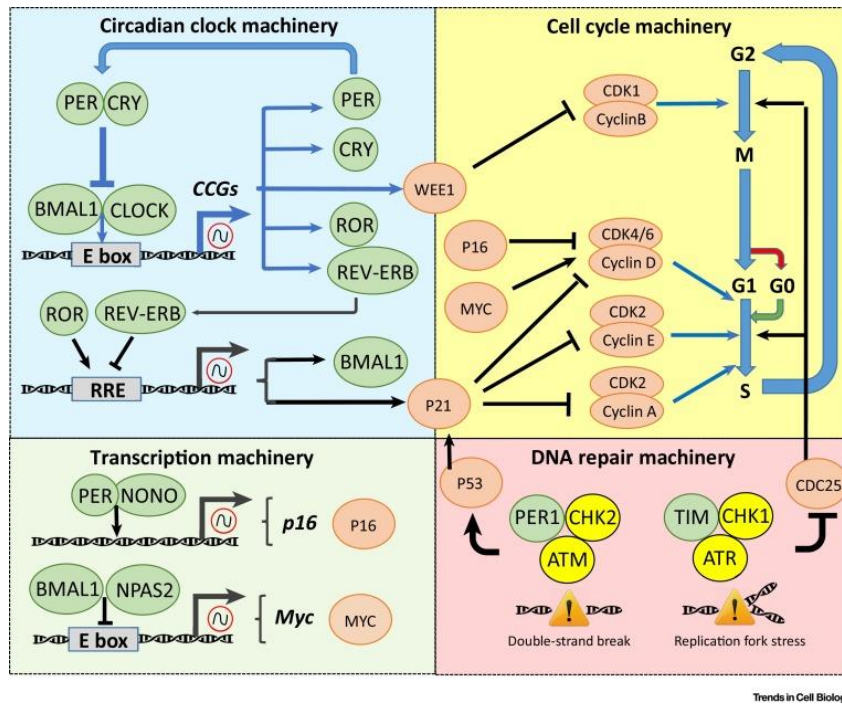


**Figure 6: The circadian clock regulation of the cell cycle.**

The circadian clock is involved in controlling the expression of cell cycle genes. The circadian clock transcriptional machinery is involved in the regulation of the *Wee1*, *P21*, *P16*, and *Myc* cell cycle genes (blue box and green box), which regulate the cell cycle progression at the G1–S, S-phase, and G2–M checkpoints (yellow box). Circadian clock proteins also control the DNA repair system, which also impact upon the control of cell cycle progression (red box). Schematic: Gaucher et al. *Trends in cell biology* 2018 [87]

For example, it has been shown that the CLOCK–BMAL1 complex regulates the circadian transcription of the cell cycle regulator gene *p21<sup>WAF1/CIP1</sup>*, thereby affecting the G1-to-S transition in a clock controlled manner [88]. Moreover, the protein NONO appears to bind to the promoter of the *p16-Ink4A* cell cycle gene, thereby mediating circadian expression in cooperation with the PER protein [82]. Recently, it has been reported that the circadian clock can function as a modulator of oncogene-induced cell fate decisions by its regulation of the *Ink4a/Arf* tumor suppressor gene. In addition to these mechanistic studies, information about the interplay between the circadian clock and the cell cycle has also emerged from time-lapse imaging studies that visualize clock regulation of

proliferation in individual cells [89]–[91]. In particular, NIH3T3 cells transfected with fluorescent clock reporter constructs show a clock-controlled progression of mitosis, suggesting that cell division is gated by the circadian clock [89]. Interestingly, in these studies the cell cycle and circadian clock appear to be phase locked in a 1:1 ratio in free running conditions, with one cellular division occurring 5 h before the peak expression of a Rev-Erb $\alpha$ -YFP clock reporter [91]. In mammals, several cell cycle regulators (e.g. *c-Myc* and *Wee1*) contain *cis*-acting E-boxes enhancer elements in their promoter regions that potentially mediate the clock regulation of their transcription, [75][92] (figure 6). Moreover, the *p21* gene, which encodes a CDK inhibitor, is regulated by the action of ROR and REVERB proteins which compete for binding to the RORE element in the p21 promoter [88].

The circadian clock control of the cell cycle also operates by the regulation of the stability of cell cycle proteins. Indeed, a recent study revealed that the CRY2 protein mediates c-MYC degradation by FBXL3 [93]. Moreover, it has been demonstrated that the abundance and phosphorylation of several cell cycle and DNA repair proteins exhibit a circadian modulation [94]. DNA damage checkpoints are an integral part of the cell cycle and control the ability of cells to pause cell cycle progression in response to DNA damage. Moreover, several proteins involved in these pathways show a dual function, allowing the activation of DNA repair systems [95]. Some circadian clock proteins modulate the DNA damage response by interacting with checkpoint response protein complexes (figure 6). For example, the PER1 protein interacts with ATM, a serine/threonine protein kinase that transmits DNA damage signals to cellular events by phosphorylating several key proteins, and CHK2 in order to promote CDC25C phosphorylation thereby arresting the G2–M phase transition, following the appearance of DNA double-strand breaks (figure 6). Likewise, following replication fork stress, timeless (TIM), a key protein of transcription-translation negative feedback loop in *Drosophila*, interacts with ataxia telangiectasia and Rad3-related protein (ATR), another serine/threonine protein kinase involved in sensing DNA damage, and CHK1 to phosphorylate and inactivate the CDC25A and CDC25C functions, thus inhibiting the cell cycle (figure 6) [96]. The CRY proteins represent another intriguing example of bridging between the clock and DNA damage. These proteins are blue-light photoreceptors directly involved in the regulation of the circadian clock in plants and animals [97]. However, they also have a characteristic structure similar to that of the photolyases, enzymes which harness blue light for light-driven electron transfer to repair UV-damaged DNA. Although in mammals CRY proteins do not exhibit DNA repair activity, they have developed a genome integrity activity mediating transcriptional responses. In response to genotoxic stress, CRY1 is phosphorylated and deubiquitinated by Herpesvirus-associated ubiquitin-specific protease (HAUSP), leading to its

stabilization. Instead, CRY2 is destabilized by FBXL3 [98]. Thus, genotoxic stress triggers changes in CRY1 and CRY2 abundance, which could affect circadian clock function.

It seems reasonable to predict that coupling of the circadian clock, the cell cycle, and the DNA damage response provide advantages for protecting cells against DNA-damaging UV exposure occurring during the light period of the day, by limiting DNA replication during the dark phase and/or boosting DNA repair machinery during the day. Indeed, it has been reported that in proliferating skin cells the DNA damage induction and repair efficiency were strictly dependent on the phase of the circadian rhythm at which the cells were exposed to UV [99].

### **1.8 The circadian clock in fish**

The fish circadian timing system is characterized by oscillators that are present in most tissues and which are regulated by direct exposure to light. The genetic organization of these oscillators closely resembles that of the mammalian clock in peripheral and central clocks and consists of a translational–transcriptional feedback in which the mRNA and protein levels of some clock genes fluctuate over the daily light-dark cycle [3], [100]–[102]. A summary of our understanding of the circadian timing system in fish is schematically represented in figure 7.

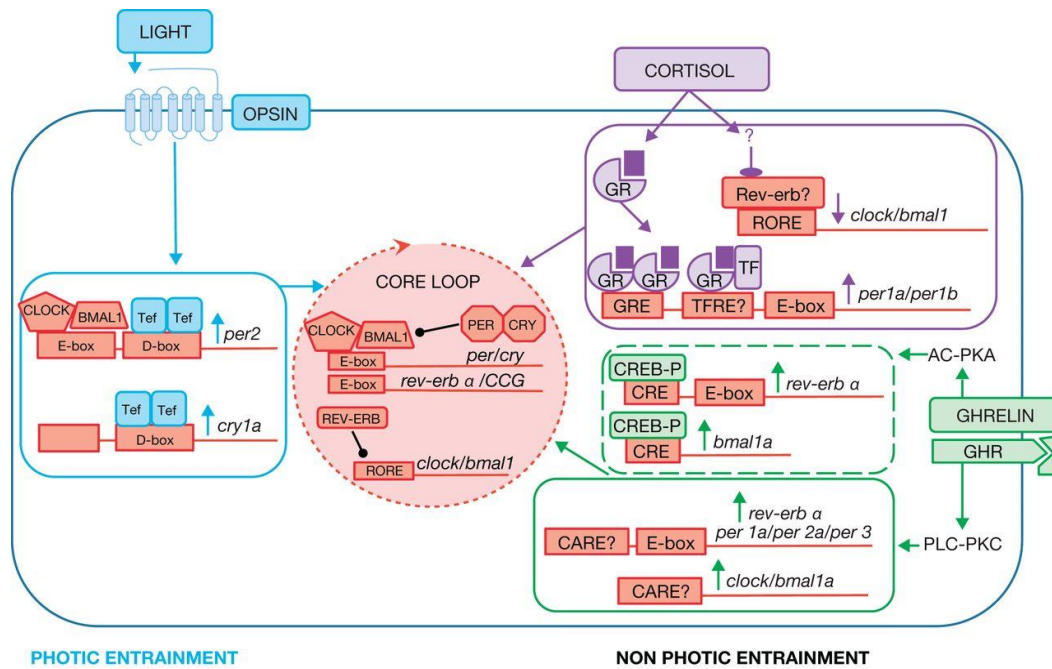


**Figure 7: Hypothetical molecular structure of the circadian oscillator in fish.**

The molecular core loop is thought to be synchronized by exogenous (light) or endogenous (hormones) temporal messengers through the induction or repression of specific clock genes. Events that occur in the cytoplasm and nuclei (gene transcription) have not been separated to simplify the figure. In each box, only putative response elements that are involved in each response (light, cortisol or ghrelin) are shown. The core clock loop is represented as the central circle in red, with some of the main elements inside. This molecular mechanism can be entrained by the light–dark cycle via the light-induced expression of *cry1* and *per2* genes, which involves functional E- and D-boxes and the TEF transcription factor in zebrafish [7], [103], [104]. Alternatively, mechanisms based on hormones such as cortisol and ghrelin can also entrain the molecular clock. Schematic: Isorna et al. *Journal of Endocrinology* 2017 [105].

The functioning of the circadian core clock is comparable in mammals and teleosts, with the sole exception that in fish there are a higher number of homologous core clock genes, as a consequence of a whole-genome duplication (WGD) event that took place in a common ancestor of extant teleosts [106]. Daily oscillation in clock genes have been reported in many tissues across several fish species, including the retina, pineal gland, brain, pituitary gland, liver, gut, gonads and head kidney[107]–[119].

### 1.8.1 Zebrafish (*Danio rerio*): a powerful model organism for circadian rhythm studies

Initially, the zebrafish proved to be an excellent model organism for developmental biology and studying the embryogenesis of vertebrates as well as high-throughput screening studies. Indeed, each

female of this species can generate a large number (between 100 and 200) of completely transparent embryos that develop rapidly and externally *in vitro*, thus facilitating the observation of the whole developmental process. The zebrafish also offers the possibility to generate transgenic lines expressing fluorescent or bioluminescent reporter genes and so has rapidly established itself as an excellent model for live imaging *in vivo*. It has progressively been established as a powerful vertebrate genetic model with well-established set of genetic tools (mutant, transgenic, knock out, knock in fish lines).

The great potential of zebrafish as a model for the study of the vertebrate circadian clock emerged with the finding that the peripheral clocks of this species can be entrained by direct exposure to light-dark cycles [8]. In fact, both core and clock-controlled genes, such as *cry1a*, *6-4Phr*, *per2*, *weel*, *per1b*, *per3*, *bmal1* and *bmal2*, show rhythmic expression in cultured tissues or cells exposed *in vitro* to light-dark entrainment conditions [120]–[124]. This contrasts with the situation in mammals where the peripheral oscillators have lost this photoreceptive capacity, but does resemble the peripheral clocks in *Drosophila* [125]. This capacity to sense light is conserved also in all the cell lines derived from zebrafish embryos and adult tissues [8], [115]. Therefore, zebrafish also serves as a useful tool to study the evolution of the circadian timing system in vertebrates.

In fish, an anatomical counterpart of the mammalian SCN has not yet been identified. However, it has been shown that the pineal gland, which is a purely secretory organ in mammals, is able to sense light and harbors a central pacemaker in zebrafish [126]. Moreover, the retina shows sustained and robust circadian oscillations [127]. Whether the pineal gland in zebrafish has a function comparable to that of the hierarchical master clock in mammals, is not yet clear. Thus, for example, it has been demonstrated that pinealectomy and ocular enucleation does not affect rhythmic locomotor activity of larval fish under LD entrainment [128]. In both the pineal gland and retina, melatonin (N-acetyl-5-methoxytryptamine), an important neuroendocrine signal, is synthesized and secreted exclusively at night, thus conveying environmental information to the circadian system [129]. The daily rhythmic production of melatonin is mediated by *Aanat2* (arylalkylamine-Nacetyltransferase 2), a rate limiting enzyme for melatonin synthesis, that is expressed in pineal photoreceptors and shows circadian-clock regulated transcription [130]. Melatonin regulates several physiological functions and coordinates some circadian outputs in zebrafish (figure 8) [128], [131]. Moreover, during embryonic development, the rhythmic pattern of melatonin and *aanat2* expression are detected enough in

advance compared to the appearance of some important clock outputs, such as the rhythmic locomotor activity [132].

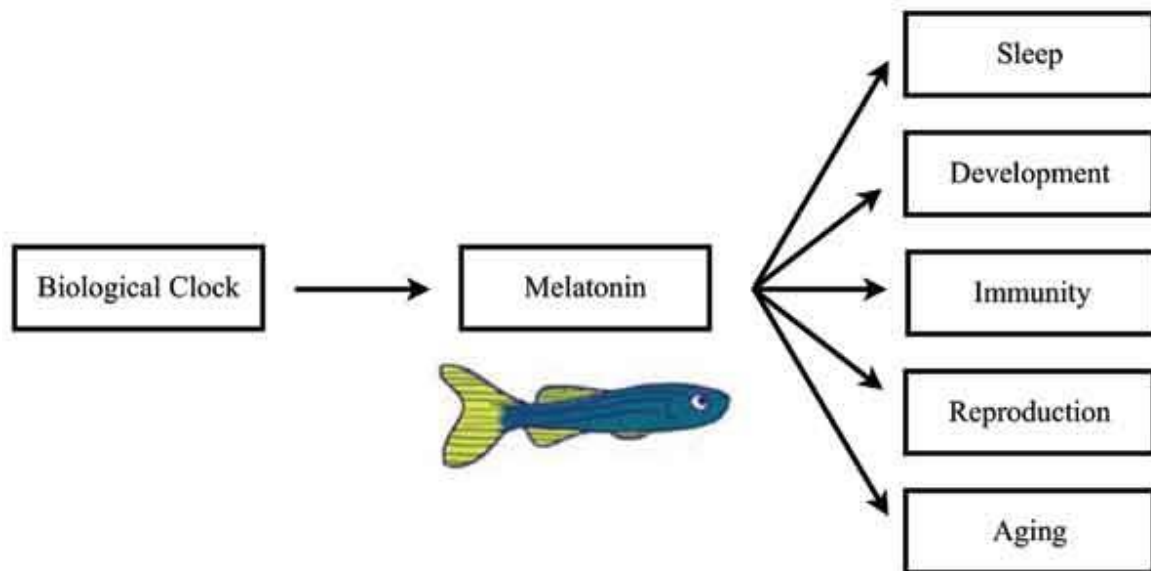


**Figure 8: Clock output processes affected by rhythmic melatonin production.**

Melatonin participates in the circadian regulation of diverse behavioral and physiological events in zebrafish, such as sleep-wake cycle, immunity response, embryonic development, reproduction. Schematic: Southwell et al. *Current Psychopharmacology* 2016 [133].

### **1.8.1.1 Zebrafish-derived cell cultures as tools to investigate circadian rhythms in vertebrates**

The zebrafish represents a powerful model organism with unique advantages for investigating how various environmental cues, such as light, impact upon the circadian timing system. Notably, it possesses directly light-entrainable peripheral circadian clocks. Therefore, unlike mammalian cell lines, that depend upon invasive transient treatments with serum or activators of signaling pathways to synchronize individual cell clocks within a culture, zebrafish cell line clocks can be synchronized non-invasively by simply exposing cultures to light–dark cycles [8]. Furthermore, zebrafish cells grow at room temperature, remain viable during long periods at confluence, and do not require a CO<sub>2</sub>-enriched atmosphere, greatly simplifying culture conditions [134]. Over the past few years, our laboratory has performed many comparative studies using cell lines established from different teleost species, such as blind cavefish. These cell lines have represented key tools to investigate the evolution of both DNA repair and the photoentrainment systems in vertebrates [115], [135], [136]. Therefore,

much of what we know about the mechanisms responding to light in fish cells has resulted from studies using these cell lines.

### **1.8.2 Light entrainable oscillator (LEO) in zebrafish**

The zebrafish pineal gland and retina organs are characterized by the presence of several photopigments such as rhodopsin, parapinopsin, vertebrate ancient opsin, exo-rhodopsin, UV opsin, and melanopsin [137]–[141]. These photoreceptors are differentially expressed across the two organs, for example exo-rhodopsin is preferentially expressed in the pineal gland, instead canonical rhodopsin is expressed preferentially in the retina [137]. The pinealocytes of the zebrafish pineal gland can perceive light through the photoreceptor rhodopsin, thus transducing the photic signal to the melatonin synthesis machinery and then affecting circadian rhythmicity via melatonin secretion [142], [143]. Moreover, in the zebrafish retina, melanopsin, a member of the non-visual opsin family, plays a key role in triggering phototransduction input pathway, thus conveying the photic signal to the circadian clock machinery [144]. In addition to the central pacemaker, zebrafish possesses peripheral organs and cells that are able to sense photic signals. Different peripheral photoreceptors have been proposed to be involved in the light input pathway in zebrafish peripheral tissues:

1. The non-visual opsins, such as melanopsin, TMT (teleost multiple tissue) opsin, neuropsin, va-opsin, the non-visual opsins [145]. In particular, TMT opsin is expressed in several peripheral tissues and even in fibroblast cell lines, in zebrafish [146].
2. The cryptochromes (Crys), in particular Cry4 [147].
3. The flavin-containing oxidase [148].

A comparative functional analysis between zebrafish and the blind cavefish *Phreatichthys andruzzii* that possesses a blind circadian clock, revealed that loss of function mutations in TMT opsin and in Opn4m2 and Opn4m1 melanopsins at least in part underlie the loss of light input pathway function in the peripheral clock in the blind cavefish; thus emphasizing the key role played by these non-visual opsins as peripheral tissue photoreceptors in teleosts [115]. Indeed, the ectopic expression of the zebrafish homologs of these genes in cavefish cells, partially restores light induced clock gene expression. These results point to extra-retinal opsins serving as key peripheral photoreceptors for peripheral and central clock entrainment in teleosts.

However, in the same study it was revealed that different wavelengths of light can differentially induce clock gene expression, thus indicating that Melanopsin and TMT-opsin are not the only photoreceptors for peripheral clocks in teleosts. Indeed, in zebrafish peripheral organs, functional genomic analyses have revealed the presence of 42 distinct opsin genes, comprising 10 known visual and 32 nonvisual opsins, which includes four new photopigment gene classes (*opn6*, *opn7*, *opn8*, and *opn9*), thus highlighting how the peripheral nonvisual light detection mechanism, in lower vertebrates, is more complex than initially appreciated [149]. It is therefore apparent that, in zebrafish, the LEO is restricted not only to a central pacemaker, but is also present in nearly all cell types.

Non-opsin-based photoreceptor systems have also been implicated in peripheral photoreception in zebrafish, including certain cryptochromes (Cry3 and Cry1b) [120] as well as flavin-containing oxidases which generate reactive oxygen species (ROS) upon exposure to light [148]. We have demonstrated that ROS mediates light-regulated gene expression. Indeed, exposure to blue light triggers increases in ROS levels via NADPH oxidase activity and elevated ROS activates the JNK and p38 MAP kinases, which in turn, induce the expression of *per2* and *cry1a* light-inducible clock genes via the effect of D-box enhancer promoter elements [7], [103], [104], [126], [150], [151]. The D-box enhancer element is a target of light signaling pathways in lower vertebrates, such as zebrafish, that enhances PAR/ E4BP4-mediated transcriptional regulation of several light inducible core clock and clock-controlled genes [104], [135], [136], [152], [153]. In particular, it has been shown that the zebrafish homolog of the thyrotroph embryonic factor (TEF), that belongs to the PAR subfamily, is able to bind to the D-box enhancer element and to transactivate the D-box-mediated gene expression [104].

### **1.8.3 Food entrainable oscillator (FEO) in zebrafish**

As for mammals, a scheduled feeding regime represents a powerful zeitgeber that synchronizes circadian rhythmicity in zebrafish [114]. Moreover, also in zebrafish, time-restricted feeding is coupled with food anticipatory activity, a typical clock output of the FEO. It has also been reported that the expression pattern of the core circadian genes (*per1*, *cry1*), in the zebrafish liver, shows a circadian phase adjusted according to inverted feeding regimes [114], while the rhythmic expression of these genes is not affected by the feeding schedules in the zebrafish brain. However, rhythmic expression of several lipid metabolic genes, in zebrafish liver, appears not susceptible to the feeding time [154]. However, to date, only few studies have been conducted to assess the anatomical site and molecular and physiological features of the FEO, in zebrafish. Therefore, many questions remain to

be answered. Does the light entrainment mechanism crosstalk or mediate the pathways of feeding entrainment, in zebrafish? What is the genetic basis and anatomical location of the FEO mechanism in zebrafish? Also, in zebrafish does the central pacemaker coordinate or regulate the peripheral clocks by systemic cues?

### **1.9 *Period2 (Per2): a multifunctional gene***

The *Per* genes are key elements of the core clock mechanism in vertebrates. Therefore, understanding the function of these genes and proteins at the molecular level represents a topic of considerable interest. The *Per* genes are involved in the regulation of many biochemical processes such as the cell cycle and metabolism, thus affecting several physiological processes such as aging, brain dysfunction, and the development of cancer. Hence, understanding *Per* gene functions will potentially help us to develop new treatments for cancer, depression, and metabolic diseases.

Vertebrates have three *Per* paralogs genes (*Per1-3*), probably the consequence of two genome duplications during early vertebrate evolution, resulting in four paralogs of which *Per4* was lost [155]. Moreover, a comparative study of *Period* genes in five teleost fish genomes including the zebrafish which has two *per1* genes, *per1a* and *per1b*, one *per2*, and one *per3*, support the notion that extra copies of teleost *per* genes resulted from the fish-specific genome duplication[156].

Within the *Per* gene family, a prominent role in the regulation of circadian rhythms is played by the *Per2* gene. Human and mouse *Per2* genes are both characterized by 23 exons, coding for transcripts of 6220 bp or 5805 bp and proteins of 1255 amino acids or 1257 amino acids, respectively. The human *Per2* gene was mapped to chromosome 2q37.3 [157], while this gene is also located on chromosome 2 in zebrafish, opossum, and the chimpanzee, instead it is placed on chromosome 1 in the mouse and on chromosome 9 in the rat. The PER2 protein is characterized by several motifs and functional domains (figure 9), which underlie its multiplicity of functions involved in the regulation of physiological processes in vertebrates, ranging from sleep-wake cycles [158], metabolism [159], hormone secretion [160] to basic cellular and molecular processes such as DNA repair [161], cell proliferation [162], and cell cycles [163]–[166].

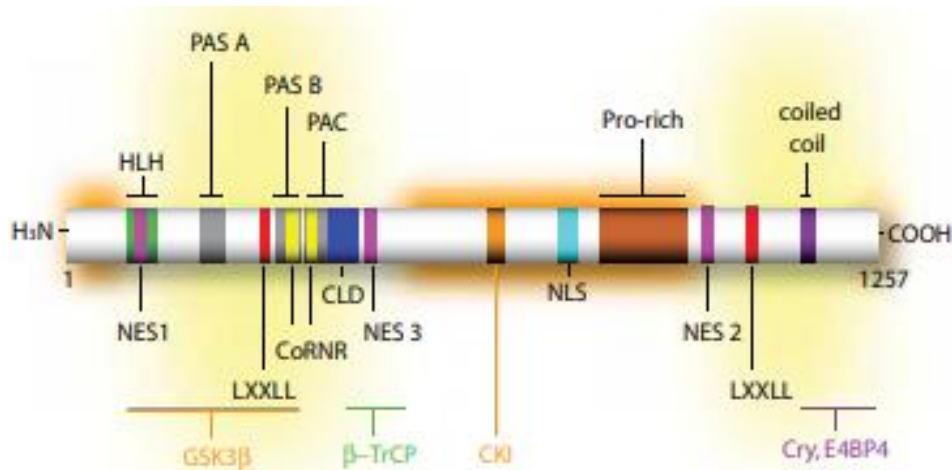


**Figure 9: Structural and functional domains of the mouse PER2 protein.**

The PAS domain consists of PAS A, PAS B, and the PAC motifs (*gray*). (HLH) Helix-loop-helix motif (*green*); (NES1, 2, and 3) nuclear export sequence (*pink*); (LXXLL) motif found in coactivators to associate with nuclear receptors (*red*); (CoRNR) motif found in corepressors to associate with nuclear receptors (*yellow*); (CLD) cytoplasmic localization domain; (CKI) casein kinase-binding site (*orange*); (NLS) nuclear localization sequence (*cyan*); (Pro-rich) proline rich sequence (*brown*); (coiled-coil) dimerization domain (*purple*). (Yellow-shaded areas) Potential protein-binding domains; (*orange-shaded areas*) localization of phosphorylation sites. Schematic: Albrecht et al. *Cold Spring Harbor Symposia on Quantitative Biology* 2007 [167]

The mouse Per2 protein includes an amino-terminal helix-loop-helix (HLH) motif, whose DNA binding function is compromised due to the presence of non-basic amino acids in the preceding n-terminal region. The most important Per2 functional region is the PAS domain, that contains two imperfect repeats (PAS A and PAS B) followed by a PAS-like PAC motif. The PAS domains are implicated in protein-protein interaction and dimerization [168]–[170]. Moreover, it has been reported that Glycogen synthase kinase-3 $\beta$  (Gsk3- $\beta$ ) interacts with the PAS A and PAS B domains of PER2 [171]. It has been proposed that PAS/PAC domains may serve as ligand-binding domains [172], binding a heme group and thereby functioning as oxygen sensors. This hypothesis is supported by the evidence that heme is a prosthetic group of the mPER2 protein [173], allowing the protein to sense redox status. Furthermore, it has been suggested that PAS/PAC domains could function as light sensors via a bound flavin adenine dinucleotide (FAD) cofactor. [174], [175]. Therefore, this evidence suggest that the PAS/PAC domain could mediate the PER2 blue light- and redox-sensing protein capacity.

The mPER2 protein is also characterized by the presence of a coiled coil motif, whose function is to strengthen the protein-protein interaction [176], [177]. Therefore, it appears that PER2 has two protein-binding domains, the PAS and the coiled coil domain, which enables the PER2 to function as a scaffold bringing other proteins or protein complexes in proximity to each other to exert a specific function. Moreover, the PER2 protein is characterized by the presence of two LXXLL motifs (figure 9)—where L is leucine and X can be any amino acid—that are generally present in coactivators and corepressors. For example, this motif has been found in some coactivators interacting with nuclear receptors such as, the steroid hormone receptor coactivator-1 (SRC-1) [178]. SRC-1 interacts with several nuclear receptors such as progesterone receptor, estrogen receptor, PPAR, or RXR, stimulating their transcriptional activity. Therefore, we could speculate that PER2 protein could accomplish a similar activity. Instead, the CoRNR box present in the PAS/PAC domain of PER2, could, potentially, mediate the PER2 nuclear receptor corepressor activity (figure 9).

*Per2* gene expression is regulated in circadian manner in the suprachiasmatic nucleus (SCN) with a shift of about 4 hr compared with *Per1* rhythmic expression [179]. Moreover, the *Per2* gene is widely expressed in several tissues in mammals. In mice, *Per2* expression in the VIP-containing region of the SCN (termed 'core') is observed only in the early subjective night. Instead, in the remaining regions of the SCN (termed 'shell'), exposure to a phase delaying light pulse significantly induces *Per2* expression, while a phase advancing light pulse results in no *Per2* induction [180]. Therefore, these results suggest a possible involvement of *Per2* in the molecular mechanism underlying the light entrainment system of the circadian clock. The *Per2* gene expression can also be regulated by other stimuli such as 5-HT<sub>1A/7</sub> receptor agonists, neuropeptide Y [181], vasoactive intestinal polypeptide [182], glucocorticoids [183], and ghrelin [184]. These characteristics point to a complicated system of transcriptional regulation of the *Per2* gene. The promoter analysis of the mammalian *Per2* gene includes two noncanonical E-box enhancers that direct the circadian expression of *Per2* through CLOCK/BMAL1 transcriptional activity [185], [186]. Interestingly, it has been observed that this CLOCK/BMAL1 regulation is tissue-specific, since the absence of BMAL1 in the liver does not affect *Per2* rhythmic expression, whereas in other tissues, loss of BMAL1 function abolishes this rhythmic expression [187]. Another important regulatory element is the DBP/E4BP4-binding element (D-box), which is crucial to establish the period length of the circadian oscillator [73], [188]. Moreover, exploring the evolution of the signal transduction pathways underlying the photoentrainment mechanism of fish peripheral clocks, our laboratory has revealed that the D-box enhancer element is necessary and sufficient to drive light-induced transcription of a wide range of

light-regulated gene [150], [189] including *per2* in fish. Therefore, whereas the D-box acts as a clock-controlled enhancer element in mammals, it would appear that it serves as a central regulatory element in light-entrainment of circadian rhythms in lower vertebrates, such as zebrafish. In mammals, the *Per2* gene appears to be induced by several signaling pathways converging on the binding of phosphorylated cAMP-responsive element (CRE) binding protein (CREB) on the CRE element located in the *Per2* promoter. The CREB protein is involved in light-induced clock resetting and is phosphorylated by ERK-MAPK kinases, *in vivo* in response to photic signals [26], and *in vitro* following glutamate treatment [190]. Moreover, light exposure at night triggers a robust increase in CRE-mediated transcription in the retinorecipient part of the SCN [191]. Despite the presence of the CRE element, the *Per2* promoter is less responsive, compared to the *Per1* promoter [192]. However, there are several other potential *cis*-regulatory elements in the *Per2* promoter; but, their functional importance has not yet been established [193].

### **1.9.1 *Per2* a regulator of the FEO?**

Some studies have reported that FAA is absent in *Per2* mutant mice [55], [56], [194]. In particular, a study has shown that total-body and liver-specific *Per2* mutant mice did not exhibit FAA [195] and that *Per2* triggers FAA via the regulation of  $\beta$ -hydroxybutyrate ( $\beta$ OHB) production, thus concluding that liver *Per2* gene function is important for this process. In contrast, a recent study showed different lines of *Per2* mutant mice (the *Idc* strain and *Brdm1* strain) exhibited robust FAA [196]. Therefore, in mammals, whether the *Per2* gene is critical for expression of FAA remains unclear. Thus, it would be extremely valuable to clarify whether *Per2* gene function is, or is not involved in the regulation of the FEO and FAA in another vertebrate model, such as the zebrafish. In zebrafish, the *per2* gene, besides being one of the main elements of the core clock, exhibits a light responsive transcription regulation across several tissues, *in vitro* and *in vivo*, thus suggesting a function in the regulation of the light entrainment mechanism of the circadian clock at the level of master and peripheral oscillators. Therefore, the zebrafish could be a useful tool to unravel *per2* gene function in the regulation of the food entrainable oscillator, in a model where the LEO and FEO could be more closely interconnected with respect to the mammals.

### **1.9.2 *Per2* involvement in the regulation of the cell cycle**

Several studies have reported the existence of robust links between the circadian clock mechanism and the cell cycle [87], [166], [197]. Indeed, disruption of the links between these two oscillator systems results in aberrant cell proliferation. Moreover, circadian clocks are frequently deregulated

in cancer cells [198]. However, we still lack a complete understanding of the molecular mechanisms underlying these connections. The PER2 protein is a strong candidate to be involved in this regulatory link. Mice with aberrant expression of the *Per2* gene are inclined to develop cancer and display altered expression of genes involved in cell cycle regulation and tumor suppression such as *Cyclin D1*, *Cyclin A*, *Myc*, and *Mdm2*. In particular, *Myc* is controlled directly by circadian regulators including *Per2*. Therefore, it appears that *Per2* has a role in tumor suppression by regulating DNA-damage-responsive and pro-apoptosis signaling [166], [199]. Moreover, *per2* rhythmic expression is altered at different stages of carcinogenesis in golden hamster buccal mucosa [200]. In addition, in oral squamous cell carcinoma, the *Per2* gene plays crucial role in cell cycle progression and the balance of cell proliferation and apoptosis by regulation of the cyclin /CDK/CKI cell cycle network [164]. Furthermore, clinical studies have revealed that *Per2* expression is reduced in cancer patients, and that it has a tumor suppressor function in breast cancer, skin tumors, hepatocellular carcinoma, colorectal cancer and head and neck squamous cell carcinoma [198], [201]–[204]. Although the above findings revealed the role for PER2 in suppressing a cancer-prone phenotype, a recent study has refuted this *per2* gene function [205]

In the last few years, it has been shown that the circadian clock can affect the cell cycle, but there is less information on how the cell cycle, can feedback on the clock and whether PER2 may play a role in this process. It has been reported that DNA damage can affect the circadian clock, thus functioning as a *zeitgeber* [206]. As DNA damage modulates the cell cycle, it may also reset the circadian clock, with the aim of optimizing the coupling between the two oscillators. A cell cycle feedback effect on the circadian clock has been demonstrated with the finding that P53, an important regulator of the cell cycle, binds a P53 response element in the *Per2* gene promoter, which overlaps with an E-box, and thereby temporally represses CLOCK–BMAL1-mediated transcription [207]. Therefore, this study reveals that P53 protein plays a role in the regulation of the *Per2* gene transcription, thus shaping its circadian behavior.

*Per2* gene function as molecular element bridging the cell cycle and circadian clock has been investigated in a detailed manner almost exclusively in mammals. However, it is important to clarify if this *per2* gene function is preserved in other vertebrates, such as zebrafish, in which previous studies have shown that both mitosis (M phase) and S phase are clock-regulated and restricted to specific times of the day in cell lines, tissues and also during embryo development [76], [77], [120], [208]–[210]. Moreover, *per2* gene expression is directly light-induced in the peripheral tissues of zebrafish

[150]. Therefore, we could speculate that the *per2* gene, might mediate the light synchronization of the cell cycle in highly proliferative tissues.

### **1.10 TGF- $\beta$ signaling pathways**

Disruption of the circadian clock system and de-synchronization of its derived rhythms have been suggested to increase the risk for several diseases and syndromes, including tumorigenesis and tumor progression [211], [212], metabolic syndromes and obesity [213], as well as Alzheimer's disease [214], [215]. However, although the molecular mechanism of the circadian clock is well characterized and the influence of the clock on multiple physiological processes has been well documented, the underlying mechanisms linking clock disruption with these disorders are not fully understood.

TGF- $\beta$  is a widely expressed and secreted protein that has been shown to play a key role in multiple cellular processes including proliferation, differentiation, migration, and survival, as well as physiological processes, including embryonic development, angiogenesis, and wound healing. [216]–[225]. Therefore, dysregulation of the TGF- $\beta$  pathway is associated with severe human disease, such as connective tissue, skeletal and muscular, reproductive and development disorders [226]. Moreover, the TGF- $\beta$  signaling pathway plays an important role in the context of cancer biology [227].

The binding of TGF- $\beta$  to one of its receptors, the TGF- $\beta$  type III receptor or the TGF- $\beta$  type II receptor, leads to the phosphorylation of SMAD2 or SMAD3, their association with SMAD4, and their translocation into the nucleus. In the nucleus, the Smad2/3-Smad4 complex act as a transcription factor, in association with various co-activators and co-repressors to activate or repress the transcription of many genes and cellular processes [228]–[231]. TGF- $\beta$  is associated with elaborate negative feedback mechanisms. These mechanisms include inhibitory SMADs (like SMAD7) and co-repressors (such as TGIF1 [229], [232]) (figure 10).

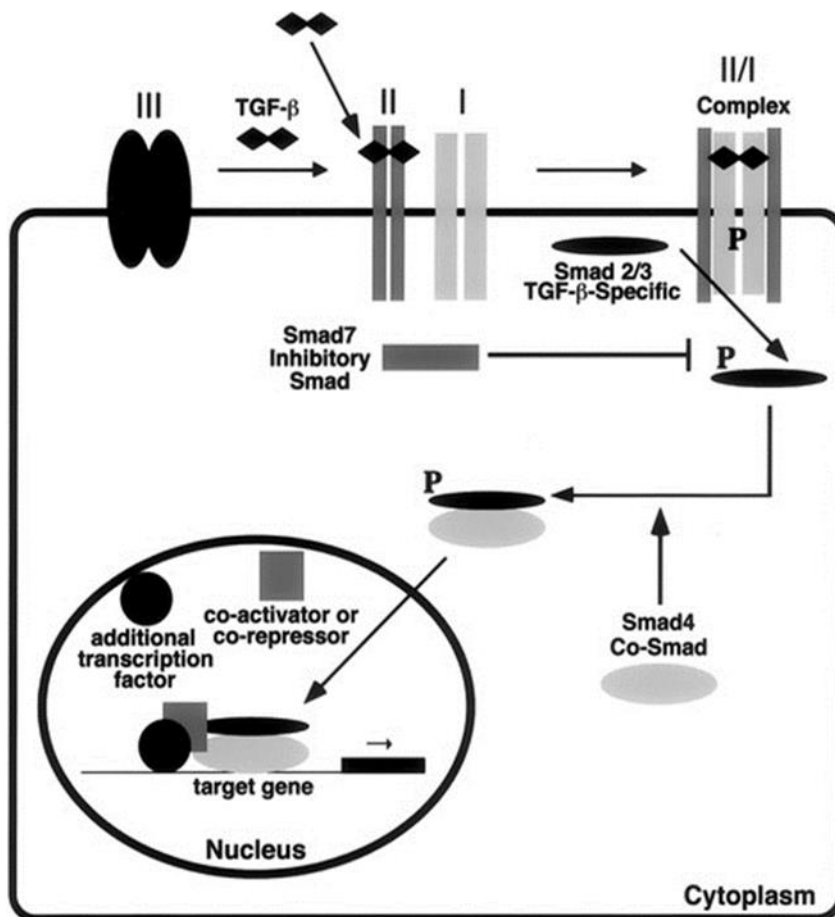


**Figure 10: Canonical TGF- $\beta$  pathways.**

After extracellular activation, TGF- $\beta$  ligands bind to the membrane associated TGF- $\beta$  type III or the TGF- $\beta$  type II receptor homodimers with high affinity. TGF- $\beta$ RII binding allows dimerization with TGF- $\beta$  type I receptor (TGF- $\beta$ RI) homodimers, activation of the TGF- $\beta$ RI kinase domain and signal transduction via phosphorylation of the C-terminus of receptor-regulated SMADs (R-SMAD), SMAD2 and SMAD3. The SMAD2/SMAD3 dimer then forms a heterotrimeric complex with SMAD4 which translocates and accumulates in the nucleus. TGF- $\beta$  dependent signaling can activate or repress hundreds of target genes through the interaction of SMADs with various transcription factors. Schematic: Wells G. *Am J Physiol Gastrointest Liver Physiol* 2000 [233].

### 1.10.1 Clock output regulation of the TGF- $\beta$ signaling pathway

An effect of TGF- $\beta$  signaling on the circadian clock was initially proposed based on the evidence that activation of ALK (TGF- $\beta$ R) receptors by TGF- $\beta$  leads to the induction of Dec1 activity and consequent resetting of the molecular oscillator [234]. This evidence was later reinforced by studies revealing that TGF- $\beta$ 2 inhibits the expression of several clock genes [235]. Moreover, it was shown that *Smad3* mRNA exhibits rhythmic expression in human cell lines and the mouse liver [236] and

that TGF- $\beta$  and phosphorylated SMAD3 (pSmad3) proteins exhibit a circadian expression pattern in the hypothalamic superchiasmatic nucleus, the site of the master clock in mammals [237]. Together, these recent findings suggest a bi-directional interaction between the circadian clock and TGF- $\beta$  signaling. More detailed studies of this interaction should shed light on important processes known to be regulated by both systems, including cell cycle, cancer development and progression, as well as other physiological processes. However, in order to understand the robustness and the evolutionary conservation of this interplay between the circadian clock and the TGF- $\beta$  signaling pathway, and in particular to be able to identify highly conserved (by inference, centrally important) regulatory elements within this mechanism it is necessary to investigate this interaction in other vertebrate model organisms, such as the zebrafish. The zebrafish is an ideal model to investigate the circadian clock regulation of the TGF- $\beta$  signaling pathway since it possesses directly light-entrainable peripheral circadian clocks, thus allowing the synchronization of the circadian clock without invasive transient treatments with serum or activators of the TGF- $\beta$  signaling pathways, that might complicate the interpretation of results.

### **1.10.2 Clock output regulation of the TGF- $\beta$ signaling pathway in zebrafish**

To explore the potential influence of the circadian clock on TGF- $\beta$  signaling in zebrafish, the laboratory of Dr. Yoav Gothilf (Tel Aviv, Israel), has tested whether TGF- $\beta$  signaling-related genes exhibit a circadian expression pattern in the zebrafish. Analysis of transcriptome data using whole zebrafish larvae, revealed 2,847 genes showed a circadian expression pattern [238]. Examination of this data revealed that TGF- $\beta$  signaling genes *Smad3a*, *Tgif1* and *Smad7* exhibit rhythmic expression in zebrafish larvae. *Smad3a* displays high levels at the end of the night and at the beginning of the light period, peaking at CT4, and then low levels at the beginning of the night. Instead, *Smad7* and *Tgif1* display high levels at the beginning of the night, with a peak at CT12, and low levels at the beginning of the light period. The expression of other TGF- $\beta$  related genes, such as *tgfb1a*, *tgfb2*, *tgfb3* and *smad3b* did not show significant circadian rhythmicity. 714 of these genes that exhibited a circadian expression pattern in larvae, also displayed circadian rhythms of gene expression in the adult zebrafish brain, [239]. Examination of this data revealed that while *Smad3a* exhibits a circadian expression pattern in the adult zebrafish brain, peaking at CT4, *Smad7*, *Tgif1* and other TGF- $\beta$  related genes do not exhibit such oscillations. The Gothilf lab also examined RNAseq data from the pineal gland of adult zebrafish, which is considered to play a key role in coordinating circadian rhythmicity in the entire organism [7]. The TGF- $\beta$  signaling genes *Smad3a*, *Tgif1* and *Smad7* were amongst 308

genes which exhibited a circadian expression pattern in the zebrafish pineal gland, peaking at CT2, CT10 and CT10, respectively [240]. Moreover, by whole mount ISH analysis of the spatiotemporal expression pattern, *Smad3a* mRNA exhibited a circadian expression pattern in the zebrafish larva head. This pattern persisted in DD, indicating that it is regulated by an endogenous circadian clock [240].

## **Aim of the thesis project**

In this thesis, in order to characterize the function of clock input and output pathways in zebrafish, I have tackled two main issues. The first concern the function of the *per2* clock gene, while the second issue concern the interactions between the circadian clock and TGF- $\beta$  signaling pathway in zebrafish.

1) Many questions remain regarding the role of *per2* in the circadian clock in zebrafish. During my PhD I tried to address the following specific questions:

- i. What is the role of *per2* in the mechanism underlying the direct light entrainment of peripheral clocks in zebrafish?
- ii. What is the contribution of *per2* to the regulation to tissue-specific clock-controlled gene networks in zebrafish?
- iii. Is *per2* critical for timekeeping by the FEO in zebrafish?
- iv. Does *per2* play a crucial role in the regulation of the cell cycle by light in zebrafish?

In order to answer these questions, together with the Gothilf group, we generated a new *per2* knockout (KO) zebrafish line. Specifically, using TALEN technology we introduced a specific loss of function, truncation mutation into the zebrafish *per2* locus, and we then characterized the resulting phenotype in the *per2* KO zebrafish line and derived cell lines.

2) Results from the Gothilf lab support the notion that *Smad3a* exhibits a circadian expression pattern regulated by the circadian clock in the whole larval head [240]. In order to more precisely examine the influence of TGF- $\beta$  signaling on peripheral circadian clock function, we have used our cell culture expertise to test these predictions with a pharmacological study using an *in vitro* zebrafish cell culture model.

## **2 Materials and Methods**

### **2.1 Animal experiments**

#### **2.1.1 Ethics statement**

Zebrafish handling procedures were performed in accordance with the German animal protection standards (Animal Protection Law, BGBI. I, 1934 (2010) and were approved by the Local Government of Baden-Wurtemberg, Karlsruhe, Germany (Az.: 35-9185.81/G-130/12). General license for fish maintenance and breeding: Az.:35-9185.64.

#### **2.1.2 Animals**

Wild type (WT) and corresponding *per2* knockout (KO) sibling AB strain zebrafish lines were raised at 28°C under a 14h:10h light/dark cycle from hatching. The lights turned on at 8:00, and turned off at 22:00. Normally, the fish were fed twice every day. To generate embryos, male and female zebrafish were paired in the evening, and spawning occurred the next day within one hour after lights on. For whole mount ISH, embryos were placed in 10 cm petri dishes with egg water containing methylene blue (0.3 p.p.m) and raised under LD cycles at 28 °C. For whole mount ISH, pigmentation was prevented by adding phenylthiourea (PTU) to the embryos water during the first two days of development. For locomotor activity analysis, embryos were transferred into 48 plates (one larva per well) during the fourth day of development and placed into the DanioVision observation chamber (Noldus Information Technology, the Netherlands).

#### **2.1.3 Feeding entrainment**

4-12 months old WT and *per2* ko zebrafish lines were used for the feeding entrainment experiments. The fish were maintained in transparent glass aquaria under normal 14h:10h light-dark conditions. Each aquarium had 24-25 adult fish. The fishes were fed once a day at mid-light (ML, 15:00, ZT7), with commercial flake (Preis aquaristik) by a self-feeding system. The amount of flake given to the fish was fixed at approximately 1% of the fish body weight per day. Before the feeding entrainment, we weighed the fish in a beaker with water and then subtracted the weight of the beaker only with the water. Then, we calibrated the food provided by the automatic feeders (Eheim). For this, we rotated the feeder several times (8-10) and then calculated the mean amount of food per rotation. The food was given from the middle and top of the aquaria.

#### **2.1.4 Locomotor activity recording of zebrafish adult fish**

The locomotor activity of zebrafish was recorded during the feeding entrainment. To quantify the fish behavior, two photoelectric sensors which were illuminated by an infrared source under light and dark conditions (E3Z-D67, Omron) were placed in the front of the aquarium. A sensor was placed close to the water surface, whereas another sensor was positioned towards the bottom of the aquarium. Adult zebrafish moved freely in the tanks. When the fish interrupted the diffused light beam emitted by the sensors, a computer connected with the sensors logged the number of interruptions and exported the data every 10 minutes by specialized software (DIO98USB, University of Murcia, Spain). Fish locomotor activity was analyzed and plotted by chronobiology software ActogramJ [241].

#### **2.1.5 Locomotor activity monitoring of zebrafish larvae**

For locomotor activity monitoring, Larvae were kept under LD conditions for three days as previously described [242], and on the 4th day of development they were transferred into 48-well plates (one larva/well) and placed into a DanioVision observation chamber. The inhibitor, or DMSO, were added to the water near the end of the light phase of the 5th day of development, approximately 30 minutes before lights-off, and larvae were then exposed to 12 hr light (3,400 lux): 12 hr dim light (40 lux) (LDim) cycles for 3 days, or to constant dim light, a condition in which larvae exhibit high amplitude clock-controlled rhythmic locomotor activity [243]. Live video tracking and analysis was conducted using the Ethovision 8.0 software (Noldus Information Technology). Activity was measured at  $6\pm 7$  days post fertilization under DimDim or  $6\pm 8$  days post fertilization under LDim, as the distance moved by a larva in 10 min time bins. The data is presented as a moving average (10 sliding points) for each group ( $n = 24$ / group). For the "wash out" experiment, in which inhibitor was administered and then removed, larvae were kept under LD cycles, the inhibitor was added to the larvae water during the 5th day of development. Starting on the 6th day of development larvae were kept under DimDim for 60 hours. On the morning of the 8th day of development the inhibitor was removed by washing, replaced with fresh water, and larvae were transferred into a 48 plate and placed into the DanioVision observation chamber. The larvae were re-entrained for 2 LDim cycles, and then kept under constant conditions (DimDim) for 24 hours, while locomotor activity (total distance moved by one larva during a 10 min time window) was measured using the Ethovision 8.0 software. The data is presented as a moving average (10 sliding points) for each group ( $n = 24$ /group). Fourier analysis was used to test differences in rhythmic locomotor activity using a previously described procedure

[242]–[245]. The time-dependent signal was converted into a frequency dependent signal using the Fast Fourier Transform (FFT). The extent to which the original signal of each larva is circadian was quantified by the ratio ('g-factor') of the power of the frequency that corresponds to the 24 hr period to the sum of powers of all frequencies. The higher the g-factor, the higher is the confidence that the larvae exhibit circadian locomotor activity. Differences in the g-factor distributions between the control and TGF- $\beta$  inhibitor treated groups were determined by the Kolmogorov-Smirnov test. The periods of locomotor activity rhythms were computed by the Lomb-Scargle periodogram ( $\alpha = 0.05$ ) with Actogram software [241], and statistical differences between inhibitor treated and control larvae were determined by t-test. Amplitude values were calculated as the difference between the second recorded peak in activity and the preceding trough, divided by 2, and the statistical differences between inhibitor treated and control larvae were determined by t-test. Phase values were calculated as the difference between the CT of the second recorded peak of activity, and the statistical differences between inhibitor treated and control larvae were determined by one-way ANOVA. For the “dark flash stimuli” experiment, used to observe larva mobility, larvae were placed in DanioVision during the 5th day of development and exposed to one LD cycle. During early light phase on the 6th day of development, the fish were subjected to 3 dark flashes of 10 seconds each, with 15 minutes of light interval between flashes. The data represents the average of three successive trials, which measured the average movement per second of each larvae, recorded 10 seconds before the flash, during the flash and 10 seconds after the dark flash.

### **2.1.6 Fin regeneration measurements**

Total regeneration was gauged by a percent regeneration metric. Briefly, this measurement required phase-contrast full-fin images be taken before amputation and at each time point after amputation. The full area (in pixels) of the fin clipped lobe, was quantified from the pre-amputation images for each fish using ImageJ (NIH). The new tissue area, from the new distal fin edge to the amputation plane, was also quantified. Percent regeneration for each fin at each time point was defined as: % regeneration =  $100 \times (\text{new tissue area} / \text{original fin area amputated})$ .

## **2.2 Cell culture methods**

### **2.2.1 Zebrafish cell culture establishment and maintenance**

The zebrafish WT and *per2* KO embryonic cell lines were derived from 24 dpf embryos while adult fin cell lines are derived from adult fins. To obtain the embryonic fibroblast cell lines we followed a

previously well-established protocol [134]. To establish the adult fin fibroblast cell lines, the fishes were anesthetized in tricaine 0.02% (Sigma Aldrich), then a small part of the fins were cut and washed once in PBS with 5% penicillin/streptomycin (Gibco BRL). Subsequently, the fins were washed once in ethanol 80% for 10 seconds and then were washed three times (each 5 minutes) in PBS with 5% penicillin/streptomycin (Gibco BRL). The fins were transferred to 200  $\mu$ l of 0.25% trypsin-EDTA (Gibco BRL) and shaken for around 1 minute. Finally, the fins, together with the trypsin solution were transferred in a 35 mm petri dish and incubated at 26°C in L-15 (Leibovitz-15) medium (Gibco BRL) supplemented with 15% fetal calf serum (Sigma Aldrich F7524) 100 units/ml penicillin, 100  $\mu$ g/ml streptomycin and 50 $\mu$ g/ml gentamicin (Gibco BRL). After an initial period of cell proliferation, typically the embryo and fin cultures ceased proliferation and then experienced a significant amount of cell mortality. In the case of the *per2* KO derived cell lines, this period was considerably longer than that observed for wild type control cells. Surviving cells were then maintained with medium changes until the numbers had increased sufficiently to achieve confluency. Then the cell lines were propagated every 7 to 10 days at a ratio of 1:4 by trypsinization with 0.25% trypsin-EDTA (Gibco BRL).

## **2.3 Molecular experiments**

### **2.3.1 RNA extraction**

Total RNA of zebrafish cell lines and tissues was extracted using Trizol reagent (Invitrogen) according to the manufacturer's instructions. 1ml Trizol reagent was added to individual frozen aliquots of tissue. The samples were then homogenized by passing 10 times through a 1 ml syringe with a 25G needle. After addition of 200  $\mu$ l of Chloroform, the samples were mixed violently and then centrifuged at 12000 rpm for 15 minutes at 4 °C. The supernatant was transferred to a new 1.5 ml eppendorf tube and 500  $\mu$ l of Isopropanol was added to precipitate the RNA. The RNA pellet was washed once with 75% ethanol, and then dissolved in RNase-free water (Promega) and stored in -80°C freezer. The concentrations of RNA samples were assessed with a NanoDrop ND-1000 spectrometer (PiqLab). The quality of the RNA was determined after electrophoresis on an agarose gel to visualize the integrity of the ribosomal 28S, 18S and 5S RNA bands. Total RNA was extracted from cells using Trizol reagent without homogenization. Then chloroform was added to extract the total RNA, and isopropanol was used to precipitate the RNA.

### 2.3.2 RT and Real-time PCR

The first strand cDNA synthesis of total RNA was performed according to the manufacturer's protocol (Promega). 600-1000 ng total RNA was diluted in 7 µl of RNase-free water, and to this was added 1 µl of 10x RQ1 DNase buffer (Promega), 1 µl of Dnase (Promega, 1u/1µl) and 1 µl of RNase inhibitor (Promega ,40 U/µl). The mixture was incubated at 37 °C for 30 minutes. After addition of 1 µl of EDTA (Promega) which stops the DNase reaction, the solution was incubated at 65 °C for 10 minutes. Then 1 µl of random hexamers (Sigma Aldrich, 200 ng/µl) were added and the mixture was incubated at 70 °C for 5 minutes. RT was performed by adding cDNA synthesis mix composed of 3 µl of RNase- free water, 4 µl of 5x M-MLV RT buffer (Thermo Scientific), 2 µl of dNTPs (Sigma Aldrich, 10 mM) and 1 µl of M-MLV reverse transcriptase (Thermo Scientific, 200 U/µl), and then incubating at 25 °C for 10 min and 42 °C for 60 min. The reaction was terminated by heating the sample to 70 °C for 15 min. the cDNAs were diluted 1:10 with distilled sterile water and stored at -20 °C until use. Real-time PCR was performed in a volume of 25 µl including 10 µl SYBR Green I Master Mix (Promega), 9 µl of PCR-grade water, 4 µl of RT product and 2 µl of forward and reverse primer mix (10µM) on an ABI StepOne Plus machine. The amplification cycle consisted of 1 cycle of 15min at 95 °C, 40 cycles of 15s at 95 °C and 30s at 60 °C, followed by the generation of a melting curve. The PCR primers were designed using Primer 3 and β-actin was used as a reference. The primer sequences of genes tested are listed in Table 1. The specificity of PCR reactions was checked by melting curve analysis. The critical threshold (CT) value is the PCR cycle number where the PCR growth curve crosses a defined threshold in the linear range of the reaction. Relative log<sub>2</sub> expression values are calculated from C<sub>max</sub>-CT , where C<sub>max</sub> is the maximum value of CT in tested samples.

**Table 1: RT-qPCR primers sequences**

<b>zf β-actin</b>	F: GCCTGACGGACAGGTCAT	R: ACCGCAAGATTCCATACCC
<b>zf per1b</b>	F: CCGTCAGTTTCGCTTTTCTC	R: ATGTGCAGGCTGTAGATCCC
<b>zf per2</b>	F: CTTCAACCACACCATACAGG	R: GTCTGACGGGGACGAGTCT
<b>zf clock1</b>	F: CTGGAGGATCAGCTGGGTAG	R: CACACACAGGCACAGACACA
<b>zf cry1a</b>	F: CAAACACTGCAGCAAAAACC	R: TCCGCTGTGTGTACATCCTC
<b>zf got1</b>	F: TCACACTAAACACCCCGGAA	R: GAGTTCACAGAGCCTTCAGT
<b>zf got2a</b>	F: GGAGGCTTCACAGTGGTTTG	R: AGCCATGCCTTTTACCTCCT

<b>zf asns</b>	F: AGGAGCACATCGAGTCTGAG	R: CTTGGCCAGGGTAATGCTTC
<b>zf glu1a</b>	F: GAAATGCGGGAAGATGGTGG	R: CAGTGAGTCGACGAGCATTG
<b>zf glud1b</b>	F: CAACACCCGATGCTGACAAA	R: AGCAGGTGGTAGTTGGAGTC
<b>zf gpt2l</b>	F: GGGTCCCGAGTACTCCAAAA	R: GCTTTCACATCCGCATCCAT
<b>zf impdh2</b>	F: TGCCGTCTGCTGTTTGTATC	R: CCGGAGTGAAAATGGTCTGT
<b>zf hsf2</b>	F: CCTTCTGGGCAAAGTTGAGCTG	R: GCTGCTTGTCTGTGTTTTCTGAATC
<b>zf myf6</b>	F: CAACGAAGCTTTTGACGCG	R: AACACGGCTCCTTCTCTATGACC
<b>zf hnf1a</b>	F: ATTGCCCCAAGCTCCTTTAT	R: TACTGCTGTCTGCGATCACC
<b>zf ppargc1b</b>	F: TGTCCTGTTACCTCCTTCC	R: TCCATGACACGTCTCTGAGC
<b>zf cyp1a</b>	F: AAACCAGTGGCAAGTCAACC	R: AAAACCAACACCTTCTCGCC
<b>zf smad3a</b>	F: ACCAAACCCTGTGTCTCCTG	R: GCTGTGAGGCATGGAAAGTT
<b>zf mef2a</b>	F: GGCTCTCCAGGGCTCTCTAT	R: CATTCTGGCTGGTGTTGATG
<b>zf cyclin A2</b>	F: CCAATAACTGAAGCCATAGCCTC	R: TACAAATATCTGGCTGAATCAAGC
<b>zf cyclin B1</b>	F: CCTTGATCAAAGACCTGGCT	R: ATGGCAGTGAAGAAATCCGT
<b>zf p21</b>	F: TGACATCAGCGGGTTTACAG	R: TTCTGCTGCTTTTCCTGACA
<b>zf timp3</b>	F: GCTGGGAGCATCTCTCACTG	R: CGTAGTGGCGTGAAGTGGTAG
<b>zf cox62a</b>	F: GGCAAACGTTTACCTGAAGATG	R: TCAGTGATGAGGGCCTTCA

### 2.3.3 Whole mount ISH

Samples were collected at 4 hr intervals throughout the 24 hr cycle during the 6th day of development, fixed for 24 hours in 4% paraformaldehyde and stored in 100% methanol at -20 °C. Exposure to the TGF- $\beta$  inhibitor LY-364947 at a concentration of 20 $\mu$ M began on the evening of the 5th day of development. Transcripts of Smad3a, Smad3b and Per1b mRNA were detected by whole mount ISH using digoxigenin-labelled antisense ribo-probes (DIG RNA labelling kit, Roche Diagnostics Ltd, Basel, Switzerland). Probes were produced as previously described and whole mount ISH analyses were carried out according to an established protocol [246]. Whole mount ISH signals in the larva head, expressed as optical density, were quantified using ImageJ software (National Institute of Health, Bethesda, MD, USA). The larva head area was chosen because of the higher expression of the studied genes in this region as compared to the trunk. Differences in signal intensities between treatments and sampling times were determined by two-way ANOVA. Specific comparison within

each treatment were performed using one-way ANOVA followed by Tukey's post-hoc test. Results are written as mean optical density  $\pm$  standard error.

### **2.3.4 TGF- $\beta$ inhibitors and indirect activator**

Pharmacological inhibition of TGF- $\beta$  signaling was carried out using a selective ATP-competitive inhibitor of TGF- $\beta$  type-1 activin receptor-like kinase (ALK-5), LY-364947 (L6293, Sigma, MO), or a selective inhibitor of both ALK-4 and ALK-5, SB-431542 (S4317, Sigma, MO). Both inhibitors were previously demonstrated to inhibit TGF- $\beta$ -Smad3 mediated signaling in zebrafish larvae [247]. For in vitro experiments, the inhibitors were dissolved in DMSO and added at working concentrations of 1, 5, 10 and 20  $\mu$ M to the cell culture medium, 30 minutes before lights on. For in vivo experiments, LY-364947 was dissolved in DMSO and was added to the larvae water during the evening of the 5th day of development, before lights off, at a final concentration of 20 $\mu$ M. The LY-364947 concentrations used in current experiments are higher than reported IC<sub>50</sub> values in cell-free binding assays, which are about 0.04 $\pm$ 0.1  $\mu$ M for the target of interest, TGF $\beta$ RI [248], [249]. Similar IC<sub>50</sub> values have also been reported in several previous cell-line based experiments [249]–[251]. However, multiple studies have used much higher concentrations of LY-364947 in cell-cultures, ranging from 5 $\mu$ M [252] and 10 $\mu$ M [253] to as high as 40 $\mu$ M [254]. LY-364947 has not been previously used with zebrafish PAC-2 cells, but has been widely used with zebrafish embryos, consistently at working concentrations of 30 $\pm$ 100 $\mu$ M [152], [247], [255]–[258]. Thus, concentrations that are higher than the IC<sub>50</sub> have been routinely used to disrupt TGF- $\beta$  signaling in cell and animal models. Accordingly, concentrations of 1 $\pm$ 20  $\mu$ M were used in the current study, consistent with the most commonly used concentrations in previous studies using the zebrafish model. Pharmacological induction of TGF- $\beta$  signaling was carried out using Alantolactone (SML0415, Sigma, MO), a sesquiterpene lactone which disrupts the Cripto-1/ActRII complexes, resulting in an indirect induction of activin/Smad3 signaling [259].

### **2.3.5 Constructs and real-time bioluminescence assays**

The zebrafish PAC-2 cell line stably expressing per1b::luc [260] were cultured and entrained to LD cycles as described elsewhere [124], [134]. 70 hours after entrainment, stably transfected cells were exposed to various concentrations of the TGF- $\beta$  inhibitors LY-36494 or SB-431542, or the TGF- $\beta$  indirect TGF- $\beta$  inducer, Alantolactone. Control groups were treated with DMSO. Real-time bioluminescence assays were performed and analyzed as described previously [124], [134], using an EnVision multilabel counter (Perkin Elmer). The periods of luciferase rhythms while the cells were

in DD conditions were computed by the Lomb-Scargle periodogram ( $\alpha = 0.05$ ) with Actogram software [241], and statistical differences between treated and control cells were determined by one-way ANOVA, followed by Tukey's post-hoc test. Amplitude values were calculated as the difference between the peak during the first constant dark (DD) cycle after exposure and the following trough, divided by 2, and the statistical differences between treated and control larvae were determined by one-way ANOVA, followed by Tukey's post-hoc test. Phase values were calculated as the CT in which luciferase activity reached its peak during the first DD cycle after exposure has occurred, and the statistical differences between treated and control larvae were determined by one-way ANOVA, followed by Tukey's post-hoc test.

### **2.3.6 Cell cycle analysis**

A total of  $2.5 \times 10^5$  cells of the WT and *per2* KO cell lines were seeded and maintained 3 days in darkness, then, on the 4th day the cells were trypsinized and collected in PBS with the addition of 1% FBS and 0.25 mM EDTA in PBS and centrifuged at 1200 rpm, 4 min, 4°C. The cell pellet was resuspended in methanol, incubated on ice for 20 min and centrifuged at 1200 rpm, 5 min, 4°C. After a wash in PBS, the pellet was incubated in PBS, containing RNase A (Thermo-Fisher Scientific) 100µg/mL for 20 min at RT. Propidium iodide (Sigma-Aldrich, Saint Louis, MO, USA) was then added at a concentration of 50µg/mL for 30 min at 4°C. Cell cycle analysis was performed on the BD Accuri C6 flow cytometer (BD Biosciences, San Jose, CA, USA)

### **2.3.7 Western blotting.**

Protein extracts were prepared by homogenizing samples in Laemmli buffer including a cocktail of phosphatase inhibitors 2 (Sigma). The samples were electrophoresed on an SDS polyacrylamide gel and transferred to a Hybond-P membrane (Amersham). Binding of the antibodies for Histone H3 and Phospho-histone H3 Ser10 (Cell Signaling) was visualized using the ECL detection system (Amersham Biosciences). Autoradiographic images were quantified with the aid of Scion Image software.

## **2.4 Transcriptome data mining**

Transcriptome data mining was performed on three previous transcriptome analysis experiments which were performed on whole zebrafish larvae [238], adult zebrafish brains [239], and adult zebrafish pineal glands [242].

## 2.5 Statistical analysis

One-way or two-way analysis of variance (ANOVA) followed by Sidak's and Tukey's multiple comparison tests were performed using GraphPad Prism 7.0. All the results are expressed as means  $\pm$  SD of biological or technical replicates. In the statistical tests  $p < 0.05$  was considered statistically significant. In each figure,  $p < 0.05$ ,  $p < 0.001$  and  $p < 0.0001$  are represented by \*, \*\* and \*\*\* respectively.

### 3 Results

#### 3.1 Characterization of the *per2* KO zebrafish line and the derived cell lines.

##### 3.1.1 Unaffected expression of circadian clock genes in *per2* mutant larvae.

Initially, in order to evaluate whether, during early development of zebrafish larvae, *per2* gene function is necessary to establish rhythmic circadian clock gene expression, we compared the expression patterns of the circadian core clock genes (*clock1*, *cry1a* and *per1b*) between the WT and *per2* mutant zebrafish larvae. Therefore, WT and *per2* mutant larvae were kept 4 days post-fertilization (dpf) in light-dark (LD) cycle (12h light-12h dark) conditions. On the fifth day post fertilization, total RNA was extracted from larvae collected at 6-h intervals for a total of 24 h (figure 11A). The gene expression levels were then assayed by qRT-PCR analysis (figure 11). Our results show that the rhythmic expression of all the core clock genes is conserved in *per2* mutant larvae (figure 11).

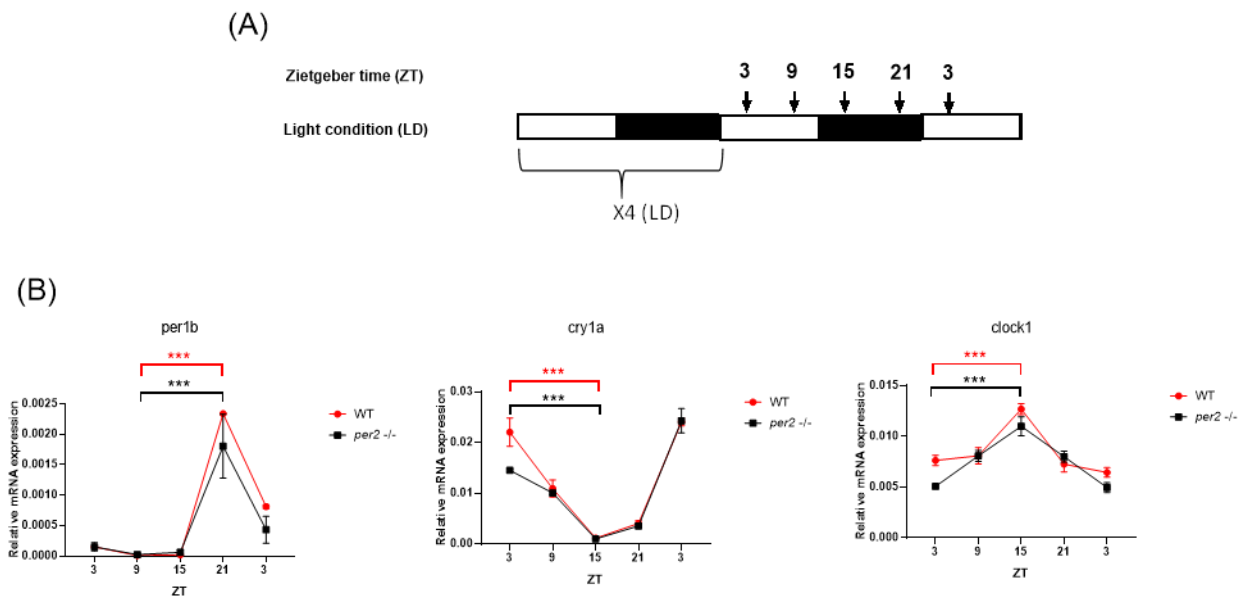


**Figure 11: Core clock gene expression in WT and *per2* KO zebrafish larvae.**

Top panel (A): schematic representation of the experimental design. The horizontal bars represent the lighting conditions before and during sampling; white boxes represent light and black boxes represent dark periods; the arrows represent the sampling times. Bottom panel (B): qRT-PCR analysis of expression levels of the circadian core clock genes (*clock1*, *cry1a*, *per1b*) in the WT and *per2* mutant larvae. Mean mRNA relative expression (n=2-3) ± SD is plotted on the y-axis, whereas *zeitgeber* time (ZT) is plotted on the x-axis. ZT0 corresponds to lights-on, ZT12 to lights-off. One-way ANOVA is applied to the data to determine the presence

of differences in gene expression over time in each genotype (table S1). In the figure are reported the levels of significance between peak and trough within the same genotype, that are calculated by post hoc analysis Tukey's test and are indicated (\*\*p < 0.01, \*p < 0.05). Acrophase (circadian peak time) of the rhythmic expression pattern of *cry1a*, *clock1* and *per1b*, were calculated, for both the genotypes, using the single cosinor procedure program (Acro.exe, version 3.5, designed by Dr. Refinetti) (table S1.1).

A possible interpretation of this result is that the regulatory role of *per2* gene is tissue-specific, rather than acting at the whole animal level. Thus, the RNA extraction of the whole-body could "hide" tissue-specific differences in core clock genes expression. Alternatively, the *per2* gene function may not be fundamental for the regulation of the core clock gene expression, at least during the first stages of the zebrafish embryo development.

### **3.1.2 Tissue-specific regulatory roles of *per2* in zebrafish peripheral tissues/organs.**

Therefore, to test the possibility that the *per2* gene may play a tissue specific role in the regulation of the circadian timing mechanism, we examined the rhythmic expression of a set of core clock genes (*cry1a*, *per2*, *clock1* and *per1b*) in brain, eyes, heart, liver, gut, muscle and fin tissues of WT and *per2* mutant zebrafish adult fish lines. WT and *per2* KO fishes were maintained in our fish facility under LD cycle (14h light-10h dark) conditions, after sacrifice all the tissues were dissected and collected for RNA extraction at 6-h intervals for a total of 24 h (figure 12A). Each sample contains tissues dissected from at least two male and two female fishes. We noticed a robust difference between the WT and the *per2* mutant adult fish in the expression of two circadian clock genes (*clock1* and *cry1a*), exclusively in heart, liver, gut and muscle tissues (figure 12B).

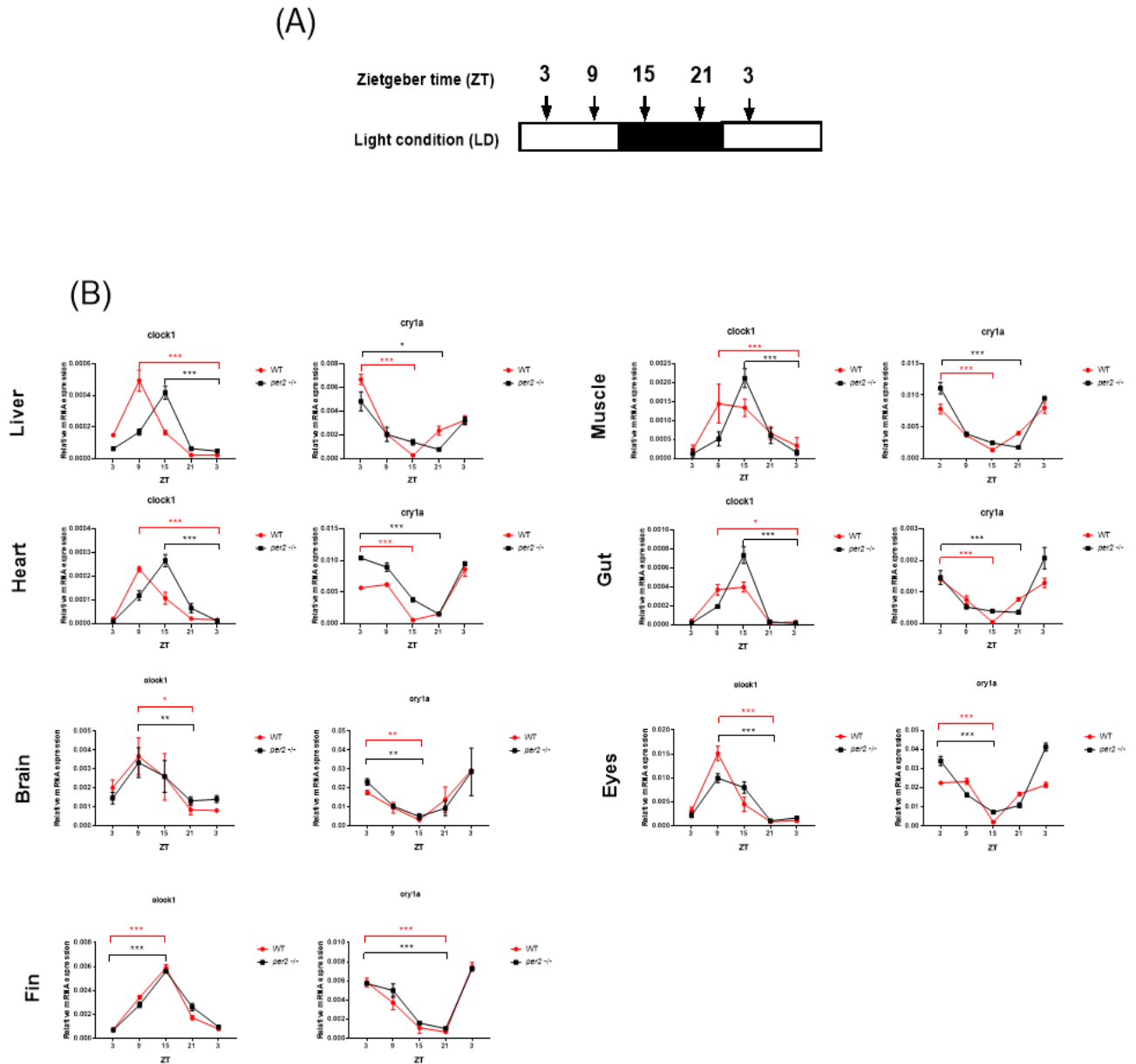


**Figure 12: Core clock gene expression in WT and *per2* KO zebrafish adult tissues.**

Top panel (A): schematic representation of the experimental design. The horizontal bars represent the lighting conditions before and during sampling; white boxes represent light and black boxes represent dark periods; the arrows represent the sampling times. Bottom panel (B): qRT-PCR analysis of expression levels of the circadian core clock genes (*clock1*, *cry1a*) in the liver, heart, gut, muscle, eyes, brain and fin tissues of WT and *per2* mutant adult fish. Mean mRNA relative expression ( $n=2-3$ )  $\pm$  SD is plotted on the y-axes, whereas *zeitgeber* time (ZT) is plotted on the x-axis. *Zietgeber* times are indicated for each sample, that contains tissues/organs from at least two male and two female fishes. ZT0 corresponds to lights-on, ZT14 to lights-off. One-way ANOVA is applied to the data to determine the presence of differences in gene expression over time in each genotype (table S2). In the figure are reported the levels of significance between peak and trough within

the same genotype, that are calculated by post hoc analysis Tukey's test and are indicated (\*\*p < 0.01, \*\*\*p < 0.001, \*\*p < 0.01, \*p < 0.05). Acrophase (circadian peak time) of the rhythmic expression pattern of *cry1a* and *clock*, were calculated for all the tissues, for both the genotypes, using the single cosinor procedure program (Acro.exe, version 3.5, designed by Dr. Refinetti) (table S1.1).

Specifically, peak level of *clock1* and the trough level of *cry1a* rhythmic expression exhibited a 6 hours phase delay in the *per2* ko heart, liver, muscle and gut compared with the corresponding wild type tissues (figure 12B). This result has several implications, first of all that the *per2* gene plays a role in shaping circadian regulation of a subset of core clock genes in a tissue specific fashion, thus impacting on the timekeeping of the physiological functions of these important peripheral organs. Moreover, it is interesting to note that rhythmic expression is affected exclusively in organs and tissues that are not peripheral in terms of the structure of the fish body and so are less exposed to light, instead a normal core clock gene expression is observed in more peripheral, light-exposed tissues, such as that in the brain, eyes and fins (figure 12B). Both the effect of direct light exposure as well as systemic signaling could be predicted to play a role in the synchronization of peripheral clocks, however to what relative extent these two signaling systems contribute to peripheral clock regulation, is not clear in fish.

### **3.1.3 Disrupted expression of circadian clock genes in *per2* mutant embryonic and adult fin primary fibroblast cell lines.**

To explore in more detail the functional contribution of Per2 to the circadian timing system, we next established cell lines from embryonic and adult fin *per2* KO and the corresponding WT sibling tissue, ideal tools to characterize core clock function in the absence of systemic signals. We noticed that the establishment of the *per2* KO cell lines was extremely slow compared with the corresponding WT siblings cell lines. Thus, while normally 1 month is required to establish both fin and embryo-derived wild type zebrafish cell lines, in the case of the *per2* KO line, this process required almost 3 months to complete. Therefore, we speculate that the slow proliferation may actually reflect part of the *per2* KO phenotype.

To analyze these cell cultures, we initially tested the expression levels of the core clock genes (*clock1*, *cry1a* and *per1b*) in the embryonic and adult fin *per2* KO and the corresponding WT sibling cell lines exposed to LD cycles. The cell lines were cultured and entrained for 3 days in LD (12h light-12h dark), then, on the fourth day, we extracted RNA at 6-h intervals for a total of consecutive 24 h. The gene expression levels were obtained by qRT-PCR analysis (figure 13).

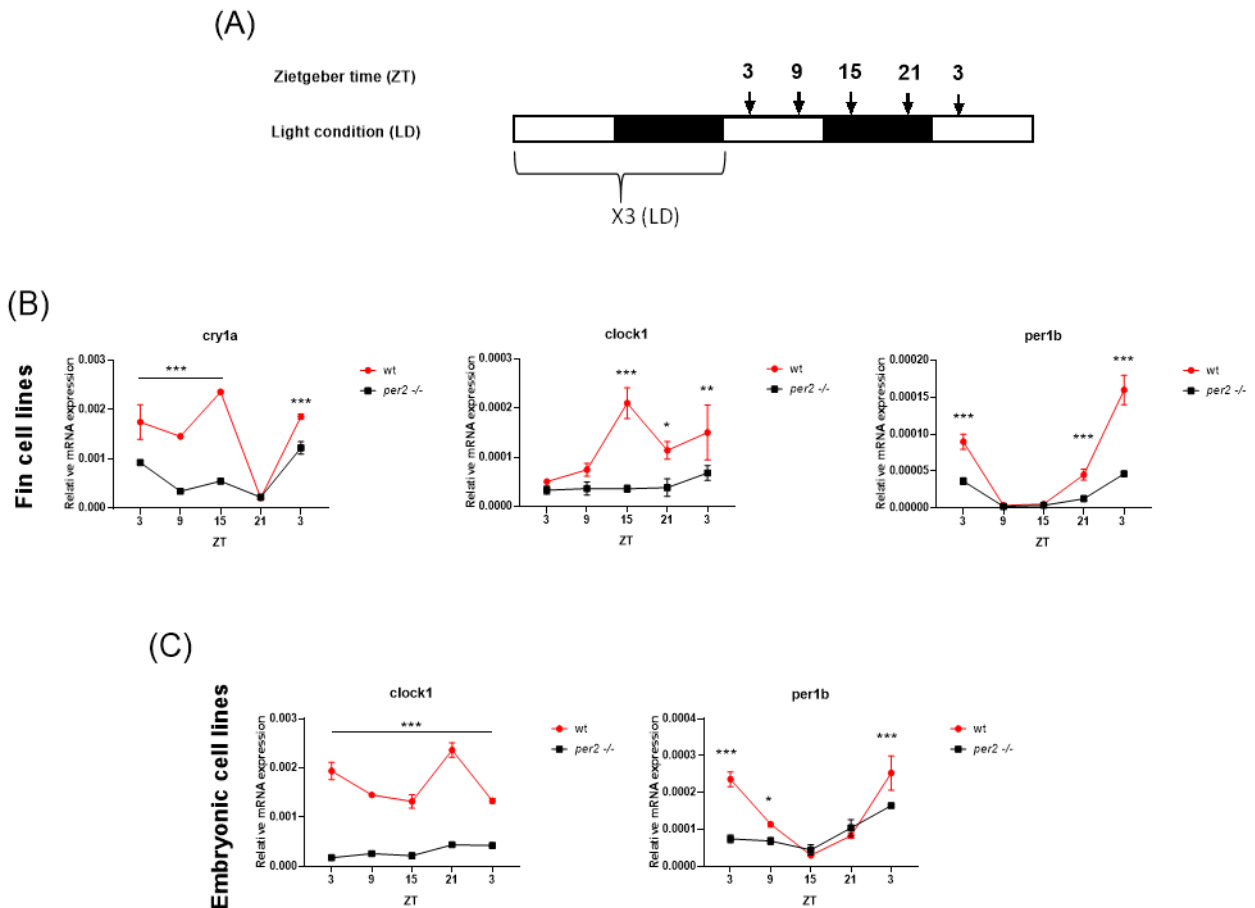


**Figure 13: Core clock gene expression in WT and *per2* mutant embryonic and adult fin primary fibroblast cell lines.**

Top panel (A): schematic representation of the experimental design. The horizontal bars represent the lighting conditions before and during sampling; white boxes represent light and black boxes represent dark periods; the arrows represent the sampling times. Bottom panel (B, C): qRT-PCR analysis of expression levels of the circadian core clock genes (*clock1*, *cry1a*, *per1b*) in WT and *per2* mutant embryonic and adult fin primary fibroblast cell lines. Mean mRNA relative expression ( $n=2-3$ )  $\pm$  SD is plotted on the y-axis, whereas *zeitgeber* time (ZT) is plotted on the x-axis. *Zietgeber* times are indicated for each sample. ZT0 corresponds to lights-on, ZT12 to lights-off. Levels of significance between the corresponding time points, of the two genotypes, are calculated by two-way ANOVA (table S3) and post hoc analysis Sidak method and are indicated (\*\* $p < 0.001$ , \*\* $p < 0.01$ , \* $p < 0.05$ ).

Results show that the rhythmic expression of all the core clock genes is absent or strongly reduced in both the *per2* KO cell types (figure 13). This striking result that contrasts with our previous *in vivo* data from embryo and adult tissue RNA analysis has alternative explanations. It may suggest that

*per2* function is required together with circulating systemic signals for maintaining circadian regulation in peripheral tissues *in vivo* but this contribution is only visualized under cell culture conditions where these systemic signals are absent. Alternatively, there may be a link between the growth properties of the cell lines and circadian clock function.

### 3.1.4 Unaffected peripheral light entrainment mechanism in cultured *per2* KO adult tissues.

In order to test these alternative explanations, we next examined the expression of the core clock genes (*clock1*, *cry1a*, and *per1b*) in different explanted cultures that were prepared using tissues from zebrafish *per2* KO and WT adult fish and were exposed to LD cycle conditions over several days. In the culture tissues, the cells are still within the context of a normal tissue structure although they will no longer experience circulating systemic factors that may serve to regulate peripheral clock function. First of all, we analyzed core clock gene expression in cultured adult zebrafish fins. WT and *per2* KO adult zebrafish fins were amputated and cultured under a cycle of 14 hours of light and 10 hours of dark, over five days. On the third day, RNA was extracted at 6-h intervals over a total sampling window of 30 h. Each sample contains fin tissues dissected from at least two male and two female fishes. The results failed to reveal any significant differences in the rhythmic expression of the core clock genes (*clock1*, *cry1a*, and *per1b*) between WT and *per2* KO zebrafish fins. Therefore, light regulated clock gene expression in zebrafish *per2* KO fin tissues, appears not to rely on *per2* function, even in the absence of systemic signals (figure 14).

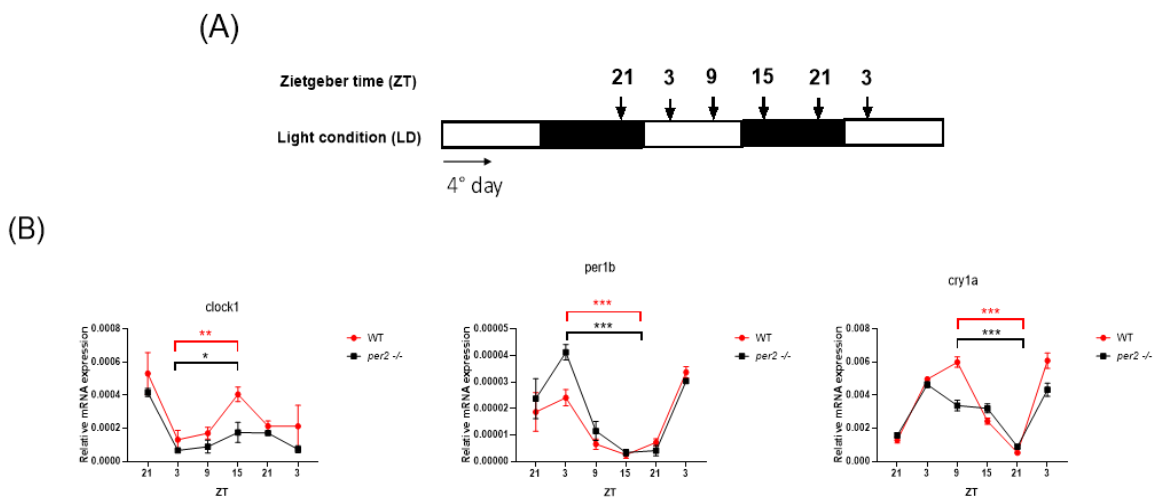


**Figure 14: Core clock gene expression in WT and *per2* mutant cultured fins.**

Top panel (A): schematic representation of the experimental design. The horizontal bars represent the lighting conditions before and during sampling; white boxes represent light and black boxes represent dark periods;

the arrows represent the sampling times. Bottom panel (B): qRT-PCR analysis of expression levels of the circadian core clock genes (*clock1*, *cry1a*, *per1b*) in the WT and *per2* mutant explanted and cultured fin tissues. Mean mRNA relative expression (n=2–3) ± SD is plotted on the y-axis, whereas *zeitgeber* time (ZT) is plotted on the x-axis. *Zietgeber* times are indicated for each sample, that contains total RNA extracted from a pool of at least 4 fins. ZT0 corresponds to lights-on, ZT14 to lights-off. One-way ANOVA is applied to the data to determine the presence of differences in gene expression over time in each genotype (table S4). Levels of significance between peak and trough within the same genotype are calculated by post hoc analysis Tukey’s test and are indicated (\*\*\*p < 0.001, \*\*p < 0.01, \*p < 0.05). Acrophase (circadian peak time) of the rhythmic expression pattern of *cry1a*, *clock1* and *per1b*, were calculated, for both the genotypes, using the single cosinor procedure program (Acro.exe, version 3.5, designed by Dr. Refinetti) (table S1.1).

Then, we performed the same experiment, but using explanted heart cultures. *In vivo*, we observed a characteristic phase shift in the rhythmic expression of *clock1* and *cry1a* genes in *per2* KO heart tissues. Therefore, we decided to evaluate *in vitro*, if the rhythmic expression of these genes was also affected in the *per2* KO cultured heart tissues. Therefore, WT and *per2* KO adult zebrafish hearts were dissected and cultured under 14 hours of light and 10 hours of dark cycle, over 3 days. On the fourth day, RNA was extracted at 6-h intervals over a total sampling window of 18 h. Each sample contains heart tissues dissected from at least two male and two female fishes. Interestingly, for the heart tissues as for the fins, the results show not differences in the rhythmic expression of the core clock genes (*clock1* and *cry1a*) between WT and *per2* KO zebrafish lines (figure 15).

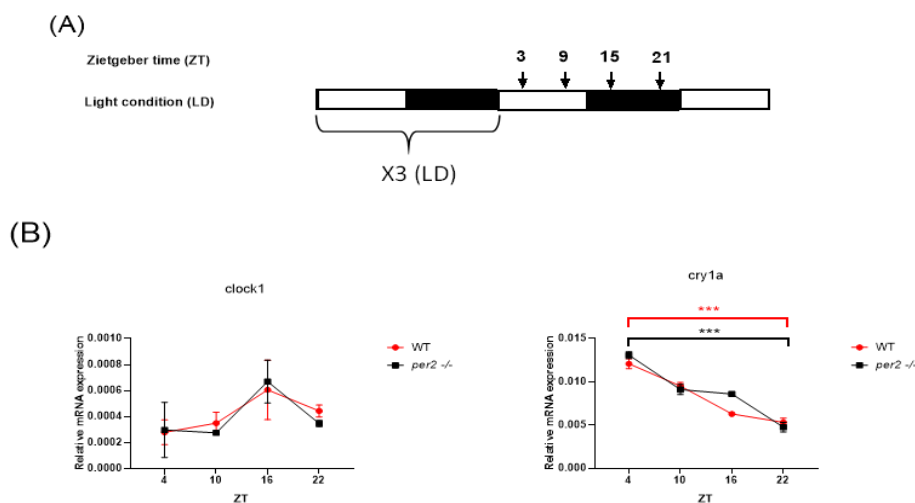


**Figure 15: Core clock gene expression in WT and *per2* KO cultured hearts.**

Top panel (A): schematic representation of the experimental design. The horizontal bars represent the lighting conditions before and during sampling; white boxes represent light and black boxes represent dark periods;

the arrows represent the sampling times. Bottom panel (B): qRT-PCR analysis of expression levels of the circadian core clock genes (*clock1*, *cry1a*) in the WT and *per2* mutant explanted and cultured heart tissues. Mean mRNA relative expression ( $n=2-3$ )  $\pm$  SD is plotted on the y-axis, whereas *zeitgeber* time (ZT) is plotted on the x-axis. *Zietgeber* times are indicated for each sample, that contains total RNA extracted from a pool of at least 4 hearts. ZT0 corresponds to lights-on, ZT14 to lights-off. One-way ANOVA is applied to the data to determine the presence of differences in gene expression over time in each genotype (table S4). Levels of significance between peak and trough within the same genotype are calculated by post hoc analysis Tukey's test and are indicated (\*\*p < 0.001, \*p < 0.01, \*p < 0.05).

This result suggests that the *per2* gene does not play a fundamental role in the direct light entrainment mechanism of the peripheral tissues in zebrafish. In the light of this result, we speculate that the abnormal clock phenotype observed in *per2* KO mutant cell lines, rather than simply resulting from the lack of circulating systemic signals, may instead reflect the cellular phenotype of the *per2* KO cells under our cell culture conditions.

### **3.1.5 *Per2* role in clock outputs: Clock-controlled gene (CCGs) expression in *per2* mutant heart, liver and muscle.**

The complexity of tissue- and day time-specific regulation of thousands of CCGs suggests that the circadian clock regulation could have a differential impact on the physiology of individual peripheral tissues. Moreover, in zebrafish we have shown that the *per2* gene plays an important role in maintaining circadian regulation of some of the main core clock genes in the zebrafish heart, liver and muscle tissues. Therefore, we performed a gene expression analysis of some putative CCGs in *per2* KO zebrafish heart, liver and muscle, in order to evaluate the possible impact of *per2* mutation on zebrafish cardiac, hepatic and skeletal muscle physiology.

For the heart, we examined the expression of (i) *p21*, a cell cycle regulator that shows a clock controlled gene expression in cell lines and during larvae development in zebrafish [209]; (ii) *mef2a*, a clock controlled transcription factor involved in the heart development and myofibril assembly processes in zebrafish [261], [262]; (iii) *timp3*, an inhibitor of the matrix metalloproteinases, a group of peptidases involved in degradation of the extracellular matrix, that was identified as being circadian clock regulated in the mouse heart [263]; (iv) *cox62a*, the nuclear-encoded polypeptide chains of cytochrome c oxidase, the terminal oxidase in mitochondrial electron transport, that shows circadian modulation in the mouse heart [264]; (v) *smad3a*, a TGF- $\beta$  signaling-related gene, exhibited a circadian expression pattern throughout the brain of zebrafish larvae [240] and in human cell lines



ZT0 corresponds to lights-on, ZT14 to lights-off. Levels of significance between the corresponding time points, of the two genotypes, are calculated by two-way ANOVA (table S5) and post hoc analysis Sidak method and are indicated (\*\*\*p < 0.001, \*\*p < 0.01, \*p < 0.05).

We then analyzed in our liver samples, the expression of (i) *cyp1a*, a gene involved in detoxification process in liver, that show a circadian expression in liver tissue in zebrafish [266]; (ii) *ppargc1b*, a gene that encode for a transcriptional coactivator that regulates multiple aspects of cellular energy metabolism, including mitochondrial biogenesis, hepatic gluconeogenesis, and  $\beta$ -oxidation of fatty acids; *ppargc1b* mRNA levels are increased in both type-1 and type-2 diabetes and may contribute to elevated hepatic glucose production in diabetic states [267]; moreover, this gene shows a circadian expression in zebrafish larvae [238]; (iii) *hnf1a*, a gene highly expressed in the liver and involved in the regulation of the expression of several liver-specific genes [268]; mutations in the *hnf1a* gene have been known to cause diabetes; moreover, this gene exhibited a circadian expression pattern in zebrafish larvae [238]; (iv) *impdh2*, a gene that show a clock controlled expression in zebrafish liver, encoding a rate-limiting enzyme in de novo purine synthesis [238].

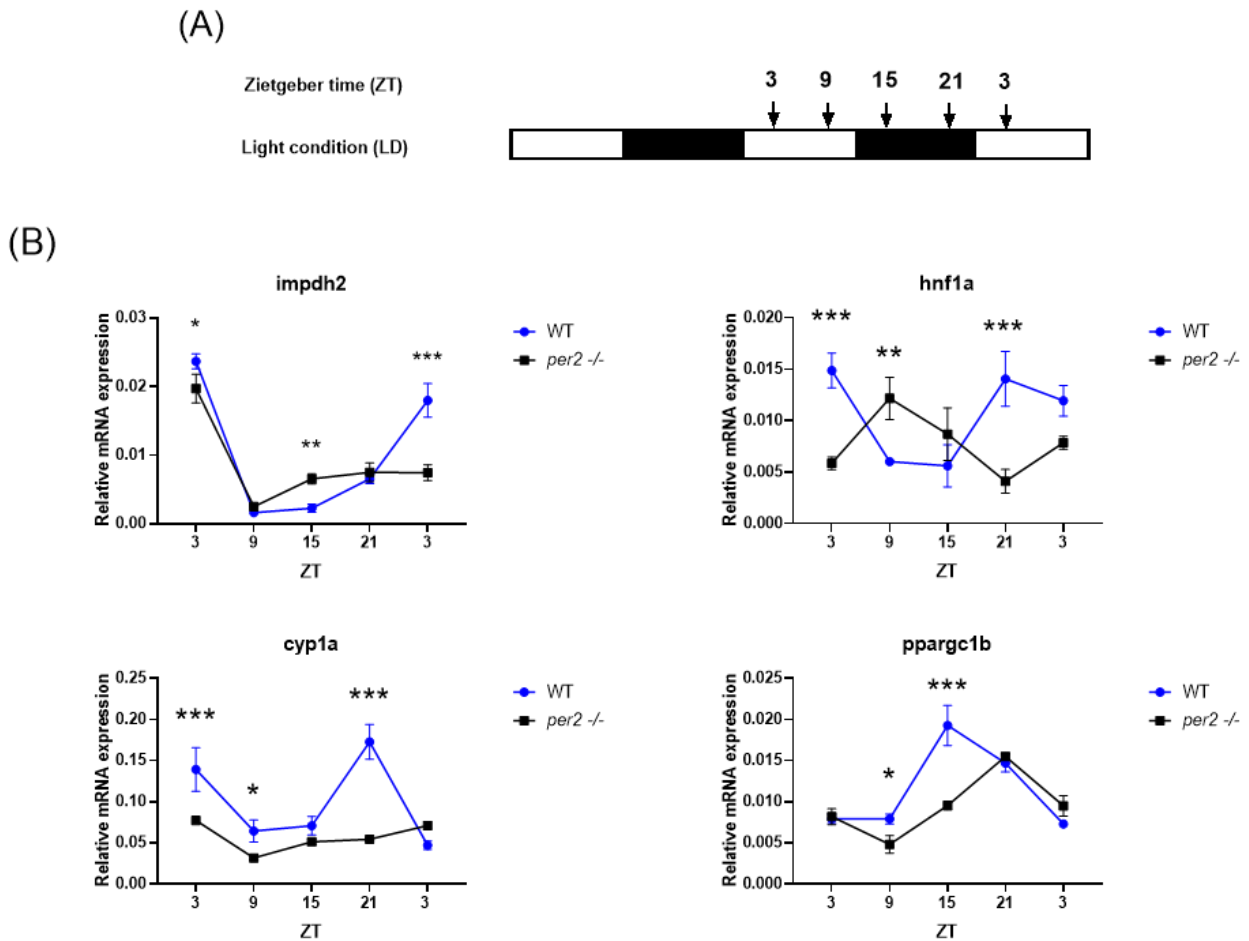


**Figure 17: Clock-controlled gene (CCGs) expression in WT and *per2* mutant zebrafish liver tissues.**

Top panel (A): schematic representation of the experimental design. The horizontal bars represent the lighting conditions before and during sampling; white boxes represent light and black boxes represent dark periods; the arrows represent the sampling times. Bottom panel (B): qRT-PCR analysis of expression levels of the four CCGs (*cyp1a*, *ppargc1b*, *hnf1a* and *impdh2*) in WT and *per2* KO liver tissues. Mean mRNA relative expression ( $n=2-3$ )  $\pm$  SD is plotted on the y-axis, whereas *zeitgeber* time (ZT) is plotted on the x-axis. *Zietgeber* times are indicated for each sample, that contains total RNA extracted from a pool of at least 4 livers. ZT0 corresponds to lights-on, ZT14 to lights-off. Levels of significance between the corresponding time points, of the two genotypes, are calculated by two-way ANOVA (table S6) and post hoc analysis Sidak method and are indicated (\*\*\* $p < 0.001$ , \*\* $p < 0.01$ , \* $p < 0.05$ ).

As shown in figure 17, the *cyp1a*, *ppargc1b* and *hnf1a* genes exhibited an altered circadian expression pattern in the *per2* KO liver tissue; for example, *cyp1a* show a general reduction of the expression levels in particular at the peak of expression; moreover, *ppargc1b* and *hnf1a* exhibit a phase delay of the rhythmic profile of 6 and 12 h respectively. On the contrary, the *impdh2* gene expression did not

appear to be strongly affected in the *per2* KO liver. These results suggest a gene-specific involvement of *per2* gene function in the regulation of the liver and heart physiology; in particular, in the liver, the *per2* gene function seems to be limited to the circadian regulation of specific pathways, instead of having a broad-spectrum impact as observed in the heart tissues

Subsequently, based on previous work [269] in which the expression of certain genes encoding key or rate-limiting enzymes involved in the biosynthetic pathways for non-essential amino acids was shown to be clock-controlled in zebrafish liver tissues, we chose to verify if the circadian expression of these genes was affected in the *per2* KO liver tissues. The metabolic pathway genes tested included *got1* and *got2a* (glutamic-oxaloacetic transaminase 1, 2a) linked to aspartate (Asp) biosynthesis pathway, *asns* (asparagine synthetase) mediating asparagine (Asn) production, *glud1b* (glutamate dehydrogenase 1b) for glutamate (Glu) synthesis, *glu1a* (glutamine synthetase 1a) catalyzing glutamine (Gln) formation and *gpt2l* (glutamic pyruvate transaminase 2, like) involved in alanine (Ala) biosynthetic reaction. As shown in figure 18, the cyclic expression of *got1*, *got2a*, *asns*, *glud1b* and *gpt2l*, in the *per2* KO liver, is affected. Specifically, *asns* shows a decrease of the peak amplitude level, *got1* and *got2a* exhibit an attenuated rhythmic expression, with the same phase shift of approximately 6 hours (as observed for core clock gene expression in the same tissue), *glud1b* show a phase delay of the rhythmic profile of 6h and *gpt2l* presented a reduction of the peak amplitude level. Instead, the rhythmic expression of *glu1a* appeared to be unaffected in the *per2* KO compared with the wild type control liver. It should be emphasized, that all the genes, except *asns*, retain a high level of expression, despite changes in the rhythmic pattern of expression.

Finally, we tested the gene expression of CCGs in the *per2* KO skeletal muscle. In particular, based on a previous study that identified putative clock-controlled genes in skeletal muscle of the zebrafish [63], [238], we tested the expression of *myf6*, *hsf2*, *igfbp3*, *igfbp5b*, *smad3a* and *mef2a*.

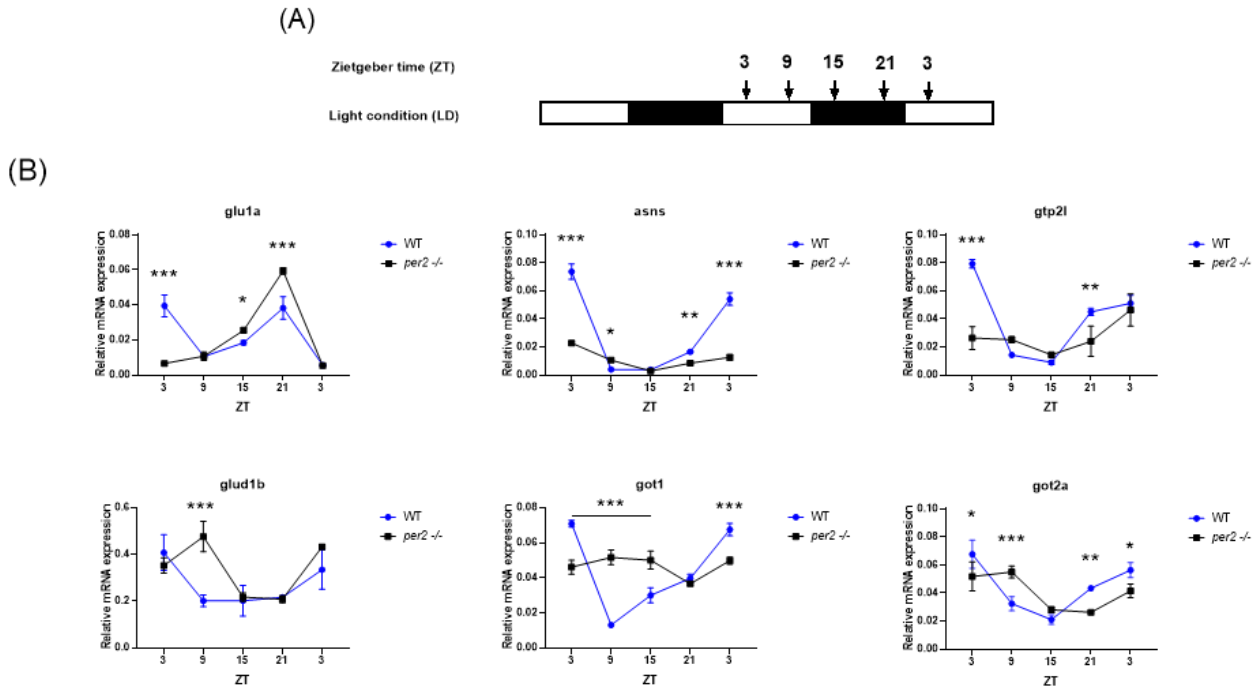


**Figure 18: Clock-controlled gene (CCGs) expression of genes encoding key or rate-limiting enzymes in non-essential amino acid pathways in WT and *per2* mutant liver tissues.**

Top panel (A): schematic representation of the experimental design. The horizontal bars represent the lighting conditions before and during sampling; white boxes represent light and black boxes represent dark periods; the arrows represent the sampling times. Bottom panel (B): qRT-PCR analysis of expression levels of the six CCGs (*got1*, *got2a*, *asns*, *glu1a*, *glud1b* and *gtp2l*) in WT and *per2* KO liver tissues. Mean mRNA relative expression ( $n=2-3$ )  $\pm$  SD is plotted on the y-axis, whereas *zeitgeber* time (ZT) is plotted on the x-axis. *Zietgeber* times are indicated for each sample, that contains total RNA extracted from a pool of at least 4 livers. ZT0 corresponds to lights-on, ZT14 to lights-off. Levels of significance between the corresponding time points, of the two genotypes, are calculated by two-way ANOVA (table S7) and post hoc analysis Sidak method and are indicated (\*\* $p < 0.001$ , \*\* $p < 0.01$ , \* $p < 0.05$ ).

However, only *myf6* and *hsf2* exhibited an expression with a clear circadian rhythmicity in the WT skeletal muscle (figure 19). The *Hsf2* gene encodes a chaperone transcriptional regulator that binds specifically to the heat-shock element in order to induces heat-shock response genes expression under conditions of heat or other stresses. The rhythmic expression of the *hsf2* gene was previously described in the pineal tissue of chicken [270], zebrafish skeletal muscle [271] and larvae [189]. The role of *hsf2* as a clock-controlled gene has been associated with the activation of specific stress-response factors in response to light [270]. *Myf6* protein belongs to a class of helix-loop-helix

transcription factors called Myogenic regulatory factors (MRFs) that play a pivotal role in myogenesis [272], [273]. *Myf6* play an important role in muscle fiber alignment in zebrafish embryos [274] and a circadian expression pattern of *myf6* gene was reported previously in skeletal muscle of zebrafish [271].

As shown in figure 19, both the *hsf2* and *myf6* genes show abnormal rhythmic expression in the *per2* KO skeletal muscle tissues. In particular, *myf6* shows a phase delay of 6 hours that matches the phase shift observed in the expression pattern of the core clock genes *cry1a* and *clock1*. Instead, *hsf2* exhibits a robust reduction of the peak expression level.

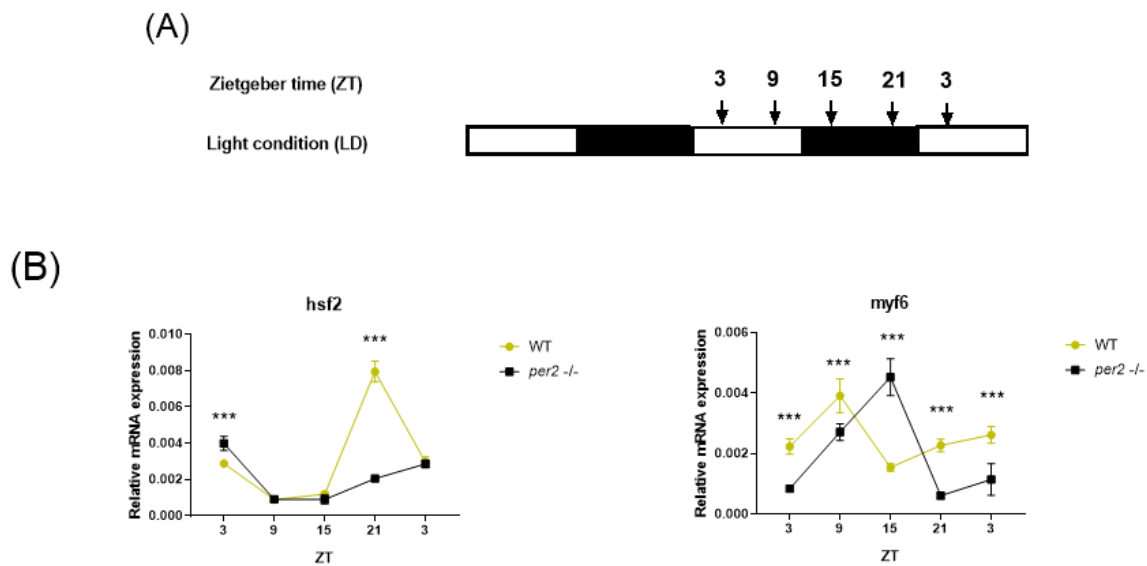


**Figure 19: Clock-controlled gene (CCGs) expression in WT and *per2* mutant zebrafish skeletal muscle tissues.**

Top panel (A): schematic representation of the experimental design. The horizontal bars represent the lighting conditions before and during sampling; white boxes represent light and black boxes represent dark periods; the arrows represent the sampling times. Bottom panel (B): qRT-PCR analysis of expression levels of the CCGs (*myf6* and *hsf2*) in WT and *per2* KO skeletal muscle tissues. Mean mRNA relative expression (n=2–3) ± SD is plotted on the y-axes, whereas *zeitgeber* time (ZT) is plotted on the x-axis. *Zeitgeber* times are indicated for each sample, that contains total RNA extracted from a pool of skeletal muscle tissues dissected from at least 4 different fishes. ZT0 corresponds to lights-on, ZT14 to lights-off. Levels of significance between the corresponding time points, of the two genotypes, are calculated by two-way ANOVA (table S8) and post hoc analysis Sidak method and are indicated (\*\*\*)p < 0.001, (\*\*p < 0.01, (\*p < 0.05).

### 3.1.6 *Per2* role in clock outputs: Locomotor activity

In collaboration with the Gothilf lab, we also characterized the phenotype of the *per2* KO larvae, using a locomotor activity – based assay (Figure 20)

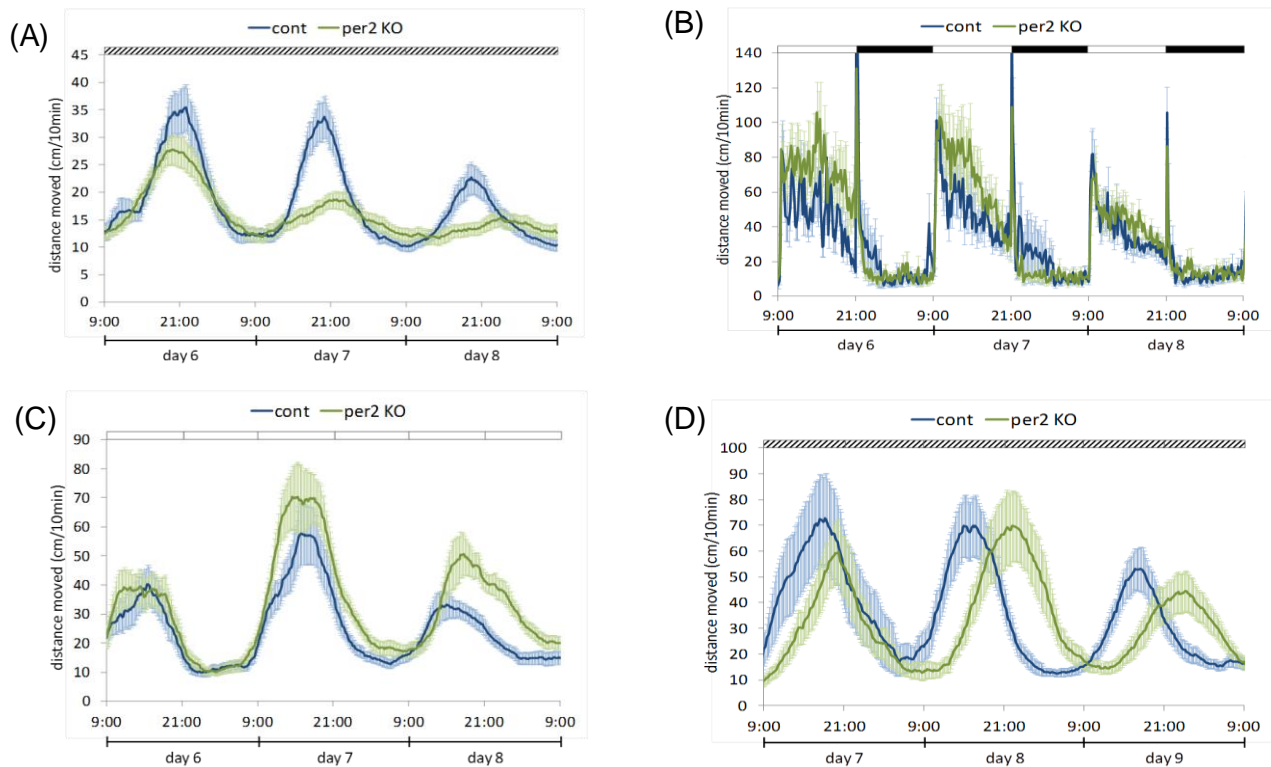


**Figure 20: Locomotor activity – based assay of the *per2* KO and WT larvae.**

(A) The locomotor activity of 6–8 days post-fertilization wild type and *per2* KO larvae under constant dim light. Larvae were kept in constant darkness and entrained by 3-h light pulse on day 5. (B) The locomotor activity of 6–8 days post-fertilization wild type and *per2* KO larvae under light-dark cycles. Larvae were kept under light-dark cycles for 5 days before the locomotor activity recording. (C) The locomotor activity of 6–8 days post-fertilization wild type and *per2* KO larvae under constant light. Larvae were kept under light-dark cycles for 5 days and then transferred to constant light. (D) The locomotor activity of 7–9 days post-fertilization wild type and *per2* KO larvae under constant dim light. Larvae were kept under light-dark cycles for 3 days and light-dim light cycles for 2 days, and then transferred to constant dim light. The horizontal bars represent the light conditions during recording: white boxes represent light, black boxes represent dark and dashed boxes represent dim light. The average distance moved (cm/10 min) is plotted on the y-axis and *zeitgeber* time (ZT) is plotted on the x-axis. Error bars stand for SE (n=24), (Gothilf lab has not yet provided statistical data analysis).

Both the WT and *per2* KO larvae, kept in constant darkness and entrained by 3-h light pulse, exhibited rhythmic locomotor activity under constant dim light conditions (figure 20A). Nevertheless, *per2* KO larvae showed a significantly lower amplitude of activity and a longer period. These results are similar to previous results obtained for *per2* knock-down in zebrafish larvae [243]. Next, WT and *per2* KO larvae locomotor activity were exposed until 5 dpf to a daily LD cycle and then behavior was measured from the 6th to the 8th dpf of LD cycle exposure (figure 20B). In this case, the *per2* KO larvae showed slightly higher locomotor activity during the light phase and a more rapid shift to a state of inactivity during the dark phase, with respect to the WT line. WT and *per2* KO larvae locomotor activity was also assayed after entrainment for 5 days under LD cycle conditions, but then assayed under constant light conditions (figure 20C). Under constant light conditions, the *per2* KO larvae exhibited a slightly higher locomotor activity during the subjective day, and a slightly longer period, with respect to the WT larvae. Finally, we measured the locomotor activity of the WT and *per2* KO larvae under constant dim light conditions (figure 20D). The larvae locomotor activity was previously entrained by exposure to light-dark cycles for 3 days and light-dim light cycles for 2 days. In this case, *Per2* KO larvae show a major phase shift and lengthening of the period of the rhythmic locomotor activity, under dim light conditions, compared to the WT larvae.

These results underline that the *per2* gene plays a crucial role to sustaining the synchronization of circadian rhythmic locomotor activity of the zebrafish larvae in the absence of the light signal (figure 20A, D). The results are somewhat consistent with the core clock gene expression analysis carried out on the different *per2* KO organs and tissues, where we observed significant differences in the rhythmic expression of the core clock genes (*clock1* and *cry1a*), exclusively in organs and the tissues experiencing lower levels of light exposure.

### **3.1.7 Role of *Per2* in clock outputs: food anticipatory activity (FAA) in zebrafish.**

Given the potential role for the *per2* gene in FEO function, we next decided to evaluate if FAA was affected in the *per2* KO zebrafish line. Therefore, the *per2* KO and WT adult zebrafish lines were maintained (25 fish/aquarium), for 18 days, under a cycle of 14 hours of light and 10 hours of dark and fed once a day at a fixed time point, in the middle of the light phase (ZT7) (LD + food), then fish were transferred to DD (darkness) and scheduled feeding was maintained (DD + food) for 7 days, and they were finally kept under DD and deprived of food (LL + fasting) for another 3,5 days. The locomotor activity was measured continuously, by means of infrared photocells, one placed at the aquarium wall 20 cm from the bottom and 5 cm from the water surface (surface photocell) and another

one placed at the aquarium wall 5 cm from the bottom and 20 cm from the water surface (deep photocell). The number of light-beam interruptions was counted and stored every 10 min by a computer connected to the photocells. A representative actogram for *per2* KO and WT zebrafish line is represented (figure 21A, F). Chi-square periodogram analysis (figure 21C, E, H, L) and mean waveforms of locomotor activity (figure 21 B, D, G, I) are reported for the LD + food and DD + food conditions in the WT (figure 21B, C, D, E) and *per2* KO (figure 21G, H, I, L) actogram. The actogram and the corresponding mean waveforms show that *per2* KO zebrafish line displayed diurnal activity and FAA under an LD cycle when feeding was restricted to a fixed time of the day. However, according to the mean waveform analysis, the *per2* KO has an activity pattern slightly different compared to the WT. Indeed, the FAA in the *per2* KO line starts around 1 h before the feeding time; instead, in the WT line, the FAA displays around 2-3 hours before the feeding time (Figure 21 B, G). However, the period ( $\tau$ ) of activity rhythms was 24 h (1440 minutes) in both the *per2* KO and WT lines (Figure 21 H, C). Therefore, we could conclude that *per2* gene function has a weak impact, under LD + restricted food conditions, on FEO timekeeping in zebrafish.

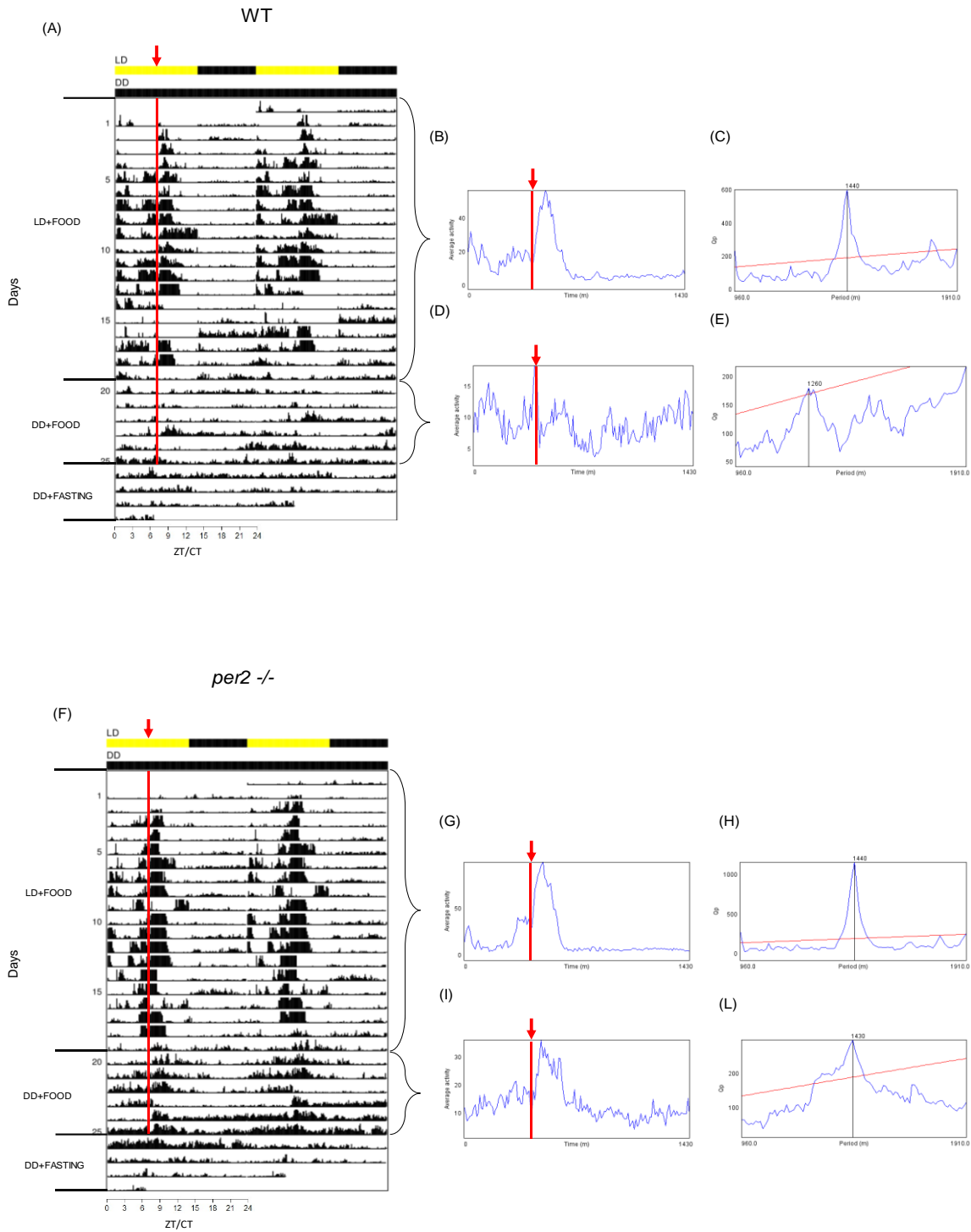


**Figure 21: Locomotor activity of *per2* KO and WT zebrafish adult lines under different light/feeding conditions.**

A representative actogram for *per2* KO (F) and WT (A) zebrafish line is represented. Fish were maintained under an LD cycle and scheduled feeding (LD+ food), then fish were transferred to DD and scheduled feeding was maintained (DD + food), and they were finally kept under DD and deprived of food (DD+ fasting).

Mealtime is indicated by the red arrow at the top of the actogram and the red line that cross the actogram from the 1th to 26th day. For convenient visualization, the data have been double plotted (48 h); the y-axis progresses in single days, with each day being plotted twice (day 1 on the right side is repeated on day 2 on the left side). The locomotor activity was measured continuously by infrared light beam-based detectors. The bars above each actogram represent the light regime; yellow and black bars represent light and dark, respectively, during the LD stage of the experiment, black bar represents dark during the DD stage of the experiment. Chi-square periodogram analysis (confidence level, 95%) for (LD+ food) and (DD + food) stages of the experiment are also shown in the actogram. The periodogram indicates the percentage of variance (Qp) of the rhythm explained by each analyzed period within a range of 960 to 1910 minutes. The highest percentage is associated with the real value of the period ( $\tau$ ). The horizontal line represents the threshold of significance, set at  $p < 0.05$  (C, E, H, L) Mean waveforms of locomotor activity is reported for each actogram. Each point has been calculated as the mean from 10-min binned data across all the experimental days for (LD + food) and (DD + food) stages of the experiment. The red line and arrow indicate the feeding time (ZT7) (B, D, G, I).

However, this does not exclude the involvement of elements of the light cycle regulated oscillator, such as *cry1a* in the setting of the timing of FAA. Therefore, in order to verify if the FAA is still conserved in the *per2* KO line in the absence of a photic signal, the fish were transferred to constant darkness and scheduled feeding was maintained (DD + food). During this experiment, the *per2* KO line continued to exhibit a free running rhythm of rhythmic activity with a period length ( $\tau$ ) of 23.83 h (1430 minutes). Curiously, the WT line shows a weak level of locomotor activity under DD + restricted feeding conditions, which reflects a shorter period (1290 minutes) with respect to the *per2* KO line. Finally, we measured the WT and *per2* KO locomotor activity under DD in order to verify the persistence of the food-entrained rhythm in the *per2* KO line. For both the WT and *per2* KO lines, the waveforms do not show a clear rhythmic pattern; possibly related to the low levels of activity, the short duration of this part of the experiment (3.5 days) and the low numbers of fish analyzed.

### **3.1.8 *Per2* function in clock outputs: circadian regulation of the cell cycle in zebrafish.**

#### **3.1.8.1 Affected cell cycle clock-controlled gene expression *per2* KO adult fin tissues.**

Disrupting circadian rhythms has been shown to have an impact on cell cycle *in vivo*. For example, in *Cry* double knockout mice, liver regeneration proceeds more slowly than normal, most likely because of constitutive upregulation of *Wee1*, a checkpoint kinase [75]. Moreover, *Per2* knockout mice shows elevated levels of *c-Myc* (a proliferative gene) and reduced *P53* (antiproliferative) expression concomitant with increased  $\gamma$ -irradiation induced rates of cell proliferation and lymphoma [166]. Therefore, in order to test whether *per2* gene function was also involved in the circadian

regulation of the cell cycle in zebrafish, we tested the gene expression of a subset of clock-controlled cell cycle regulators *p21*, *cyclin B1* and *cyclin A2*, in the *per2* KO zebrafish adult fin tissues. *P21* is a cell cycle inhibitor that play a key role at the level of G1/S cell cycle checkpoint, while *cyclin B1* and *cyclin A2* are both involved in the cell cycle progression through the G2/M cell cycle checkpoint. WT and *per2* mutant fishes were kept in LD cycle (14h light-10h dark) and fins were amputated and collected for RNA extraction at 6-h intervals for a total of consecutive 24 h. Each sample contains fins from at least two female fish and two male fish.

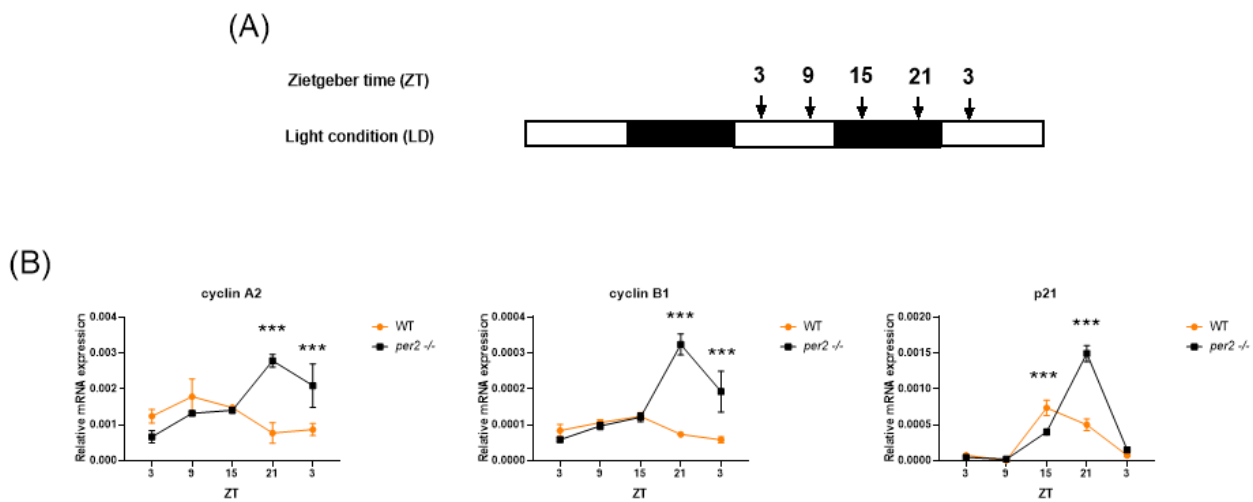


**Figure 22: Clock-controlled gene expression of the cell cycle regulators (*cyclin A2*, *cyclin B1* and *p21*) in adult fin tissues of WT and *per2* mutant fish.**

Top panel (A): schematic representation of the experimental design. The horizontal bars represent the lighting conditions before and during sampling; white boxes represent light and black boxes represent dark periods; the arrows represent the sampling times. Bottom panel (B): qRT-PCR analysis of expression levels of some cell cycle CCGs (*cyclin A2*, *cyclin B1* and *p21*) in adult fin tissues of WT and *per2* mutant fishes. Mean mRNA relative expression (n=2–3) ± SD is plotted on the y-axis, whereas *zeitgeber* time (ZT) is plotted on the x-axis. *Zeitgeber* times are indicated for each sample, that contains total RNA extracted from a pool of at least 4 fins. ZT0 corresponds to lights-on, ZT14 to lights-off. Levels of significance between the corresponding time points, of the two genotypes, are calculated by two-way ANOVA (table S9) and post hoc analysis Sidak method and are indicated (\*\*\*p < 0.001, \*\*p < 0.01, \*p < 0.05).

The results revealed that the rhythmic expression in *per2* ko zebrafish adult fins is strongly affected for all the cell cycle genes, with a phase shift of 6h for *p21* and *cyclin B1* and 12 h shift for *cyclin A2* (figure 22). Moreover, all genes show an increase of the peak expression level in the *per2* KO fins. It is interesting to note that in the *per2* KO fin tissue, the *p21* gene exhibited a rhythmic expression

pattern similar to that of *cyclin A2* and *cyclin B1*, although these genes regulate the passage through different cell cycle checkpoints, thus suggesting that the cell cycle progression in the caudal fin tissues could be affected. In general, we can conclude that *per2* gene function impacts on the rhythmic expression of key cell cycle regulators in the highly proliferative fin tissue.

### **3.1.8.2 Clock-controlled cell cycle gene expression in *per2* KO adult fin and embryonic fibroblast cell lines.**

Based on the previous results we next tested whether the rhythmic expression of *p21*, *cyclin A2* and *cyclin B1* was also affected in the *per2* KO fibroblast cell lines. WT and *per2* KO embryonic and adult fin cell lines were cultured for 3 days in LD (12h light-12h dark), then on the fourth day, RNA was extracted at 6-h intervals over a total sampling window of 24 h.

The rhythmic expression of *p21*, *cyclin A2* and *cyclin B1* is strongly affected in the *per2* KO cell lines, with a significant reduction of the basal level of expression, of all these cell cycle regulators, in the embryonic cell lines (figure 23). In the *per2* KO adult fin cell line, the expression level of *p21* is much higher than WT, with a possible 6h phase delay of the rhythmic profile (figure 23). This latter result is consistent with the *p21* gene expression pattern observed in the *per2* KO fin tissue (figure 22B). In general, this different gene expression pattern of *p21*, in different cell lines, points to cell type-specific modulation of cell cycle by *per2* in zebrafish. In contrast, the expression level of *cyclin A2* and *cyclin B1* in the *per2* KO adult fin cell lines are comparable to the WT.

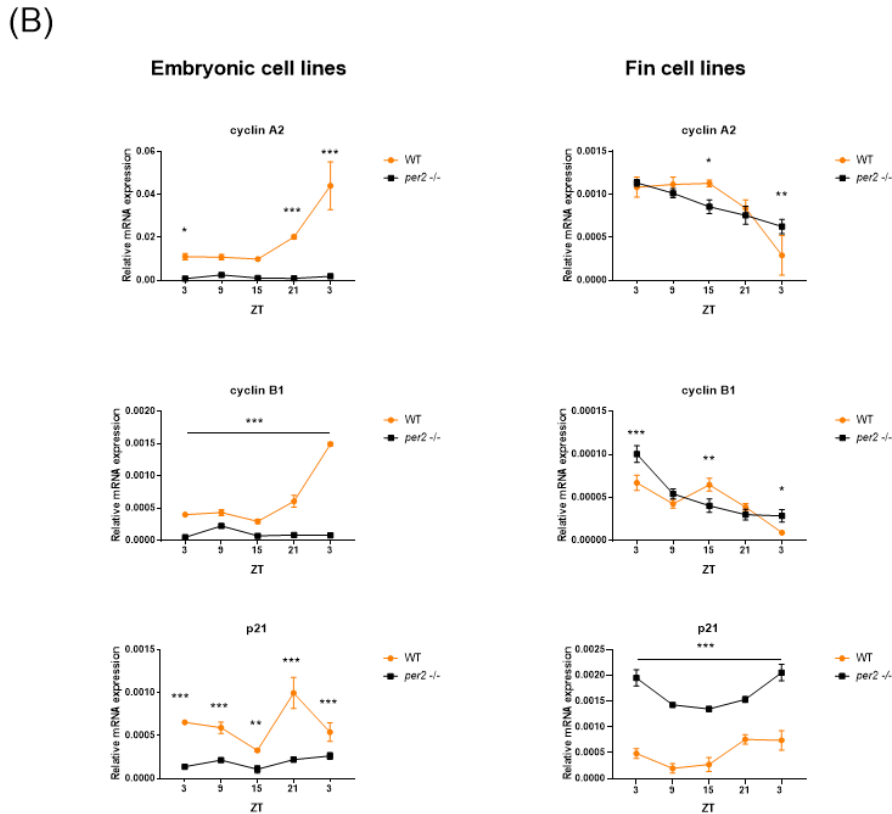
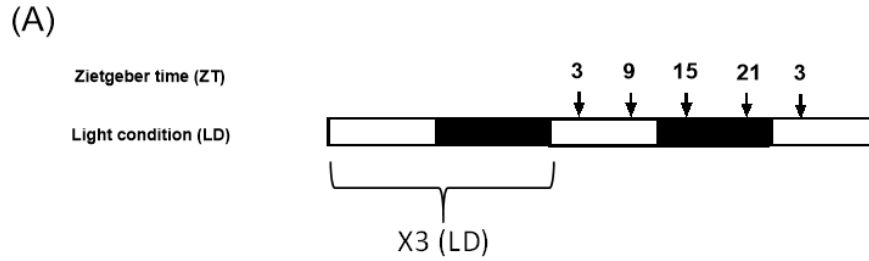


**Figure 23: Clock-controlled gene expression of *p21* in WT and *per2* mutant adult fin and embryonic fibroblast cell lines.**

Top panel (A): schematic representation of the experimental design. The horizontal bars represent the lighting conditions before and during sampling; white boxes represent light and black boxes represent dark periods; the arrows represent the sampling times. Bottom panel (B): qRT-PCR analysis of expression levels of *p21*, *cyclin A2* and *cyclin B1* genes in embryonic and adult fin WT and *per2* KO cell lines. Mean mRNA relative expression ( $n=2-3$ )  $\pm$  SD is plotted on the y-axis, whereas *zeitgeber* time (ZT) is plotted on the x-axis. *Zietgeber* times are indicated for each sample. ZT0 corresponds to lights-on, ZT14 to lights-off. Levels of significance between the corresponding time points, of the two genotypes, are calculated by two-way ANOVA (table S10) and post hoc analysis Sidak method and are indicated (\*\*\* $p < 0.001$ , \*\* $p < 0.01$ , \* $p < 0.05$ ).

### 3.1.8.3 Circadian pattern of M phase progression in *per2* KO adult fin tissues.

Previously, it has been shown that M phase progression, in zebrafish adult fin tissues, exhibits a light-entrained circadian clock regulation [210]. Therefore, we tested whether the photic entrainment of rhythmic M phase is affected in the *per2* KO zebrafish adult fin tissues. We used a western blot assay to quantify levels of the phospho-H3 protein, a marker for mitosis, in the whole fin protein extracts of the WT and *per2* KO zebrafish line. The fishes were previously maintained under an LD cycle (14h light-10h dark) and whole fin protein extracts were prepared from pools of at least 4 fins at 6-h intervals for over a 24 h sampling period.

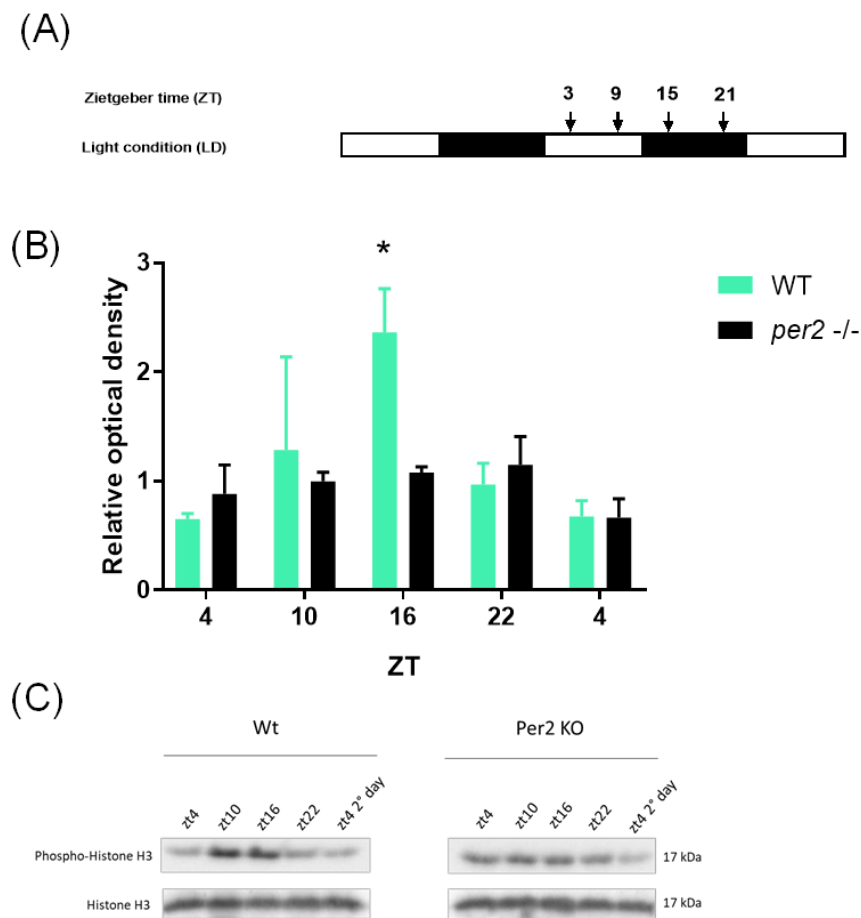


**Figure 24: Western blot analysis and quantification of the phospho-H3 protein in fin whole protein extracts of the WT and *per2* KO zebrafish line.**

Top panel (A): schematic representation of the experimental design. The horizontal bars represent the lighting conditions before and during sampling; white boxes represent light and black boxes represent dark periods; the arrows represent the sampling times. Middle panel (B): Western blot analysis and quantification of Phospho-Histone H3 (P-H3) ser10 expression level normalized to using Histone H3 (H3) as loading control.

The histogram presents average densitometric values of two independent experiments on the y-axis and *zeitgeber time* (ZT) on the x-axis. *Zietgeber* times are indicated for each sample, that contain whole fin protein extract obtained from at least 4 adult fins. ZT0 corresponds to lights-on, ZT14 to lights-off. Levels of significance between the corresponding time points, of the two genotypes, are calculated by two-way ANOVA (table S11) and post hoc analysis Sidak method and are indicated (\*\*\*p < 0.001, \*\*p < 0.01, \*p < 0.05). Lower panel (C): Representative western blot image of two (n=2) independent experiments.

WT fin tissues exhibited a peak of phospho-H3 protein levels around ZT16, consistent with the results from previous reports [210] (Figure 24). Instead, in the *per2* KO fin tissues this peak is significantly reduced, thus, confirming abnormal circadian clock regulation of cell cycle progression in the *per2* KO proliferative fin tissues. Moreover, the abnormal circadian clock regulation of M phase progression, together with the affected circadian gene expression of *p21*, a important inhibitor acting at the level of G1/S cell cycle checkpoint, could be indicators of a specific cell cycle phase deregulation.

### 3.1.8.4 Abnormal cell cycle progression in the *per2* KO embryonic fibroblast cell lines

In order to characterize cell cycle progression in more detail in the absence of *per2* gene function we next compared cell cycle progression in *per2* KO embryonic fibroblast cell lines with the corresponding WT cell line. We performed FACS analysis of WT and *per2* KO embryonic fibroblast cell lines. The cells were maintained for 3 days in darkness, then labeled with propidium iodide and sorted by FACS, as percentage (%) of cells in G1, S and G2/M phase of the cell cycle.

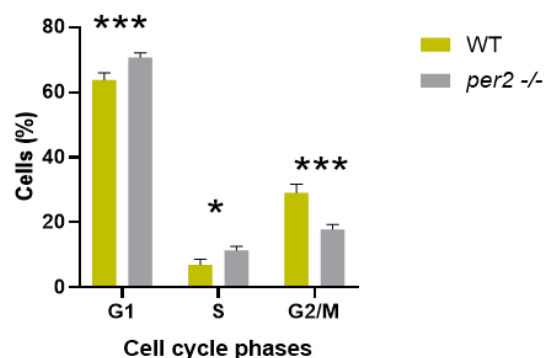


**Figure 25 : Cell cycle FACS analysis of the *per2* KO and WT embryonic fibroblast cell lines.**

Mean cell (%) (n=4) ± SD is plotted on the y-axis, cell cycle phases (G1, S, G2/M) are plotted on the x-axis. Levels of significance between the corresponding time points, of the two genotypes, are calculated by two-

way ANOVA (table S12) and post hoc analysis Sidak method and are indicated (\*\*\* $p < 0.001$ , \*\* $p < 0.01$ , \* $p < 0.05$ ).

The results showed that the phase distribution of the cells differs between the WT and *per2* KO lines (figure 25). In particular, the *per2* KO has a lower number of cells in the G2/M phase and a higher number of cells in G1 with respect to the WT, while there is only a slight difference between the % of cells in S phase. The higher number of the *per2* KO cells in G1 phase could result from cell cycle arrest or delay at G1 phase. As consequence of such an arrest/delay in G1 phase, a lower number of the *per2* KO cells result in G2/M phase, which could explain the circadian clock dysregulation of the M phase progression observed in the *per2* KO adult fins.

#### **3.1.8.5 The regenerative capacity of the zebrafish caudal fin is not affected in the *per2* KO line.**

Based on the reduced circadian rhythmicity of M phase progression and the abnormal cell cycle progression observed in the adult fins and embryonic fibroblast cells of the *per2* KO line, we next tested whether the regenerative capacity of the caudal fin was affected in the *per2* KO adult line. Zebrafish, as well as other teleosts, is able to regenerate rapidly (within 15 days post amputation (dpa)) the amputated caudal fin, restoring both size and shape. Therefore, we amputated half the caudal fin from wild-type and *per2* KO fishes and then monitored the regrowth over 18 dpa. WT and *per2* mutant fishes were kept in LD (14h light-10h dark) conditions and half of each caudal fin was amputated at ZT3 of dpa 0 from at least 5 fish for each line. Then, images of the regrowth process were taken for a period of 18 days. Results revealed no significant differences in the fin regrowth rate of the *per2* KO line with respect to WT control fish (figure 26).

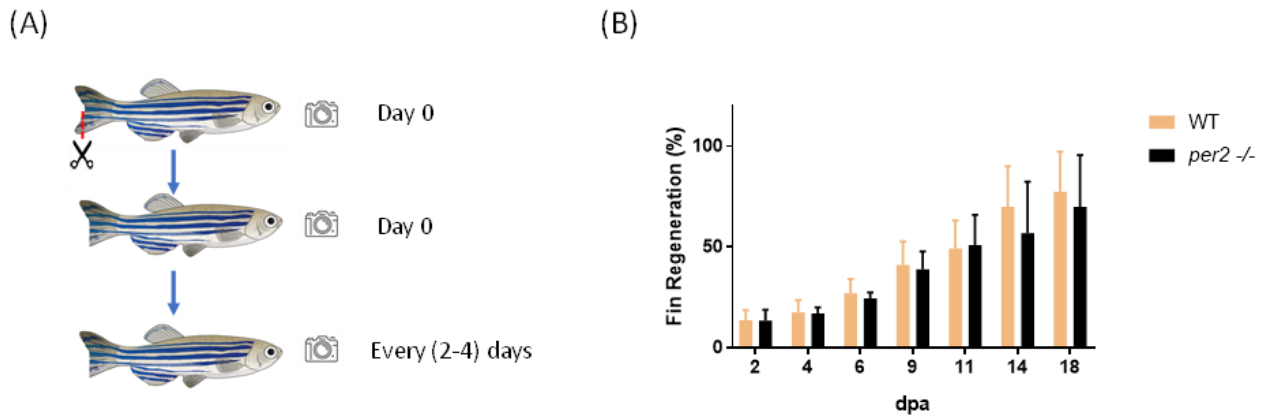


**Figure 26: Fin regeneration of the WT and *per2* KO zebrafish line over 18 days post amputation (dpa).** Left panel (A): Schematic illustration of the experimental scheme. The full area (in pixels) of the fin clipped lobe, was quantified from the pre-amputation images for each fish. The new tissue area, from the new distal fin edge to the amputation plane, was also quantified every (2-4) days. Right panel (B): Fin regeneration of the WT and *per2* KO zebrafish line over 18 days post amputation. The histogram presenting the mean fin regeneration (%) ( $n=5$ )  $\pm$  SD on the y-axes and the days post amputation (dpa) on the x-axis. Percent regeneration for each fin at each time point was defined as: % regeneration =  $100 \times (\text{new tissue area} / \text{original fin area amputated})$ .

### 3.2 TGF- $\beta$ signaling pathway affects the circadian clock in zebrafish

#### 3.2.1 Disruption of TGF- $\beta$ signaling interferes with the molecular circadian clock in zebrafish PAC-2 cells.

Previous studies have demonstrated that TGF- $\beta$  influences the expression of several clock genes in human cell lines and the mouse liver [236]. In order to more precisely examine the influence of TGF- $\beta$  signaling on peripheral circadian clock function, we tested the effect of pharmacologically blocking TGF- $\beta$  signaling on the molecular circadian oscillator in zebrafish PAC-2 cells stably transfected with a clock gene promoter-reporter construct, Tg(-3.1)*per1b::luc* [124]. Cells were exposed to 3 LD (12h light:12h dark) cycles for entrainment. Then, 30 minutes before lights on a selective ATP-competitive inhibitor of the TGF- $\beta$  receptor ALK5, LY-364947, was added to the cell culture medium at different concentrations (1, 5, 10, 20  $\mu$ M). This inhibitor was previously shown to inhibit TGF- $\beta$ -Smad3 mediated signaling in zebrafish larvae [247]. Cells were maintained in LD for an additional 2 days and then transferred to DD. Luciferase activity was monitored and compared with that of vehicle treated control cells ( $n = 4/\text{group}$ ). The addition of TGF- $\beta$  inhibitor LY-364947 altered the clock controlled rhythmic activity of the *per1b* promoter in a dose-dependent manner (figure 27)

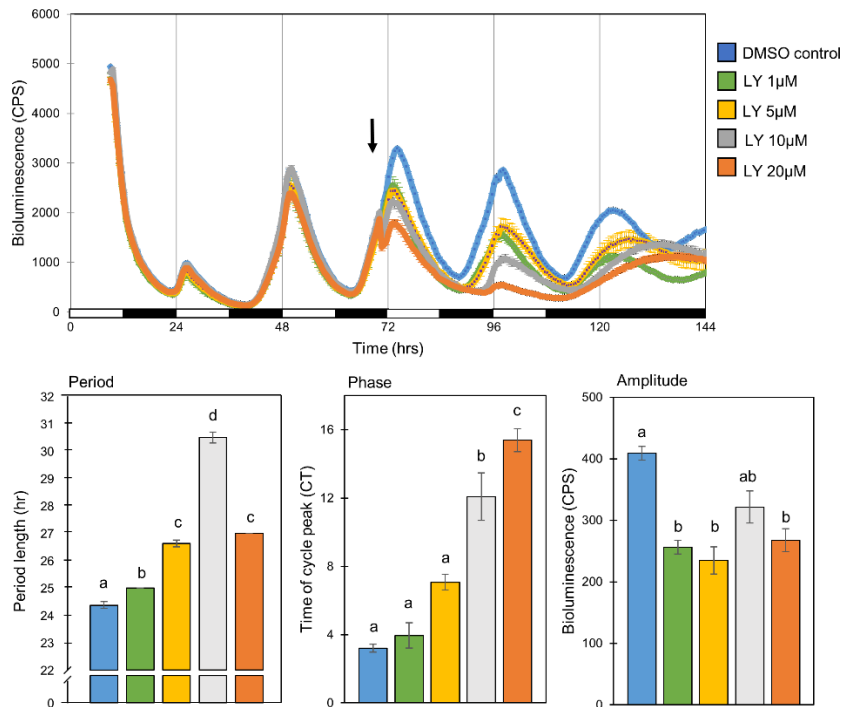


**Figure 27: The molecular circadian oscillator in PAC-2 cells is significantly altered by TGF- $\beta$  inhibition.**

Rhythmic *Per1b* promoter activity in the zebrafish PAC-2 cell line was significantly altered by the addition of the TGF- $\beta$  inhibitor LY-364947 in a dose-dependent manner in comparison to DMSO treated control (n = 4-12/group). Upper panel: Luciferase bioluminescence, driven by the *per1b* promoter, is plotted on the y-axis and time (hours) on the x-axis. The horizontal bars represent the lighting conditions during the measurements; white boxes represent light periods and black boxes represent dark periods. Lower panel: cells which were exposed to LY-364947 exhibit rhythms of longer period (p<0.001, one-way ANOVA), a phase delay (p<0.001, one-way ANOVA), and a lower amplitude of expression (p<0.001, one-way ANOVA). Different letters represent statistically different values within each parameter (p<0.05, Tukey's test). This experiment was repeated twice, resulting in comparable results. The results are from one representative experiment.

Treatment with the TGF- $\beta$  inhibitor LY-364947 led to a significant lengthening of the period of rhythmic *per1b* promoter driven transcription at all inhibitor concentrations (25 $\pm$ 0, 26.62 $\pm$ 0.12, 30.5 $\pm$ 0.2, 27 $\pm$ 0.0 hr for 1, 5, 10 and 20  $\mu$ M, respectively, compared to 24.37 $\pm$ 0.12 for the DMSO treated control, p<0.001, one-way ANOVA, p<0.05, Tukey's post-hoc). This led to a significant dose-dependent phase delay at higher (10 and 20  $\mu$ M) inhibitor concentrations (the time of the first peak after the cells were transferred to DD was at CT 3.95 $\pm$ 0.74, 7.08 $\pm$ 0.46, 12.08 $\pm$ 1.4 and 15.4 $\pm$ 0.67 for 1, 5, 10 and 20  $\mu$ M, respectively, compared to CT 3.2 $\pm$ 0.24 for the DMSO treated control, p<0.001, one-way ANOVA, p<0.05, Tukey's post-hoc). The treatment also led to a reduction in the amplitude of rhythmic *per1b* promoter activity during the first DD cycle after exposure to all concentrations

(256.25±20.51, 234.62±22.38, 321.5±26.12, 267.33±18.78 CPS for 1, 5, 10 and 20 μM, respectively, compared to 409±11.04 for the DMSO treated control,  $p<0.001$ , one-way ANOVA,  $p<0.005$ , Tukey's post-hoc). We also tested an alternative TGF-β inhibitor for both TGF-β receptors ALK-4 and ALK-5, SB-505124. Inhibition with SB-505124 resulted in very similar effects on amplitude and period of *per1b* promoter activity, but with insignificant effects on phase (figure 28).

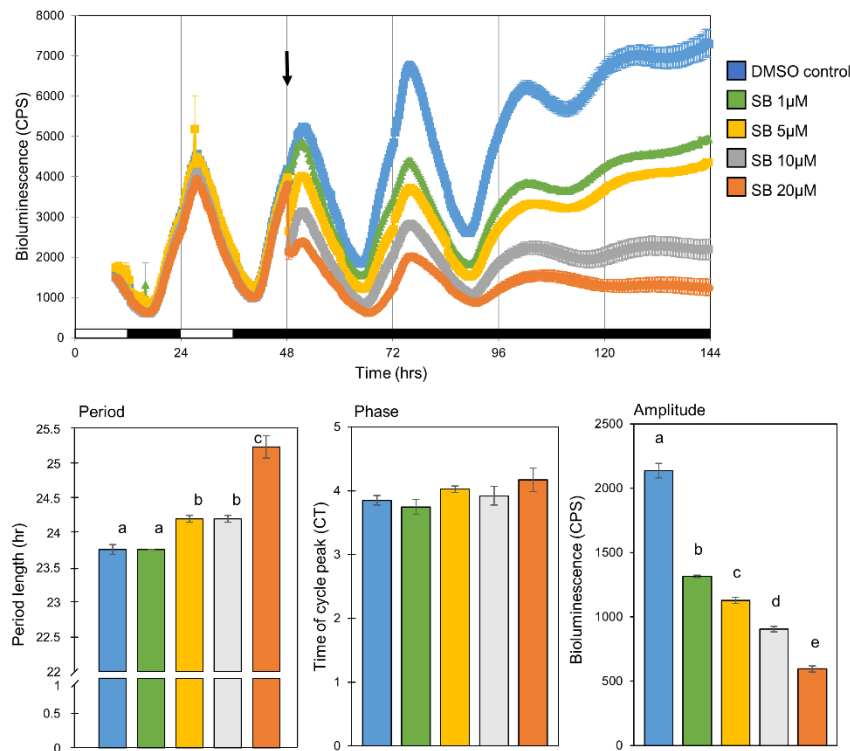


**Figure 28: The molecular circadian oscillator in PAC-2 cells is significantly altered by TGF-β inhibition by SB-505124.**

Rhythmic *per1b* promoter activity in the zebrafish PAC-2 cell line was significantly altered by the addition of the TGF-β inhibitor SB-505124 in a dose-dependent manner in comparison to DMSO treated control (n = 8/group). Upper panel: bioluminescence is plotted on the y-axis and time (hours) on the x-axis. The horizontal bars represent the lighting conditions before and during sampling; white boxes represent light periods and black boxes represent dark periods. Lower panel: effects of inhibition on length, phase, and amplitude of *per1b* promoter activity. Different letters represent statistically different values within each parameter ( $p<0.05$ , one-way ANOVA, Tukey's test). Treatment led to a significant lengthening of the period of *per1b* promoter activity (23.76±0.05, 24.2±0.05, 24.2±0.05, 25.24±0.16 hr for 1, 5, 10 and 20 μM, respectively, compared to 24.35±0.12 for the DMSO-treated), and reduction in the amplitude (1313.75±9.37, 1128±24.02, 903±20.26, 594.19±23.29 CPS for 1, 5, 10 and 20 μM, respectively, compared to 2136.25±57.29 for the DMSO-treated

control), but not to a significant phase delay (the time of the first peak after the cells were transferred to DD was at CT  $3.74\pm 0.12$ ,  $4.025\pm 0.05$ ,  $3.92\pm 1.5$ ,  $4.17\pm 0.19$  hr for 1, 5, 10 and 20  $\mu\text{M}$ , respectively, compared to  $3.85\pm 0.07$  for the DMSO-treated control).

These results indicate that TGF- $\beta$  signaling is essential for the rhythmic promoter activity of a key clock gene in the PAC-2 zebrafish cell line, and therefore demonstrates the importance of TGF- $\beta$  signaling for normal function of the circadian clock mechanism.

In order to further demonstrate the influence of the TGF- $\beta$  signaling pathway on the core circadian clock mechanism, we tested the effects of TGF- $\beta$  signaling activation on the molecular circadian oscillator in PAC-2 cells. This was done by applying the compound Alantolactone, which disrupts Cripto-1/ActRII complexes resulting in an indirect induction of activin/Smad3 signaling [259]. Cells were exposed to 3 LD cycles for entrainment, then, at CT 23.5 Alantolactone was added to the cell culture medium at different concentrations (1, 5 and 10  $\mu\text{M}$ ,  $n = 8$ / group) and cells were transferred to constant darkness. Luciferase activity was monitored and compared with that of vehicle-treated control cells. The addition of Alantolactone to the culture media disrupted the clock-driven transcription from the *per1b* promoter (figure 29), with a significant dose-dependent reduction in the amplitude of rhythmic *per1b* reporter expression under DD ( $1542.31\pm 27.76$ ,  $968.69\pm 16.07$  CPS for 1 and 5  $\mu\text{M}$  Alantolactone respectively, compared to  $2151.31\pm 18.44$  for the DMSO-treated, during the first DD cycle after exposure,  $p < 0.001$ , one-way ANOVA,  $p < 0.001$ , Tukey's post-hoc). The period of *per1b* promoter activity was reduced upon treatment with the activator ( $24.01\pm 0.05$ ,  $23.17\pm 0.05$  hr for 1 and 5  $\mu\text{M}$ , respectively, compared to  $24.99\pm 0.05$  for the DMSO treated control,  $p < 0.001$ , one-way ANOVA,  $p < 0.05$ , Tukey's post-hoc). However, Alantolactone did not effect the phase of *per1b*-driven rhythmic expression (the time of the first peak after the cells were transferred to DD was at CT  $21.42\pm 0.07$ ,  $21.74\pm 0.1$  for 1 and 5  $\mu\text{M}$ , respectively, compared to CT  $21.48\pm 0.05$  for the DMSO-treated control,  $p < 0.001$ , one-way ANOVA,  $p < 0.05$ , Tukey's post-hoc). The highest concentration (10 $\mu\text{M}$ ) of Alantolactone tested completely abolished rhythmic expression.

The different effects of treatment with the inhibitor and activator on the period length of the rhythmic promoter driven luciferase activity in the PAC-2 zebrafish cell line indicate that this modulation of the circadian expression pattern is the result of a pathway-specific pharmacological treatment, rather than a more general, non-specific effect.

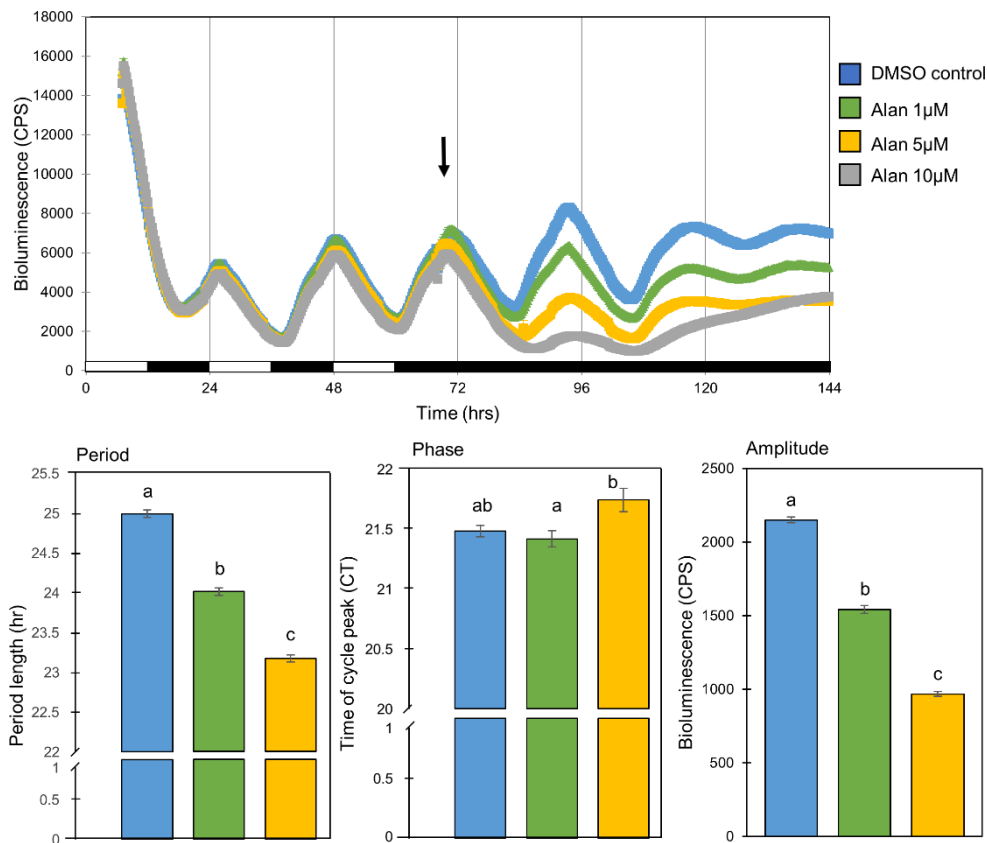


**Figure 29: The molecular circadian oscillator in PAC-2 cells is significantly altered by TGF- $\beta$  induction.** Rhythmic *per1b* promoter activity in the zebrafish PAC-2 cell line was significantly altered by the addition of the indirect TGF- $\beta$  inducer Alantolactone to the culture media in a dose-dependent manner in comparison to DMSO treated control (n = 8/group). Upper panel: bioluminescence is plotted on the y-axis and time (hours) on the x-axis. The horizontal bars represent the lighting conditions during bioluminescence measurements; white boxes represent light periods and black boxes represent dark periods. Lower panel: cells which were exposed to Alantolactone exhibit lower amplitude (p<0.001, one-way ANOVA), a phase delay (p<0.001, one-way ANOVA), and shorter periods of rhythms (p<0.001, one-way ANOVA). Different letters represent statistically different values within each parameter (p<0.05, Tukey's test).

### 3.2.2 TGF- $\beta$ inhibition leads to phase delay of *per1b* mRNA rhythms in zebrafish larvae.

After demonstrating that pharmacological inhibition of TGF- $\beta$  influences the circadian clock of zebrafish cell lines *in vitro*, we next tested the influence of this inhibition at the whole organism level by testing its effect on the clock-controlled rhythmic expression pattern of *per1b* mRNA. Zebrafish larvae were kept under LD cycles for 5 days. Near the end of the light phase of the 5th day of development, the TGF- $\beta$  inhibitor LY-364947 (20µM) or diluted DMSO alone (control) was added to the larvae water, and larvae were transferred to DD conditions. During the 6th and 7th days of

development fish were collected at 4 hr intervals and *per1b* mRNA levels were measured by whole mount ISH (n = 15/group). *Per1b* mRNA expression levels were significantly affected by sampling time (p<0.001, two-way ANOVA), and there was a significant interaction between treatment and sampling time (p<0.001, two-way ANOVA). Thus, consistent with our previous cell culture experimental results, the circadian expression pattern of *per1b* mRNA was significantly altered in larvae exposed to the TGF- $\beta$  inhibitor, demonstrating a phase delay of circadian expression in comparison to the control group (figure 30).

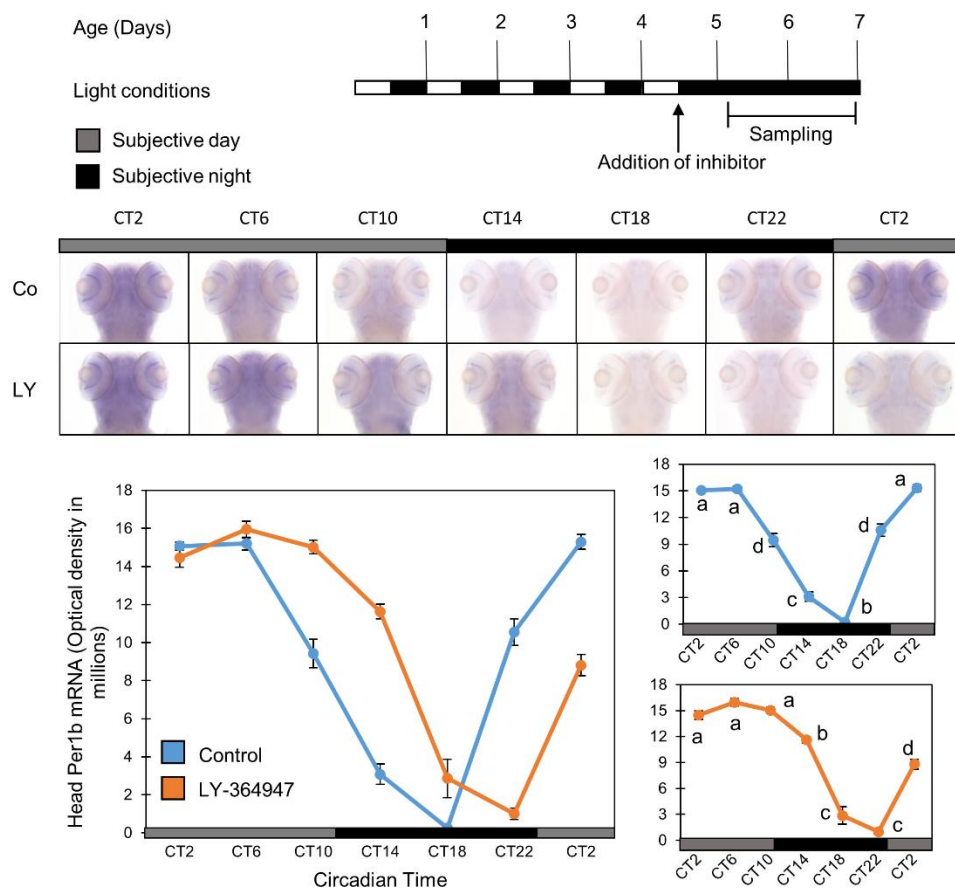


**Figure 30: *Per1b* mRNA circadian expression pattern in zebrafish larvae is phase-shifted by TGF- $\beta$  inhibition.**

Zebrafish larvae were treated with TGF- $\beta$  inhibitor LY-364947 (20  $\mu$ M), and the expression pattern of *Per1b* was evaluated by whole mount ISH. *Per1b* expression was detected throughout the head region and its circadian expression pattern was altered in the presence of the TGF- $\beta$  inhibitor, exhibiting a phase delay of circadian expression in comparison to a control group (DMSO). *Per1b* mRNA expression was significantly affected by sampling time (p<0.001, two-way ANOVA), and by an interaction between treatment and sampling time (p<0.001, two-way ANOVA) (n = 15/group). Upper panel: Schematic representation of the experimental

design. The horizontal bars represent the light conditions before and during sampling; white boxes represent light and black boxes represent dark periods. Middle panel: whole mount ISH signals for *Per1b* mRNA (dorsal views of the heads) of representative specimens. Grey bars represent subjective day and black bars represent subjective night. Circadian times are indicated for each sample. CT0 corresponds to “subjective lights on”, CT12 to “subjective lights-off”. Lower panel-left: Quantification of signal intensities in the heads of treated and control larvae. Values represent the mean  $\pm$  SE optical densities of the head signals. Lower panel-right: Different letters represent statistically different values within each treatment ( $p < 0.05$ , one-way ANOVA, Tukey's test). This experiment was repeated twice, resulting in similar outcomes. The results are from one representative experiment.

This observed phase delay is similar to the phase delay of *Per1b* promoter activity rhythms in PAC-2 cells upon exposure to the TGF- $\beta$  inhibitor (figure 27).

### **3.2.3 TGF- $\beta$ inhibition reversibly disrupts clock-controlled rhythmic locomotor activity in zebrafish larvae.**

Studies of the influence of TGF- $\beta$  signaling on the circadian clock have been limited so far to its influence on the core molecular mechanism [234], [275]. Therefore, we next aimed to test whether TGF- $\beta$  signaling also influences a behavioral output of the clock, namely clock-controlled circadian rhythms of locomotor activity [7], [276].

The influence of a TGF- $\beta$  inhibitor on larval locomotor activity was tested following a previously described experimental protocol [245]. Larval clocks were entrained by exposure to 3 LD cycles and two 12 hr light:12 hr dim light cycles (LDim) and then transferred to constant dim light (DimDim). Locomotor activity was recorded under DimDim during the 6th-7th days of development in the presence of the TGF- $\beta$  inhibitor LY-364947 (20  $\mu$ M) which was added to the larvae water during the 5th day of development ( $n = 24$ /group). Circadian rhythms of locomotor activity were significantly disrupted in larvae treated with the TGF- $\beta$  inhibitor in comparison with the DMSO treated controls (figure 31;  $p < 0.001$ , Kolmogorov-Smirnov test). Inhibitor-treated larvae exhibited a significantly lower amplitude ( $1.52 \pm 0.48$  and  $4.15 \pm 0.84$  cm/10 min for inhibitor-treated and control larvae respectively,  $p < 0.001$ , t-test), similar to the decrease in amplitude of *per1b* promoter activity following the TGF- $\beta$  inhibition observed in our previous *in vitro* experiments.

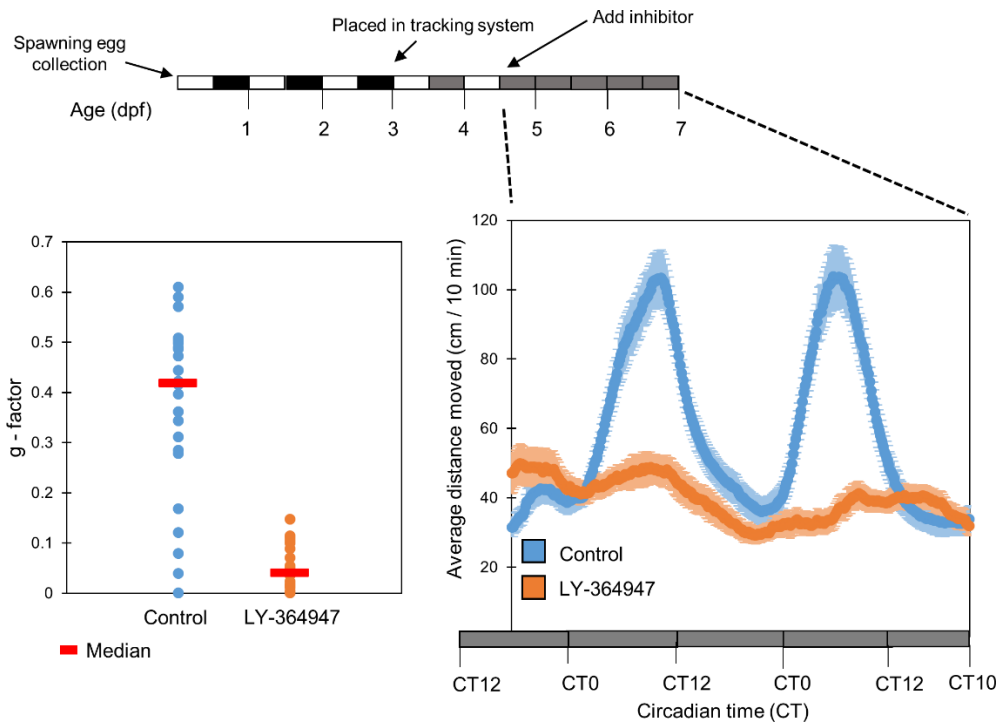


**Figure 31: TGF- $\beta$  inhibition abolishes clock-controlled rhythmic locomotor activity in zebrafish larvae.**

Clock-controlled rhythmic locomotor activity of zebrafish larvae under constant dim light was abolished after treatment with the TGF- $\beta$  inhibitor LY-374947 (20 $\mu$ M) in comparison to a control group (DMSO). Embryos were raised under LD for 3 days, raised under LDim in the DanioVision chamber for 2 days, the inhibitor was then applied and locomotor activity (distance moved every 10 min) was monitored under constant Dim. The data is presented as a moving average (10 sliding points) for each group (n = 24/group). Larvae exhibited a significant reduction in the amplitude of rhythmic locomotor activity ( $p < 0.001$ , t-test, bottom right panel). The horizontal bars represent the lighting conditions before and during the experiment. White boxes represent light, black boxes represent dark and grey boxes represent dim light (upper panel). TGF- $\beta$  inhibitor-treated larvae exhibited significantly lower g-factor values (fitness to a circadian rhythm) in comparison to control larvae ( $p < 0.001$ , Kolmogorov-Smirnov test), indicating that their locomotor activity is less circadian (bottom left panel). The median is represented for each group (red line).

Light exposure has been extensively documented to have an acute effect on the locomotor activity of zebrafish larvae, independently of regulation by the endogenous circadian clock [277]. Therefore, we next aimed to determine whether this “masking” effect of light could overcome the effect of the TGF-

$\beta$  inhibitor, and restore or prevent disruption in rhythmic locomotor activity of the larvae. Larvae were entrained to 3 LD and 2 LDim cycles and locomotor activity was monitored on the 6th-8th day of development under LDim cycles in the presence or absence of the inhibitor ( $n = 24/\text{group}$ ). Circadian rhythms of locomotor activity were significantly altered in larvae treated with TGF- $\beta$  inhibitor in comparison with the DMSO treated controls ( $p < 0.001$ , Kolmogorov-Smirnov test; figure 32).

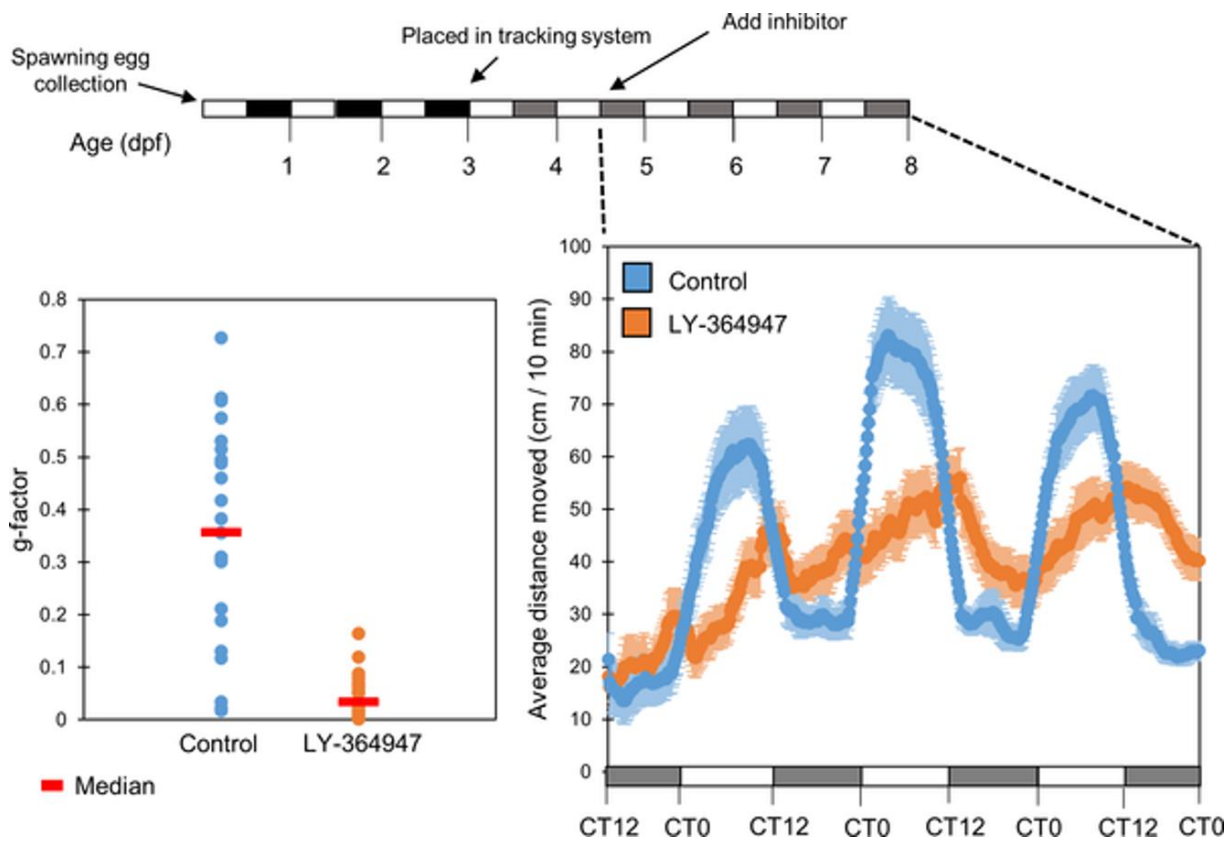


**Figure 32: TGF- $\beta$  inhibition disrupts circadian locomotor activity rhythms under light:Dim light cycles.**

Larval rhythmic locomotor activity under LDim was significantly disrupted ( $p < 0.05$ , t-test), but not completely abolished, after treatment with the TGF- $\beta$  inhibitor LY-374947 ( $20\mu\text{M}$ ) in comparison with the DMSO control group. Embryos were raised under LD for 3 days, raised under LDim in the DanioVision chamber for 2 days, the inhibitor was added and locomotor activity (distance moved every 10 min) was monitored under LDim cycles. The data is presented as a moving average (10 sliding points) for each group ( $n = 24/\text{group}$ ) (bottom right panel). The horizontal bars represent the lighting conditions before and during the experiment. White boxes represent light, black boxes represent dark and grey boxes represent dim light (upper panel). TGF- $\beta$  inhibitor treated larvae exhibited significantly lower g-factor values in comparison with control larvae ( $p < 0.001$ , Kolmogorov-Smirnov test), indicating that their locomotor activity is significantly less circadian

(bottom left panel). The median is represented for each group (red line). This experiment was repeated twice, resulting in similar outcomes. The results are from one representative experiment.

Inhibitor-treated larvae exhibited a significantly longer period of rhythmic locomotor activity ( $25.86 \pm 0.75$  and  $23.19 \pm 1.34$  hr for treated and control larvae, respectively,  $p < 0.05$ , t-test). Consequently, inhibitor-treated larvae displayed a delayed phase (peaking at  $CT11 \pm 4.4$  and  $CT5 \pm 5.22$  hr for inhibitor-treated and control larvae, respectively,  $p < 0.001$ , t-test), reminiscent of the period lengthening and phase delay observed in the activity of *per1b* promoter activity *in vitro* (figure 27), and the phase delay in *per1b* mRNA expression *in vivo* (figure 30).

Treated larvae also exhibited a lower amplitude rhythm ( $2.49 \pm 1.02$  and  $3.98 \pm 1.16$  cm/10 min for inhibitor treated and controlled larvae, respectively,  $p < 0.05$ , t-test), reminiscent of the decrease in the amplitude of *per1b* promoter activity *in vitro*. The alteration of locomotor activity circadian rhythms, even under LDim cycles, further reinforces the importance of TGF- $\beta$  signaling for the function of the circadian system.

Given the striking effect of TGF- $\beta$  inhibition on larval circadian locomotor activity, and to rule out the possibility of an irreversible toxic effect, we examined whether this effect could be reversed. Larvae were kept under LD cycles during the first 5 days of development, and then placed in DD during the 6th-7th days of development in the presence of TGF- $\beta$  inhibitor LY-364947 (20 $\mu$ M). On the morning of the 8th day of development, the inhibitor was removed by washing. Larvae were re-entrained by two LDim cycles, and then kept under DimDim conditions for an additional 24 hours, during which their locomotor activity was recorded ( $n = 23$ /group). 24 hours after removal of the inhibitor, normal circadian rhythmicity of locomotor activity in inhibitor-treated larvae was completely recovered (figure 33). 24 hours following inhibitor washout there were no significant differences in the g-factor distribution between control and inhibitor-treated larvae ( $p = 0.12$ , Kolmogorov-Smirnov test), as well as no significant difference in amplitude ( $2.37 \pm 0.31$  and  $2.8 \pm 0.63$  cm/10 min for inhibitor-treated and control larvae, respectively,  $p = 0.32$ , t-test) period length ( $24.77 \pm 0.26$  and  $25.19 \pm 0.52$  hr for treated and control larvae, respectively,  $p = 0.58$ , t-test) or phase ( $CT7.5 \pm 1.07$  and  $CT8 \pm 0.28$  hr for treated and control larvae respectively,  $p = 0.73$ , t-test). This indicates that the effect of pharmacological TGF- $\beta$  inhibition on the circadian rhythms of locomotor activity is specific and reversible.

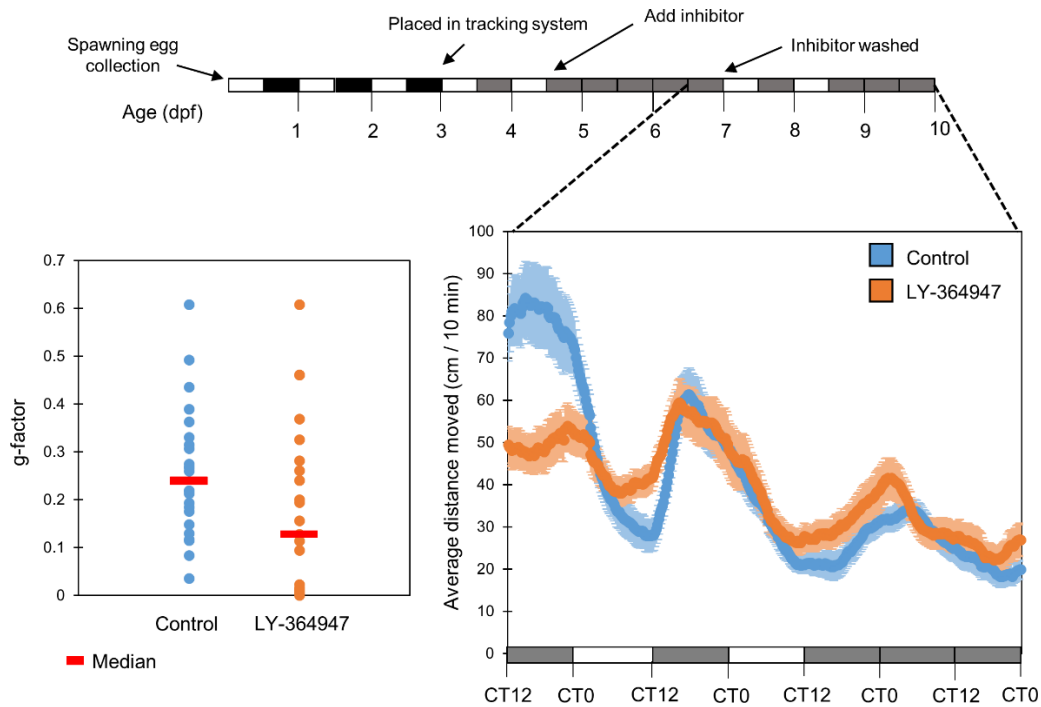


**Figure 33: The effect of TGF- $\beta$  inhibition on clock-controlled rhythmic locomotor activity in zebrafish larvae is reversible.**

Embryos were raised under LD for 3 days, raised under LDim in the DanioVision chamber for 2 days, the inhibitor (20 $\mu$ M LY-374947) was applied for an additional 2 DimDim cycles. After washing off the inhibitor, the larvae were entrained by 2 LDim cycles and locomotor activity (distance moved every 10 min) was monitored under constant Dim. Following removal of the TGF- $\beta$  inhibitor, normal circadian rhythmicity of locomotor activity in treated larvae was recovered. A day following inhibitor wash out there were no significant differences in the g-factor distribution between DMSO and inhibitor treated larvae ( $p = 0.12$ , Kolmogrov-Smirnov test), as well as no significant differences in amplitude ( $p = 0.32$ , t-test), phase ( $p = 0.73$ , t-test) or period length ( $p = 0.58$ , t-test) (bottom left panel). The data is presented as a moving average (10 sliding points) for each group ( $n = 23$ /group). The median is represented for each group (red line). This experiment was repeated twice, resulting in similar outcomes. The results are from one representative experiment

To rule out the possibility that LY-364947 simply impairs larval mobility by for example influencing skeletal muscle functionality, we performed an additional assay for the behavioral response to light-to-dark transitions. The behavioral response of the larvae to a sudden light transition is not regulated by the circadian clock [278], and therefore can be examined to test whether the TGF- $\beta$  inhibitor affects larval mobility. During the early light phase of the 6th day of development, larvae were subjected to 3 dark flashes of 10 seconds each, with 15 minutes of light interval between flashes, in the presence of the TGF- $\beta$  inhibitor LY-364947 (20 $\mu$ M). Locomotor activity was recorded before,

during and after the dark flashes. No statistical difference was observed between the response of inhibitor-treated and control DMSO treated larvae ( $n = 24/\text{group}$ ) to dark flashes (figure 34;  $p = 0.28$ , t-test), indicating that LY-364947 does not generally impair larval mobility.

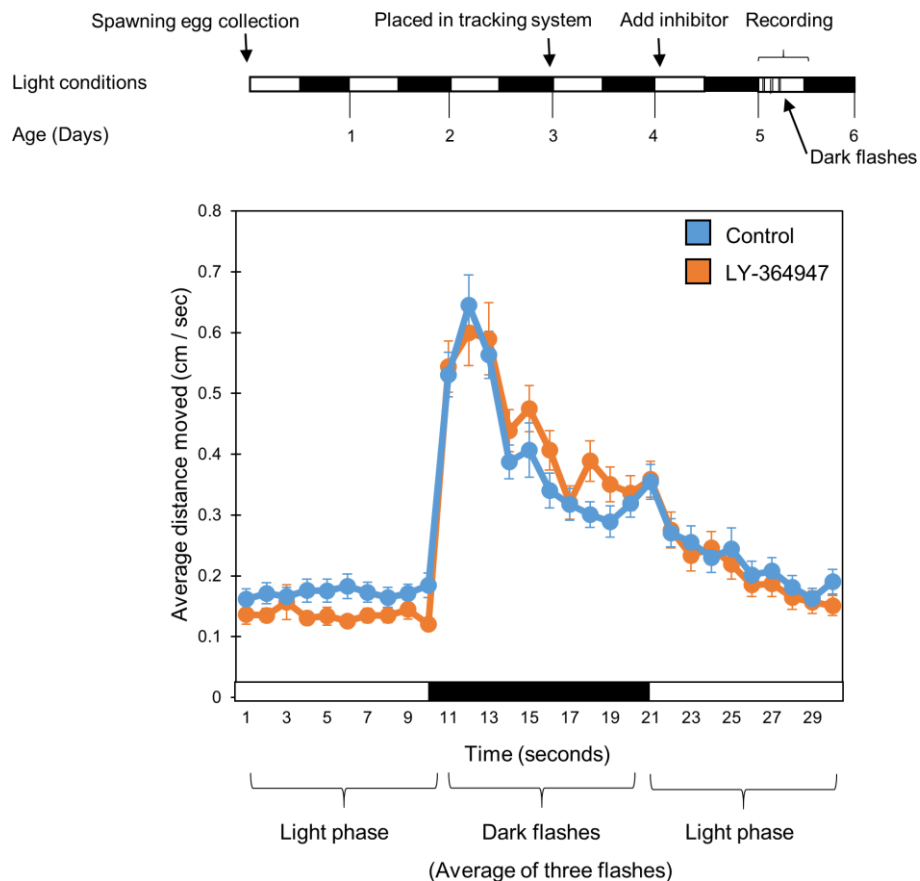


**Figure 34: Locomotor activity levels in response to dark flashes is not affected by TGF- $\beta$  inhibition.** Larvae were kept under LD cycles. On day 5, the inhibitor or DMSO as control, was added. Larvae were subjected to 3 dark flashes of 10 seconds each, which are known to induce startle response, with 15 minutes intervals of light between flashes, and their activity was recorded (upper panel). No statistical difference was observed between the activity of control (DMSO) and the TGF- $\beta$  inhibitor (LY-374947, 20 $\mu$ M) treated groups during the dark flashes ( $p = 0.28$ , t-test), indicating that TGF- $\beta$  inhibition does not impair larval mobility (lower panel). Each line represents the average of three succeeding trials, which measured the average movement per second of each group of larvae, recorded from 10 second before the flash, during the flash, and 10 second after the flash. Black and white horizontal boxes represent the light phase and dark flashes, respectively. This experiment was repeated twice, resulting in similar outcomes. The results are from one representative experiment.

## 4 Discussion

We have investigated the function of the *per2* gene in clock input and output pathways in adult and embryonic zebrafish. We have generated a *per2* KO zebrafish line and performed a gene expression analysis of sets of core clock and clock-controlled genes in different organs, tissues, cell lines and larvae. Our results have revealed a tissue-specific function for the *per2* gene in the regulation of the circadian clock, as well as clock-controlled genes in zebrafish peripheral tissues. Furthermore, our data do not support a role for *per2* in the regulation of FAA in zebrafish under LD conditions. Finally, we have shown that disruption of *per2* gene function in our cell line models has a significant impact on the profile of cell cycle control gene expression, *in vivo* it does not appear to contribute to the timing of cell proliferation during tissue regeneration in zebrafish. Concerning clock output pathways, we have focused our attention on the circadian clock regulation of the TGF- $\beta$  signaling pathway in zebrafish. In particular, by *in vitro* as well as *in vivo* analysis, we show the existence of a bidirectional interaction between the circadian clock and TGF- $\beta$  signaling pathways at the molecular and behavioral levels, thus reinforcing the notion of a functional link between the circadian clock and TGF- $\beta$  signaling in zebrafish.

### 4.1 Contribution of the *per2* gene to light input pathways in zebrafish

The *per2* gene is one of the key elements of the circadian clock core mechanism in vertebrates. Many studies that have been performed in mammals have concluded that *per2* is a multifunctional gene that enables the cross-talk between the circadian timing system and the transcription of clock-controlled genes (CCGs). One of the defining features of the circadian clock is that it regulates the daily rhythmicity of most aspects of physiology and behavior. Therefore, the presence of multifunctional elements within the core clock transcription-translation feedback loop would appear to make a lot of sense. Among the first functions to be attributed to the *per2* gene, was a role in the light input pathway to the clock. Consistent with this role, *per2* gene expression is photoinducible in the mammalian SCN. Moreover, the *per2* gene exhibits a light inducible, D-box-mediated gene expression in zebrafish peripheral tissues [7], [150]. However, our analysis of core clock gene expression in *per2* KO embryos and different adult tissues, such as heart, liver, fin, eyes, brain, gut, and muscle, exposed to a light dark cycle failed to reveal any significant abnormalities. These results could indicate a possible compensation for loss of *per2* gene function by alternative modulators of the direct-light entrainable peripheral clock mechanism. More specifically, we could speculate that the *per2* gene function in direct light exposed tissues as well as the relatively transparent embryos, could be compensated for

by the action of other light inducible genes such as *cry1a* that could heterodimerize with other *per* paralogous genes, such as *per1b*, *per1a* and *per3*. Furthermore, the higher light intensities may also serve to compensate for a reduced effectiveness of photic input. However, a 6 hr phase delay was observed in the expression of the core clock genes *clock1* and *cry1a* in the *per2* KO adult gut, liver, heart and muscle tissues. One possible interpretation of this result is that since these organs are internal structures, they might experience lower light intensities than peripheral tissues such as the fins and consequently the loss of *per2* function results in a shift in the timing of rhythmic expression of these two clock genes. In tissues experiencing a reduced light intensity, light inducible *cry1a* gene expression may not be sufficient to effectively entrain the clocks, thus generating a complete dependence of the circadian timing system on systemic signals and so resulting in the observed phase differences in the loss of function mutants.

In support of a gene and tissue specific regulation by PER2, it is known that this protein shares amino acid sequence motifs with both coactivators and corepressors of hormone receptors. For example, the mouse PER2 protein is characterized by two LXXLL motifs in both of its predicted protein–protein interaction domains. This motif is present in different coactivators which interact with nuclear receptors such as the steroid hormone receptor coactivator-1 (SRC-1) [178]. This coactivator interacts with several nuclear receptors, thereby conferring transcriptional transactivation function. Moreover, the presence of the CoRNR boxes in the PAS/PAC domain of the mouse PER2 protein are indicative of corepressor function [279]. Furthermore, consistent with PER2 regulatory targets not being restricted to E-box elements, this protein has been implicated in the transcriptional regulation of the *bm11* gene via its regulation of retinoic acid—related orphan receptor response element (RORE) binding sites in zebrafish. In particular, the Per2 protein upregulates *bm11b* gene expression by directly binding to the Rora nuclear receptor [280]. This situation is reminiscent of a mechanism observed in mammals where PER2 binds to Rev-erba to enhance *bm11b* expression [281], thus pointing to evolutionary conservation of this transactivation mechanism involving elements of the Rora/Rev-erba clock stabilizing loop. Interestingly, a RORE element has also been identified in the zebrafish *clock1* promoter, an observation that would potentially account for the dysregulation of *clock1* gene expression in certain tissues. The only unresolved issue remains how changes in the profile and timing of *Clock1* and *Cry1a* mRNA expression does not lead to corresponding alterations in the rhythmic expression of other core clock component genes. Of course, we still lack crucial evidence for changes in clock protein levels which may not precisely mirror the observed mRNA

patterns. Nevertheless, it will be an important goal to understand the functional consequence of combined changes in *Clock1* and *Cry1a* expression for the function of the circadian clock mechanism.

#### **4.2 Characterization of *per2* gene function in a zebrafish *in vitro* system.**

In order to clarify the functional contribution of *per2* to the circadian timing system in zebrafish in the absence of systemic signals, we established cell lines from embryonic and adult fin tissues derived from *per2* KO and the corresponding WT sibling fish. In the mutant cell line, we observed an absence or strong attenuation of rhythmic clock gene expression that contrasts with the relatively normal rhythmic clock gene expression observed in wild type cell line as well as mutant and wild type, adult and embryonic tissues. We interpret this striking result by several alternative explanations. In one scenario, in the *in vivo* context of the embryo or adult fish, loss of *per2* function fails to impact on light entrainment or core function of the clock since systemic signals derived from a central clock perhaps located in the central nervous system and entrained indirectly by retina-derived light input, are able to “rescue” the entrainment and normal function of the peripheral clocks. Instead, in cell cultures, in the absence of these systemic entraining signals, the cell peripheral clocks are reliant on *per2* function for entrainment and so we observe a strong disruption of clock gene expression under light dark cycle conditions. In an alternative explanation, the disrupted clock gene expression in the cell lines is the result of an abnormal growth state of these cells. Indeed, it is important to note that the *per2* KO cell lines took considerably longer than wild type cells to be established in culture, an observation possibly pointing to the existence of some abnormalities in cell growth and proliferation. Given that these cell cultures clearly experienced a pronounced bottleneck in their early growth, then cells which survived the early stages of this selective process may have been exhibited changes in their clock gene expression profile. In this scenario, the presence of a disrupted clock may have compensated for other cellular properties that resulted from the *per2* KO. To test these two hypotheses, we prepared explant cultures of adult fins and hearts and examined clock gene expression under light dark cycle conditions. In these cultures, we observed normal rhythmic clock gene expression profiles, a result that would tend to favor our second hypothesis where it is the particular growth or cell proliferation phenotype of the cell lines that accounts for the abnormal clock gene expression rather than the lack of a key systemic entraining factor.

#### **4.3 *Per2* gene function affects clock-controlled gene expression**

The role of *per2* in the phase setting of the tissue specific rhythmic expression of the core clock genes in zebrafish, *in vivo*, raises a new question: Does the *per2* gene play a role in the circadian clock

regulation of tissue specific physiology, *in vivo*? In order to address this question, first of all, we performed an analysis of CCG expression in the liver, heart and muscle of the *per2* KO line. In particular, we focused attention on the expression of genes that are involved in the regulation of molecular mechanisms which underlie important physiological processes ranging from metabolism, development, and maintenance of homeostasis, to basic cellular processes, including cell growth and division (proliferation), cell movement (migration), controlled cell death (apoptosis) and cell differentiation. We observed in *per2* KO heart tissues a significant impact of *per2* gene function on the rhythmic expression of the *p21*, *timp3*, *mef2a*, *cox62a* and *smad3a* genes. This apparent broad influence of the *per2* gene on clock-controlled gene expression in the heart, suggest that *per2* may play a key role in the circadian clock-mediated regulation of important cardiac functions. Indeed, it has already been demonstrated that disruption of circadian rhythms is a major contributor to heart pathophysiology. Furthermore, there is an increased sensitivity to myocardial infarction in the morning compared to the evening [282]. In mice the overexpression of a dominant-negative form of the CLOCK protein in cardiomyocytes, abolishes the rhythmic expression of several cardiac CCGs, which overrides the circadian clock response in infarct size after ischemia/reperfusion [283]. Therefore, cardiac-specific circadian rhythms are clearly important contributors for the heart's response to external stress. However, the molecular mechanisms underlying the circadian clock regulation of cardiac function are still poorly understood. In parallel, we investigated the involvement of the *per2* gene in the circadian clock regulation of liver-specific CCGs *cyp1a*, *ppargc1b*, *hnf1a*, *impdh2*, *got1*, *got2a*, *asns*, *glula*, *glud1b* and *gpt2l*. The results revealed a pathway-specific influence of the *per2* gene on clock-controlled gene expression in the liver. In particular, we observed, in *per2* KO liver tissues, a reduction of the peak expression level of *cyp1a*, and a phase shift of the expression pattern for *ppargc1b* and *hnf1a*. However, the *impdh2* gene shows a normal rhythmic expression pattern. Likewise, we analyzed the clock-controlled expression of genes encoding key or rate-limiting enzymes involved in the biosynthetic pathways for non-essential amino acids, in order to verify the role of the *per2* gene in the regulation of this important liver-specific metabolic process. Here again we observed a pathway-specific effect of the loss of *per2* gene function. The *got1*, *got2a*, *asns*, *glud1b* and *gpt2l* genes all showed loss of rhythmic expression in the *per2* KO liver, whereas the rhythmic expression of *glula* appeared to be unaffected. The *Per2* gene has already been associated with the regulation of liver-specific metabolic pathways in mammals. In particular, Rev-erba and PPARα interact with the PER2 protein in the liver to regulate the transcription of their target genes [281]. Moreover, using *per2* KO mice, it has been shown that PER2 directly represses the nuclear receptor

PPAR $\gamma$ , critical for adipogenesis, insulin sensitivity, and inflammatory response, by affecting its recruitment to target promoters and thereby transcriptional activation [284]. Furthermore, *Per2* KO lines are more predisposed to liver fibrosis after carbon tetrachloride injection compared with wild-type controls. Therefore, these previous findings together with our own CCG expression analysis support the notion that the *per2* gene plays an important and selective role in liver physiology. Finally, we revealed disruption of rhythmic expression of the clock-controlled genes *myf6* and *hsf2* in the *per2* KO skeletal muscle. The *Myf6* gene exhibits a 6 hr phase shift of the expression pattern similar to that of *clock1*, while *hsf2* exhibits a strong reduction of the amplitude of its rhythmic expression in the skeletal muscle. It is interesting to note how the peak expression of the *hsf2* gene precedes the light phase in the WT line, thus suggesting that the clock regulation of the *hsf2* gene could play an important role in the anticipation of protein-damaging stresses generated during daytime locomotor activity. Therefore, in the future, it will be interesting to evaluate if the mechanism underlying the response to proteotoxic stresses is affected in the *per2* KO zebrafish line.

CCG expression analysis of liver, muscle and heart in the *per2* KO line implies that the *per2* gene may contribute to the regulation of CCG expression via two different mechanisms: a) The expression of the CCGs that exhibit a 6 hours phase shift of their rhythmic pattern in the mutant may rely on the same mechanism that sets the phase of rhythmic *clock1* and *cry1a* gene expression while b) the clock-controlled genes that exhibit a reduced rhythm amplitude in the mutant may be targeted by a distinct molecular mechanism. Therefore, in the future, a sequence analysis of the promoter region of these different classes of genes would be valuable to identify new *cis*-acting elements which could be targeted by transcriptional protein complexes in which the *per2* gene may exert its coactivator or corepressor functions.

#### **4.4 *Per2* gene function influences circadian output systems in zebrafish**

We next revealed that *per2* not only regulates the molecular circadian clock, but also clock-controlled behavior. We observed a severe impact on rhythmic locomotor activity of the *per2* KO larvae, mainly, under constant dark conditions, whereas minor effects were revealed under constant light and light/dark cycle conditions. We speculate that this major effect observed under constant dark conditions could reflect the absence of light-driven acute changes in locomotor activity, combined with the alteration of clock-controlled behavioral output due to the loss of Per2 function.

The *per2* gene function involvement in the circadian regulation of the cell cycle has been widely demonstrated in mammals [161], [164]–[166], [200], [204]. Here we observed a robust effect of the loss of *per2* gene function on setting the phase of rhythmic expression pattern of *p21*, *cyclin B1* and *cyclin A2* in adult fin tissues. All genes show an increase of the peak expression level and 6 hours phase delay of the rhythmic expression pattern in the *per2* KO fins. It is important to note that in the same tissues where we observe abnormal expression of these cell cycle regulators, rhythmic expression of the core clock genes is apparently normal indicating that the *per2*-regulated expression of clock-controlled cell cycle regulators in peripheral tissues is clearly a distinct mechanism from the transcriptional control circuits within the core circadian clock mechanism itself. Namely the cell cycle control represents a specific, clock output function for *per2*. We also observed that the rhythmic expression of *p21*, *cyclin A2* and *cyclin B1* is strongly affected in the *per2* KO cell lines, with a significant reduction of the basal level of expression of all these cell cycle regulators in the embryo-derived cell cultures, suggesting that *per2* plays a role in setting the basal expression levels of these three cell cycle regulators. In the *per2* KO adult fin-derived cell line, the expression level of *p21* is much higher than WT, with a possible 6h phase delay of the rhythmic expression, indicating that *per2* plays a negative role in regulating the expression of *p21*. Based on previous reports, it is tempting to speculate that P53 plays a role in the mechanism whereby Per2 regulates *p21* expression. Thus, it has been demonstrated that the P53 protein, in response to DNA damage, activates the transcription of a variety of genes, including the cell cycle inhibitor *p21* and it has also been reported that the PER2 protein modulates P53 stability and transcriptional activity in normal human cells [285]. Instead, the expression levels of *cyclin A2* and *cyclin B1* genes were not affected in these *per2* KO adult fin cell lines. Thus, our results point to considerable cell type specificity in the control of cell cycle regulators by Per2. Given the remarkable impact of *per2* gene function on the regulation of the expression levels of these important regulators of the cell cycle, we speculate that *per2* may play a key role during the early stages of the zebrafish embryonic development. However, the normal early embryonic development observed in *per2* KO mutants would tend to argue against this.

Previously, it has been shown that M phase progression in zebrafish adult fin tissue, shows a light-entrained, circadian clock regulation [210]. Our quantification of the levels of mitosis throughout the light dark cycle, revealed a dampened M-phase rhythm in the *per2* KO fin tissues. The dysregulation of M phase progression, together with the affected circadian gene expression of *p21*, could indicate that *per2* may play a functional role at the level of G1/S cell cycle checkpoint. In order to characterize in more detail the cell cycle progression in the absence of *per2* gene function we also compared cell

cycle progression in *per2* KO embryo-derived fibroblast cell lines with the corresponding WT cell line. The results of the FACS analysis revealed that the *per2* KO has a lower number of cells in the G2/M phase and a higher number of cells in G1 with respect to the WT. The higher number of the *per2* KO cells in G1 phase indicates a cell cycle delay in G1 phase. This result would be consistent with a positive role for *per2* in regulating the progression of the cell cycle via the G1/S cell cycle checkpoint. However, further investigations are necessary to unravel the molecular mechanism underlying *per2* regulation of the cell cycle in zebrafish. In order to verify the impact of *per2* gene function on regulation of the cell cycle in zebrafish *in vivo*, we tested whether the regenerative capacity of the caudal fin was affected in the *per2* KO adult line. Our results failed to show any significant difference in the fin regrowth rate of the *per2* KO line with respect to WT control fish following fin amputation. However, this result does not exclude that other tissues that are characterized by a high regenerative capacity in zebrafish, such as the heart, may show an abnormal regrowth rate. Indeed, the heart regeneration process in zebrafish may involve the contribution of different molecular mechanisms and signaling pathways with respect to the fin tissues. Given the robust alteration in rhythmic expression of the core clock and clock-controlled genes in the *per2* KO heart, in the future, it will be interesting to verify if the heart regeneration capacity of the *per2* ko line is affected.

#### **4.4.1 Does *per2* gene function play a role in the regulation of the FEO in zebrafish?**

In the last few years, it has been hypothesized that the *per2* gene plays a role in the regulation of the FEO. In particular, it was reported that FAA was absent in *per2* KO mice maintained under a restricted feeding regime [55], [56], [194]. This finding suggested a possible connection between the FEO and the light entrainable oscillator (LEO) in mammals. However, it has been recently reported that different lines of *Per2* mutant mice (both the *lhc* and *Brdm1* strains) exhibited robust FAA [196]. To date, the contribution of *per2* gene function to the regulation of the FEO remains unclear. Our results revealed that the *per2* KO line exhibited normal FAA under LD conditions. This result is consistent with the results published by Pendergast and colleagues [196], which demonstrated that the *Brdm1 mPeriod2* loss of function line as well as other single *Period* gene mutant mouse strains have normal FAA. In zebrafish, it has been demonstrated that FAA persists under restricted feeding and constant conditions of illumination [114]. The persistence of FAA in the *per2* KO line that we have observed under LD conditions does not exclude a potential contribution of LEO clock components in compensating for the loss of *per2* function. Therefore, we also tested the *per2* KO and

WT lines for evidence of continuing FAA activity under constant darkness conditions. Our preliminary results do not allow us to draw a definitive conclusion, since both lines show a free running rhythm of rhythmic locomotor activity, although the WT line shows a weaker level of locomotor activity with respect to the *per2* KO line. However, clearly this experiment will need to be repeated carefully in order to be able to draw clearer conclusions.

#### **4.5 Interactions between the circadian clock and TGF- $\beta$ signaling pathway in zebrafish**

Previous studies have implied the presence of connections between the circadian clock and TGF- $\beta$  signaling [236], [237], [242], [275], [286], however, the precise details of the mechanisms that bridge these two signaling systems remain poorly understood. In collaboration with the Gothilf lab, we have explored the interactions between the circadian clock and TGF- $\beta$  signaling at the molecular and behavioral levels by the use of zebrafish cell-lines as well as by *in vivo* analysis. Furthermore, we have demonstrated that TGF- $\beta$  is necessary for normal circadian clock function. The results of the transcriptome analysis performed by the Gothilf lab tend to support previous studies indicating that *Smad3* is expressed with a circadian rhythm [236], [237], and reveal that *Smad3* rhythmic expression is present both in whole zebrafish larvae and the adult zebrafish brain, with peak levels at the beginning of the subjective day. In support of a clock control of *Smad3* expression, our study of alterations in gene expression in the *per2* KO mutant line revealed a loss of rhythmic *Smad3* expression in the heart. Furthermore, the expression of two additional TGF- $\beta$  related genes, *Smad7* and *Tgfb1*, also appears to be under circadian clock control in the zebrafish embryo and in adult zebrafish pineal glands with a peaking of expression during the middle of the dark period. It is tempting to speculate that the different phases of expression for these TGF- $\beta$  related genes may reflect regulation by different enhancer elements that are targeted by the circadian clock. For example, the E-box and RORE enhancers which direct circadian rhythms of CCGs gene expression in zebrafish [10] show different phases of rhythmic expression which differ by around 12 hours, with E-box (Clock:Bmal) driven expression peaking in the early light period while RORE (RevErb /ROR) driven expression peaks during the early night [287].

Previous results have revealed that *Smad3a* is rhythmically expressed in both central and peripheral circadian clock pacemakers, namely in the mouse SCN and zebrafish pineal [237], the mouse liver as well as in various cell-lines [236]. While studies in mammals have suggested that the expression of TGF- $\beta$  itself is under circadian clock regulation [237], the Gothilf lab zebrafish transcriptome analysis failed to detect rhythmic expression of either *Tgfb*, *Tgfb2*, or *Tgfb3*. It is therefore possible that the

precise elements of the mechanism linking the clock with TGF- $\beta$  signaling have been subject to change during vertebrate evolution. An important limitation of our studies has been the reliance on measuring mRNA levels to explore circadian clock regulation. Of course, this does not automatically mean that protein levels are subject to the same pattern of temporal control. However, given that cycling protein levels for TGF- $\beta$  signaling pathway elements have been reported in the mammalian SCN [237], it seems likely that a comparable protein rhythmicity also exists in zebrafish. However, it will clearly be vital to validate many of our results by western blotting or quantitative *in situ* immunohistochemistry analysis using antibodies that are raised against zebrafish proteins.

We have revealed that pharmacological inhibition of TGF- $\beta$  results in a lengthening of the period length and a consequent phase delay and a decrease in amplitude of rhythmic expression of the core clock gene *per1b* in PAC-2 cells, and a phase delay in the rhythmic expression of *per1b* mRNA *in vivo*. Since *per1b* represents a component of the core circadian clock mechanism, these documented shifts in *per1b* promoter activity and mRNA expression are highly likely to reflect a general alteration in the dynamic properties of the molecular mechanism of the circadian clock itself. Interestingly, pharmacological indirect activation of TGF- $\beta$  signaling using Alantolactone also caused a decrease in amplitude and a shortening of the period length of rhythmic *per1b* expression in PAC-2 cells. We have interpreted this result as indicating that any disruption to the TGF- $\beta$  signaling cascade, will in turn disrupt the activity of the molecular circadian clock. However, it is also important to keep in mind that these effects might also be due to the effects of Alantolactone on other cellular pathways, even though previous evidence suggests that Alantolactone does not have any significant effect on non-cancerous cells as judged by analyzing various parameters [259]. Nevertheless, in support of a consistent effect of disrupted TGF- $\beta$  signaling on the circadian clock function, is previous evidence from Kon et al. [234] which showed that intraperitoneal injection of TGF- $\beta$  towards the end of the night caused a 3 hours advance in rhythmic *Per1* expression in the kidney and adrenal gland. Differences in the precise consequence for clock rhythmicity between the two studies might be due to the inherent differences in the length of the treatment (chronic vs. acute). Pharmacological inhibition of TGF- $\beta$  affected not only the molecular circadian clock, but also clock-controlled behavior as measured by alterations in the kinetics of clock-controlled rhythms of locomotor activity in larvae. This effect on locomotor activity was observed under various lighting conditions which failed to mask the effects of the inhibitor. Interestingly, the period lengthening and phase delay in rhythmic locomotor activity of inhibitor-treated larvae closely resembled the observed period lengthening and phase delay in *per1b* transcription that we documented *in vitro*. Therefore, it is

reasonable to conclude that the effects we have documented upon inhibition of TGF- $\beta$  signaling at the behavioral level are based upon corresponding changes in the molecular mechanism of the core circadian clock that we have revealed in our cell line model. In this regard, it will be interesting to test whether TGF- $\beta$  inhibition influences other circadian controlled behaviors, such as temporal feeding patterns. Furthermore, it is important to consider that the two ways interaction between the circadian clock and TGF- $\beta$  signaling may potentially influence other outputs of both systems. Thus, the circadian expression pattern of *smad3* may in turn influence the timing of *smad2/3: smad4* dependent transcription, and thereby indirectly lead to circadian oscillations in *smad*-controlled genes. In addition, the influence of *smad2/3: smad4* on *Per1* function may potentially influence the expression of CCGs that is independent of a direct influence by TGF- $\beta$  signaling. Generally, a better understanding of the cross talk between these two key cellular mechanisms will be an important goal for future studies given that shared outputs of TGF- $\beta$  signaling and the circadian clock include the cell cycle and apoptosis, and common outcomes upon disruption of these two interconnected systems include tumorigenesis and tumor progression.

## 5 Supplementary Information

WT vs. <i>per2</i> KO embryos					
One-way ANOVA					
<i>Clock1</i>		<i>Cry1a</i>		<i>Per1b</i>	
WT	<i>Per2</i> KO	WT	<i>Per2</i> KO	WT	<i>Per2</i> KO
***p<0.001	***p<0.001	***p<0.001	***p<0.001	***p<0.001	***p<0.001
Tukey's post-test (peak vs trough)					
<i>Clock1</i>		<i>Cry1a</i>		<i>Per1b</i>	
WT	<i>Per2</i> KO	WT	<i>Per2</i> KO	WT	<i>Per2</i> KO
***p<0.001	***p<0.001	***p<0.001	***p<0.001	***p<0.001	***p<0.001

**Table S1:** Statistical analysis of the figure 11. Significant thresholds are indicated by asterisks (\*\*\* p<0.001, \*\*p<0.01, \*p<0.05).

Figure 12	Gene	Genotype	Goodness of fit	95% CI (h)	P value	Acrophase (h)
Brain	Clock1	WT	0,001	17,5 to 17,7	p < 0.001	17,6
		Per2 KO	0,015	18,37 to 19,23	p < 0.01	18,8
	Cry1a	WT	0,053	10,72 to 12,48	p < 0.05	11,6
		Per2 KO	0,028	10,97 to 12,23	p < 0.02	11,6
Gut	Clock1	WT	0,024	19,51 to 20,49	p < 0.02	20,0
		Per2 KO	0,065	21,5 to 23,3	p > 0.05 (ns)	22,4
	Cry1a	WT	0,062	11,31 to 13,09	p > 0.05 (ns)	12,2
		Per2 KO	0,034	10,92 to 12,28	p < 0.02	11,6
Eyes	Clock1	WT	0,041	16,85 to 18,35	p < 0.05	17,6
		Per2 KO	0,01	19,05 to 19,75	p < 0.005	19,4
	Cry1a	WT	0,062	11,31 to 13,09	p > 0.05 (ns)	12,2
		Per2 KO	0,034	10,92 to 12,28	p < 0.02	11,6
Muscle	Clock1	WT	0,028	20,04 to 21,16	p < 0.02	20,6
		Per2 KO	0,039	22,27 to 23,73	p < 0.05	23,0
	Cry1a	WT	0,018	11,07 to 12,13	p < 0.01	11,6
		Per2 KO	0,088	11,14 to 13,26	p > 0.05	12,2
Liver	Clock1	WT	0,023	16,43 to 17,57	p < 0.01	17,0
		Per2 KO	0,059	20,95 to 22,65	p < 0.05	21,8
	Cry1a	WT	0,03	10,94 to 12,26	p < 0.02	11,6
		Per2 KO	0,09	11,12 to 13,28	p > 0.05 (ns)	12,2
Fin	Clock1	WT	0,011	21,41 to 22,19	p < 0.005	21,8
		Per2 KO	0,004	22,74 to 23,26	p < 0.001	23,0
	Cry1a	WT	0,03	12,78 to 14,02	p < 0.02	13,4
		Per2 KO	0,017	13,53 to 14,47	p < 0.01	14,0
Heart	Clock1	WT	0,043	18,07 to 19,53	p < 0.05	18,8
		Per2 KO	0,017	21,91 to 22,89	p < 0.01	22,4
	Cry1a	WT	0,018	13,53 to 14,47	p < 0.01	14,0
		Per2 KO	0,023	13,45 to 14,55	p < 0.01	14,0
<b>Figure 11</b>						
Embryo	Clock1	WT	0,019	11,69 to 12,71	p < 0.01	12,2
		Per2 KO	0,005	12,54 to 13,06	p < 0.005	12,8
	Cry1a	WT	0,103	21,29 to 23,51	p > 0.05 (ns)	22,4
		Per2 KO	0,0	22,98 to 23,02	p < 0.001	23,0
	Per1b	WT	0,099	3,92 to 6,08	p > 0.05 (ns)	5,0
		Per2 KO	0,094	3,94 to 6,06	p > 0.05 (ns)	5,0
<b>Figure 14</b>						
Fin cultured	Clock1	WT	0,173	5,1 to 8,1	p > 0.05 (ns)	6,6
		Per2 KO	0,12	5,36 to 7,84	p > 0.05(ns)	6,6
	Cry1a	WT	0,173	5,1 to 8,1	p > 0.05 (ns)	6,6
		Per2 KO	0,12	5,36 to 7,84	p > 0.05 (ns)	6,6
	Per1b	WT	0,006	9,92 to 10,48	p < 0.005	10,2
		Per2 KO	0,008	10,47 to 11,13	p < 0.005	10,8

**Table S1.1:** Acrophase (circadian peak time) of the rhythmic expression pattern of *cry1a*, *clock1* and *per1b* in embryo and organs/tissues (figure 11, 12 and 14), were calculated, using the single cosinor procedure program (Acro.exe, version 3.5, designed by Dr. Refinetti).

	One-way ANOVA				Tukey's post-test (peak vs trough)			
	<i>Clock1</i>		<i>Cry1a</i>		<i>Clock1</i>		<i>Cry1a</i>	
	WT	<i>Per2</i> KO	WT	<i>Per2</i> KO	WT	<i>Per2</i> KO	WT	<i>Per2</i> KO
<b>Liver</b>	***p<0.001	***p<0.001	***p<0.001	*p<0.05	***p<0.001	***p<0.001	***p<0.001	*p<0.05
<b>Gut</b>	***p<0.001	***p<0.001	***p<0.001	***p<0.001	***p<0.001	***p<0.001	***p<0.001	***p<0.001
<b>Muscle</b>	**p<0.01	***p<0.001	***p<0.001	***p<0.001	***p<0.001	***p<0.001	***p<0.001	***p<0.001
<b>Heart</b>	***p<0.001	***p<0.001	***p<0.001	***p<0.001	***p<0.001	***p<0.001	***p<0.001	***p<0.001
<b>Brain</b>	*p<0.05	**p<0.01	***p<0.001	***p<0.001	*p<0.05	**p<0.01	**p<0.01	**p<0.01
<b>Eyes</b>	***p<0.001	***p<0.001	***p<0.001	***p<0.001	***p<0.001	***p<0.001	***p<0.001	***p<0.001
<b>Fin</b>	***p<0.001	***p<0.001	***p<0.001	***p<0.001	***p<0.001	***p<0.001	***p<0.001	***p<0.001

**Table S2:** Statistical analysis of the figure 12. Significant thresholds are indicated by asterisks (\*\*\* p<0.001, \*\*p<0.01, \*p<0.05).

<b>WT vs. <i>per2</i> KO fin cell lines</b>					
<i>Cry1</i>	Sidak's post-test	Two-way ANOVA	<i>Clock1</i>	Sidak's post-test	Two-way ANOVA
ZT3	*** p<0.001	*** p<0.001	ZT3	ns p>0.05	*** p<0.001
ZT9	*** p<0.001		ZT9	ns p>0.05	
ZT15	*** p<0.001		ZT15	***p<0,001	
ZT21	ns p>0.05		ZT21	*p<0.05	
ZT3 2° day	*** p<0.001		ZT3 2° day	**p<0.01	
<b>WT vs. <i>per2</i> KO embryonic cell lines</b>					
<i>Per1b</i>	Sidak's post-test	Two-way ANOVA			
ZT3	*** p<0.001	*** p<0.001			
ZT9	ns p>0.05				
ZT15	ns p>0.05				
ZT21	*** p<0.001				
ZT3 2° day	*** p<0.001				
<b>WT vs. <i>per2</i> KO embryonic cell lines</b>					
<i>Clock1</i>	Sidak's post-test	Two-way ANOVA	<i>Per1b</i>	Sidak's post-test	Two-way ANOVA
ZT3	*** p<0.001	*** p<0.001	ZT3	*** p<0.001	*** p<0.001
ZT9	*** p<0.001		ZT9	*p<0.05	
ZT15	*** p<0.001		ZT15	ns p>0.05	
ZT21	*** p<0.001		ZT21	ns p>0.05	
ZT3 2° day	*** p<0.001		ZT3 2° day	*** p<0.001	

**Table S3:** Statistical analysis of the figure 13. Significant thresholds are indicated by asterisks (\*\*\* p<0.001, \*\*p<0.01, \*p<0.05).

One-way ANOVA						
	<i>Clock1</i>		<i>Cry1a</i>		<i>Per1b</i>	
	WT	<i>Per2</i> KO	WT	<i>Per2</i> KO	WT	<i>Per2</i> KO
<b>Cultured Fin</b>	*** p<0.001	*** p<0.001	*** p<0.001	*** p<0.001	*** p<0.001	*** p<0.001
<b>Cultured heart</b>	ns p>0.05	ns p>0.05	*** p<0.001	*** p<0.001		
<b>Tukey's post-test (peak vs trough)</b>						
	<i>Clock1</i>		<i>Cry1a</i>		<i>Per1b</i>	
	WT	<i>Per2</i> KO	WT	<i>Per2</i> KO	WT	<i>Per2</i> KO
<b>Cultured Fin</b>	**p<0.01	*p<0.05	*** p<0.001	*** p<0.001	*** p<0.001	*** p<0.001
<b>Cultured heart</b>	ns p>0.05	ns p>0.05	*** p<0.001	*** p<0.001		

**Table S4:** Statistical analysis of the figure 14 and figure 15. Significant thresholds are indicated by asterisks (\*\*\* p<0.001, \*\*p<0.01, \*p<0.05).

<b>WT vs. <i>per2</i> KO heart tissues</b>					
<i>Timp3</i>	Sidak's post-test	Two-way ANOVA	<i>P21</i>	Sidak's post-test	Two-way ANOVA
ZT3	*** p<0.001	*** p<0.001	ZT3	ns p>0.05	*** p<0.001
ZT9	*** p<0.001		ZT9	*** p<0.001	
ZT15	*p<0.05		ZT15	*** p<0.001	
ZT21	ns p>0.05		ZT21	ns p>0.05	
ZT3 2° day	**p<0.01		ZT3 2° day	ns p>0.05	
<i>Mef2a</i>	Sidak's post-test	Two-way ANOVA	<i>Cox62a</i>	Sidak's post-test	Two-way ANOVA
ZT3	*** p<0.001	*** p<0.001	ZT3	*** p<0.001	*** p<0.001
ZT9	ns p>0.05		ZT9	ns p>0.05	
ZT15	ns p>0.05		ZT15	*** p<0.001	
ZT21	*** p<0.001		ZT21	*** p<0.001	
ZT3 2° day	*** p<0.001		ZT3 2° day	*** p<0.001	
<i>Smad2a</i>	Sidak's post-test	Two-way ANOVA			
ZT3	*** p<0.001	*** p<0.001			
ZT9	*p<0.05				
ZT15	ns p>0.05				
ZT21	**p<0.01				
ZT3 2° day	ns p>0.05				

**Table S5:** Statistical analysis of the figure 16. Significant thresholds are indicated by asterisks (\*\*\* p<0.001, \*\*p<0.01, \*p<0.05).

<b>WT vs. <i>per2</i> KO liver tissues</b>					
<i>Impdh2</i>	Sidak's post-test	Two-way ANOVA	<i>Hnf1a</i>	Sidak's post-test	Two-way ANOVA
ZT3	**p<0.01	*** p<0.001	ZT3	*** p<0.001	*** p<0.001
ZT9	ns p>0.05		ZT9	**p<0.01	
ZT15	**p<0.01		ZT15	ns p>0.05	
ZT21	ns p>0.05		ZT21	*** p<0.001	
ZT3 2° day	*** p<0.001		ZT3 2° day	ns p>0.05	
<i>Cyp1a</i>	Sidak's post-test	Two-way ANOVA	<i>Ppargc1b</i>	Sidak's post-test	Two-way ANOVA
ZT3	*** p<0.001	*** p<0.001	ZT3	ns p>0.05	*** p<0.001
ZT9	*p<0.05		ZT9	*p<0.05	
ZT15	ns p>0.05		ZT15	*** p<0.001	
ZT21	*** p<0.001		ZT21	ns p>0.05	
ZT3 2° day	ns p>0.05		ZT3 2° day	ns p>0.05	

**Table S6:** Statistical analysis of the figure 17. Significant thresholds are indicated by asterisks (\*\*\* p<0.001, \*\*p<0.01, \*p<0.05).

<b>WT vs. <i>per2</i> KO liver tissues</b>					
<i>Glu1a</i>	Sidak's post-test	Two-way ANOVA	<i>Asns</i>	Sidak's post-test	Two-way ANOVA
ZT3	*** p<0.001	*** p<0.001	ZT3	*** p<0.001	*** p<0.001
ZT9	ns p>0.05		ZT9	*p<0.05	
ZT15	*p<0.05		ZT15	ns p>0.05	
ZT21	*** p<0.001		ZT21	**p<0.01	
ZT3 2° day	ns p>0.05		ZT3 2° day	*** p<0.001	
<i>Gtp2l</i>	Sidak's post-test	Two-way ANOVA	<i>Glud1b</i>	Sidak's post-test	Two-way ANOVA
ZT3	*** p<0.001	*** p<0.001	ZT3	ns p>0.05	*** p<0.001
ZT9	ns p>0.05		ZT9	*** p<0.001	
ZT15	ns p>0.05		ZT15	ns p>0.05	
ZT21	**p<0.01		ZT21	ns p>0.05	
ZT3 2° day	ns p>0.05		ZT3 2° day	ns p>0.05	
<i>Got1</i>	Sidak's post-test	Two-way ANOVA	<i>Got2b</i>	Sidak's post-test	Two-way ANOVA
ZT3	*** p<0.001	*** p<0.001	ZT3	*p<0.05	*** p<0.001
ZT9	*** p<0.001		ZT9	*** p<0.001	
ZT15	*** p<0.001		ZT15	ns p>0.05	
ZT21	ns p>0.05		ZT21	**p<0.01	
ZT3 2° day	*** p<0.001		ZT3 2° day	*p<0.05	

**Table S7:** Statistical analysis of the figure 18. Significant thresholds are indicated by asterisks (\*\*\* p<0.001, \*\*p<0.01, \*p<0.05).

<b>WT vs <i>per2</i> KO muscle tissues</b>					
<i>Hsf2</i>	Sidak's post-test	Two-way ANOVA	<i>Myf6</i>	Sidak's post-test	Two-way ANOVA
ZT3	*** p<0.001	*** p<0.001	ZT3	*** p<0.001	*** p<0.001
ZT9	ns p>0.05		ZT9	**p<0.01	
ZT15	ns p>0.05		ZT15	*** p<0.001	
ZT21	*** p<0.001		ZT21	*** p<0.001	
ZT3 2° day	ns p>0.05		ZT3 2° day	*** p<0.001	

**Table S8:** Statistical analysis of the figure 19. Significant thresholds are indicated by asterisks (\*\*\* p<0.001, \*\*p<0.01, \*p<0.05).

<b>WT vs. <i>per2</i> KO fin tissues</b>					
<b><i>P21</i></b>	<b>Sidak's post-test</b>	<b>Two-way ANOVA</b>	<b><i>Cyclin A2</i></b>	<b>Sidak's post-test</b>	<b>Two-way ANOVA</b>
ZT3	ns p>0.05	*** p<0.001	ZT3	ns p>0.05	*** p<0.001
ZT9	ns p>0.05		ZT9	ns p>0.05	
ZT15	*** p<0.001		ZT15	ns p>0.05	
ZT21	*** p<0.001		ZT21	*** p<0.001	
ZT3 2° day	ns p>0.05		ZT3 2° day	*** p<0.001	
<b><i>Cyclin B1</i></b>	<b>Sidak's post-test</b>	<b>Two-way ANOVA</b>			
ZT3	ns p>0.05	*** p<0.001			
ZT9	ns p>0.05				
ZT15	ns p>0.05				
ZT21	*** p<0.001				
ZT3 2° day	*** p<0.001				

**Table S9:** Statistical analysis of the figure 22. Significant thresholds are indicated by asterisks (\*\*\* p<0.001, \*\*p<0.01, \*p<0.05).

WT vs. <i>per2</i> KO Embryonic cell lines			WT vs. <i>per2</i> KO Fin cell lines		
<i>P21</i>	Sidak's post-test	Two-way ANOVA	<i>P21</i>	Sidak's post-test	Two-way ANOVA
ZT3	*** p<0.001	*** p<0.001	ZT3	*** p<0.001	*** p<0.001
ZT9	*** p<0.001		ZT9	*** p<0.001	
ZT15	**p<0.01		ZT15	*** p<0.001	
ZT21	*** p<0.001		ZT21	*** p<0.001	
ZT3 2° day	*** p<0.001		ZT3 2° day	*** p<0.001	
WT vs. <i>per2</i> KO Embryonic cell lines			WT vs. <i>per2</i> KO Fin cell lines		
<i>Cyclin A2</i>	Sidak's post-test	Two-way ANOVA	<i>Cyclin A2</i>	Sidak's post-test	Two-way ANOVA
ZT3	*p<0.05	*** p<0.001	ZT3	ns p>0.05	**p<0.01
ZT9	ns p>0.05		ZT9	ns p>0.05	
ZT15	ns p>0.05		ZT15	*p<0.05	
ZT21	*** p<0.001		ZT21	ns p>0.05	
ZT3 2° day	*** p<0.001		ZT3 2° day	**p<0.01	
<i>Cyclin B1</i>	Sidak's post-test	Two-way ANOVA	<i>Cyclin B1</i>	Sidak's post-test	Two-way ANOVA
ZT3	*** p<0.001	*** p<0.001	ZT3	*** p<0.001	*** p<0.001
ZT9	*** p<0.001		ZT9	ns p>0.05	
ZT15	*** p<0.001		ZT15	**p<0.01	
ZT21	*** p<0.001		ZT21	ns p>0.05	
ZT3 2° day	*** p<0.001		ZT3 2° day	*p<0.05	

**Table S10:** Statistical analysis of the figure 23. Significant thresholds are indicated by asterisks (\*\*\* p<0.001, \*\*p<0.01, \*p<0.05).

<b>WT vs. <i>per2</i> KO fin tissues</b>		
	<b>Sidak's post-test</b>	<b>Two-way ANOVA</b>
ZT4	ns p>0.05	Interaction: ns p>0.05  Sampling time: **p<0.01
ZT10	ns p>0.05	
ZT16	*p<0.05	
ZT22	ns p>0.05	
ZT4 2° day	ns p>0.05	

**Table S11:** Statistical analysis of the figure 24. Significant thresholds are indicated by asterisks (\*\*p<0.01, \*p<0.05).

<b>WT/<i>per2</i> KO Embryonic cell lines (FACS analysis)</b>		
<b>Cell cycle phases</b>	<b>Sidak's post-test</b>	<b>Two-way ANOVA</b>
<b>G1</b>	*** p<0.001	*** p<0.001
<b>S</b>	*p<0.05	
<b>G2/M</b>	*** p<0.001	

**Table S12:** Statistical analyses of the figure 25. Significant thresholds are indicated by asterisks (\*\*p<0.01, \*p<0.05).



## 6 References

- [1] C. S. PITTENDRIGH, “On temporal organization in living systems.,” *Harvey Lect.*, vol. 56, pp. 93–125.
- [2] C. S. Pittendrigh, “Temporal organization: reflections of a Darwinian clock-watcher.,” *Annu. Rev. Physiol.*, vol. 55, no. 1, pp. 16–54, Oct. 1993.
- [3] U. Albrecht, “Timing to Perfection: The Biology of Central and Peripheral Circadian Clocks,” *Neuron*, vol. 74, no. 2, pp. 246–260, Apr. 2012.
- [4] M. Menaker, J. S. Takahashi, and A. Eskin, “The physiology of circadian pacemakers.,” *Annu. Rev. Physiol.*, vol. 40, no. 1, pp. 501–26, Mar. 1978.
- [5] A. Balsalobre, F. Damiola, and U. Schibler, “A serum shock induces circadian gene expression in mammalian tissue culture cells.,” *Cell*, vol. 93, no. 6, pp. 929–37, Jun. 1998.
- [6] Y. Fukada and T. Okano, “Circadian clock system in the pineal gland.,” *Mol. Neurobiol.*, vol. 25, no. 1, pp. 19–30, Feb. 2002.
- [7] G. Vatine, D. Vallone, Y. Gothilf, and N. S. Foulkes, “It’s time to swim! Zebrafish and the circadian clock,” *FEBS Lett.*, vol. 585, no. 10, pp. 1485–1494, 2011.
- [8] P. Sassone-Corsi, D. Whitmore, and N. S. Foulkes, “Light acts directly on organs and cells in culture to set the vertebrate circadian clock.,” *Nature*, vol. 404, no. 6773, pp. 87–91, 2000.
- [9] M. P. Gerkema, W. I. L. Davies, R. G. Foster, M. Menaker, and R. A. Hut, “The nocturnal bottleneck and the evolution of activity patterns in mammals.,” *Proceedings. Biol. Sci.*, vol. 280, no. 1765, p. 20130508, Aug. 2013.
- [10] C. L. Partch, C. B. Green, and J. S. Takahashi, “Molecular architecture of the mammalian circadian clock,” *Trends Cell Biol.*, vol. 24, no. 2, pp. 90–99, 2014.
- [11] E. S. Maywood, J. E. Chesham, J. A. O’Brien, and M. H. Hastings, “A diversity of paracrine signals sustains molecular circadian cycling in suprachiasmatic nucleus circuits,” *Proc. Natl. Acad. Sci.*, vol. 108, no. 34, pp. 14306–14311, Aug. 2011.
- [12] F. W. Turek, “Circadian Neural Rhythms in Mammals,” *Annu. Rev. Physiol.*, vol. 47, no. 1, pp. 49–64, Oct. 1985.
- [13] M. R. Ralph, R. G. Foster, F. C. Davis, and M. Menaker, “Transplanted suprachiasmatic nucleus determines circadian period.,” *Science*, vol. 247, no. 4945, pp. 975–8, Feb. 1990.
- [14] R. Refinetti, C. M. Kaufman, and M. Menaker, “Complete suprachiasmatic lesions eliminate circadian rhythmicity of body temperature and locomotor activity in golden hamsters,” *J. Comp. Physiol. A*, vol. 175, no. 2, pp. 223–232, Aug. 1994.
- [15] M. S. Kafka, P. J. Marangos, and R. Y. Moore, “Suprachiasmatic nucleus ablation abolishes circadian rhythms in rat brain neurotransmitter receptors,” *Brain Res.*, vol. 327, no. 1–2, pp. 344–7, Feb. 1985.

- [16] C. P. Coomans *et al.*, “The suprachiasmatic nucleus controls circadian energy metabolism and hepatic insulin sensitivity.,” *Diabetes*, vol. 62, no. 4, pp. 1102–8, Apr. 2013.
- [17] S. Hattar, H. W. Liao, M. Takao, D. M. Berson, and K. W. Yau, “Melanopsin-Containing Retinal Ganglion Cells: Architecture, Projections, and Intrinsic Photosensitivity,” *Science (80-. )*, vol. 295, no. 5557, pp. 1065–1070, Feb. 2002.
- [18] I. Provencio, G. Jiang, W. J. De Grip, W. P. Hayes, and M. D. Rollag, “Melanopsin: An opsin in melanophores, brain, and eye.,” *Proc. Natl. Acad. Sci. U. S. A.*, vol. 95, no. 1, pp. 340–5, Jan. 1998.
- [19] H. J. Bailes and R. J. Lucas, “Melanopsin and inner retinal photoreception.,” *Cell. Mol. Life Sci.*, vol. 67, no. 1, pp. 99–111, Jan. 2010.
- [20] R. J. Lucas, S. Hattar, M. Takao, D. M. Berson, R. G. Foster, and K.-W. Yau, “Diminished Pupillary Light Reflex at High Irradiances in Melanopsin-Knockout Mice,” *Science (80-. )*, vol. 299, no. 5604, pp. 245–247, Jan. 2003.
- [21] S. Panda *et al.*, “Melanopsin (Opn4) requirement for normal light-induced circadian phase shifting.,” *Science*, vol. 298, no. 5601, pp. 2213–6, Dec. 2002.
- [22] N. F. Ruby *et al.*, “Role of melanopsin in circadian responses to light.,” *Science*, vol. 298, no. 5601, pp. 2211–3, Dec. 2002.
- [23] S. Panda *et al.*, “Melanopsin is required for non-image-forming photic responses in blind mice.,” *Science*, vol. 301, no. 5632, pp. 525–7, Jul. 2003.
- [24] J. Hannibal, “Neurotransmitters of the retino-hypothalamic tract,” *Cell Tissue Res.*, vol. 309, no. 1, pp. 73–88, Jul. 2002.
- [25] J. Hannibal, M. Møller, O. P. Ottersen, and J. Fahrenkrug, “PACAP and glutamate are co-stored in the retinohypothalamic tract.,” *J. Comp. Neurol.*, vol. 418, no. 2, pp. 147–55, Mar. 2000.
- [26] D. D. Ginty *et al.*, “Regulation of CREB phosphorylation in the suprachiasmatic nucleus by light and a circadian clock.,” *Science*, vol. 260, no. 5105, pp. 238–41, Apr. 1993.
- [27] U. Albrecht, Z. S. Sun, G. Eichele, and C. C. Lee, “A differential response of two putative mammalian circadian regulators, mper1 and mper2, to light.,” *Cell*, vol. 91, no. 7, pp. 1055–64, Dec. 1997.
- [28] K. Bae, X. Jin, E. S. Maywood, M. H. Hastings, S. M. Reppert, and D. R. Weaver, “Differential functions of mPer1, mPer2, and mPer3 in the SCN circadian clock.,” *Neuron*, vol. 30, no. 2, pp. 525–36, May 2001.
- [29] C. S. Colwell, “Linking neural activity and molecular oscillations in the SCN,” *Nat. Rev. Neurosci.*, vol. 12, no. 10, pp. 553–569, Oct. 2011.
- [30] A. Balsalobre *et al.*, “Resetting of circadian time in peripheral tissues by glucocorticoid signaling.,” *Science*, vol. 289, no. 5488, pp. 2344–7, Sep. 2000.

- [31] T. Yamamoto *et al.*, “Acute Physical Stress Elevates Mouse *Period1* mRNA Expression in Mouse Peripheral Tissues via a Glucocorticoid-responsive Element,” *J. Biol. Chem.*, vol. 280, no. 51, pp. 42036–42043, Dec. 2005.
- [32] A. B. Reddy *et al.*, “Glucocorticoid signaling synchronizes the liver circadian transcriptome,” *Hepatology*, vol. 45, no. 6, pp. 1478–1488, Jun. 2007.
- [33] A. C. Liu, W. G. Lewis, and S. A. Kay, “Mammalian circadian signaling networks and therapeutic targets,” *Nat. Chem. Biol.*, vol. 3, no. 10, pp. 630–639, Oct. 2007.
- [34] B. FRISCH and J. ASCHOFF, “Circadian rhythms in honeybees: entrainment by feeding cycles,” *Physiol. Entomol.*, vol. 12, no. 1, pp. 41–49, Mar. 1987.
- [35] T. Boujard’ and J. F. Leatherland, “Circadian rhythms and feeding time in fishes\*,” 1992.
- [36] H. Abe and S. Sugimoto, “Food-anticipatory response to restricted food access based on the pigeon’s biological clock,” *Anim. Learn. Behav.*, vol. 15, no. 4, pp. 353–359, Dec. 1987.
- [37] S. C. Edmonds and N. T. Adler, “Food and light as entrainers of circadian running activity in the rat,” *Physiol. Behav.*, vol. 18, no. 5, pp. 915–919, May 1977.
- [38] B. Jilge and H. Stähle, “Restricted food access and light-dark: impact of conflicting zeitgebers on circadian rhythms of the rabbit.,” *Am. J. Physiol.*, vol. 264, no. 4 Pt 2, pp. R708-15, Apr. 1993.
- [39] R. E. Mistlberger, “Food-anticipatory circadian rhythms: concepts and methods,” *Eur. J. Neurosci.*, vol. 30, no. 9, pp. 1718–1729, Nov. 2009.
- [40] F. K. Stephan, J. M. Swann, and C. L. Sisk, “Anticipation of 24-hr feeding schedules in rats with lesions of the suprachiasmatic nucleus.,” *Behav. Neural Biol.*, vol. 25, no. 3, pp. 346–63, Mar. 1979.
- [41] K.-A. Stokkan, S. Yamazaki, H. Tei, Y. Sakaki, and M. Menaker, “Entrainment of the Circadian Clock in the Liver by Feeding,” *Science (80-. )*, vol. 291, no. 5503, pp. 490–493, Jan. 2001.
- [42] F. Damiola, N. Le Minh, N. Preitner, B. Kornmann, F. Fleury-Olela, and U. Schibler, “Restricted feeding uncouples circadian oscillators in peripheral tissues from the central pacemaker in the suprachiasmatic nucleus.,” *Genes Dev.*, vol. 14, no. 23, pp. 2950–61, Dec. 2000.
- [43] R. Hara *et al.*, “Restricted feeding entrains liver clock without participation of the suprachiasmatic nucleus.,” *Genes Cells*, vol. 6, no. 3, pp. 269–78, Mar. 2001.
- [44] G. Asher, H. Reinke, M. Altmeyer, M. Gutierrez-Arcelus, M. O. Hottiger, and U. Schibler, “Poly(ADP-Ribose) Polymerase 1 Participates in the Phase Entrainment of Circadian Clocks to Feeding,” *Cell*, vol. 142, no. 6, pp. 943–953, Sep. 2010.
- [45] A. Mukherji, A. Kobiita, and P. Chambon, “Shifting the feeding of mice to the rest phase creates metabolic alterations, which, on their own, shift the peripheral circadian clocks by 12

- hours,” *Proc. Natl. Acad. Sci.*, vol. 112, no. 48, pp. E6683–E6690, Dec. 2015.
- [46] T. Wu, Y. Ni, F. Zhuge, and Z. Fu, “Resetting Process of Peripheral Circadian Gene Expression after the Combined Reversal of Feeding Schedule and Light/Dark Cycle Via a 24-h Light Period Transition in Rats,” *Physiol. Res*, vol. 59, pp. 581–590, 2010.
- [47] A. J. Davidson, B. J. Aragona, R. M. Werner, E. Schroeder, J. C. Smith, and F. K. Stephan, “Food-anticipatory activity persists after olfactory bulb ablation in the rat.,” *Physiol. Behav.*, vol. 72, no. 1–2, pp. 231–5, Jan. 2001.
- [48] A. J. Davidson, B. J. Aragona, T. A. Houpt, and F. K. Stephan, “Persistence of meal-entrained circadian rhythms following area postrema lesions in the rat.,” *Physiol. Behav.*, vol. 74, no. 3, pp. 349–54, Oct. 2001.
- [49] R. E. Mistlberger and D. G. Mumby, “The limbic system and food-anticipatory circadian rhythms in the rat: ablation and dopamine blocking studies,” *Behav. Brain Res.*, vol. 47, no. 2, pp. 159–168, Apr. 1992.
- [50] N. Le Minh, F. Damiola, F. Tronche, G. Schütz, and U. Schibler, “Glucocorticoid hormones inhibit food-induced phase-shifting of peripheral circadian oscillators,” *EMBO J.*, vol. 20, no. 24, pp. 7128–7136, Dec. 2001.
- [51] S. Pitts, E. Perone, and R. Silver, “Food-entrained circadian rhythms are sustained in arrhythmic *Clk/Clk* mutant mice,” *Am. J. Physiol. Integr. Comp. Physiol.*, vol. 285, no. 1, pp. R57–R67, Jul. 2003.
- [52] K.-F. Storch and C. J. Weitz, “Daily rhythms of food-anticipatory behavioral activity do not require the known circadian clock,” *Proc. Natl. Acad. Sci.*, vol. 106, no. 16, pp. 6808–6813, Apr. 2009.
- [53] J. S. Pendergast, G. A. Oda, K. D. Niswender, and S. Yamazaki, “Period determination in the food-entrainable and methamphetamine-sensitive circadian oscillator(s).,” *Proc. Natl. Acad. Sci. U. S. A.*, vol. 109, no. 35, pp. 14218–23, Aug. 2012.
- [54] M. Iijima, S. Yamaguchi, G. T. J. van der Horst, X. Bonnefont, H. Okamura, and S. Shibata, “Altered food-anticipatory activity rhythm in Cryptochrome-deficient mice,” *Neurosci. Res.*, vol. 52, no. 2, pp. 166–173, Jun. 2005.
- [55] J. Mendoza, U. Albrecht, and E. Challet, “Behavioural food anticipation in clock genes deficient mice: confirming old phenotypes, describing new phenotypes,” *Genes, Brain Behav.*, vol. 9, no. 5, pp. 467–77, Mar. 2010.
- [56] C. A. Feillet, J. A. Ripperger, M. C. Magnone, A. Dulloo, U. Albrecht, and E. Challet, “Lack of Food Anticipation in *Per2* Mutant Mice,” *Curr. Biol.*, vol. 16, no. 20, pp. 2016–2022, 2006.
- [57] C. B. Peek *et al.*, “Circadian clock NAD<sup>+</sup> cycle drives mitochondrial oxidative metabolism in mice.,” *Science*, vol. 342, no. 6158, p. 1243417, Nov. 2013.
- [58] D. Landgraf *et al.*, “Oxyntomodulin regulates resetting of the liver circadian clock by food.,”

*Elife*, vol. 4, p. e06253, Mar. 2015.

- [59] F. Dang *et al.*, “Insulin post-transcriptionally modulates Bmal1 protein to affect the hepatic circadian clock,” *Nat. Commun.*, vol. 7, p. 12696, 2016.
- [60] C. A. Feillet, J. Mendoza, P. Pévet, and E. Challet, “Restricted feeding restores rhythmicity in the pineal gland of arrhythmic suprachiasmatic-lesioned rats,” *Eur. J. Neurosci.*, vol. 28, no. 12, pp. 2451–2458, Dec. 2008.
- [61] M. O. Dietrich *et al.*, “Agrp Neurons Mediate Sirt1’s Action on the Melanocortin System and Energy Balance: Roles for Sirt1 in Neuronal Firing and Synaptic Plasticity,” *J. Neurosci.*, vol. 30, no. 35, pp. 11815–11825, Sep. 2010.
- [62] A. Satoh *et al.*, “SIRT1 Promotes the Central Adaptive Response to Diet Restriction through Activation of the Dorsomedial and Lateral Nuclei of the Hypothalamus,” *J. Neurosci.*, vol. 30, no. 30, pp. 10220–10232, Jul. 2010.
- [63] K. Bozek *et al.*, “Regulation of Clock-Controlled Genes in Mammals,” *PLoS One*, vol. 4, no. 3, p. e4882, Mar. 2009.
- [64] J. Gaucher, E. Montellier, and P. Sassone-Corsi, “Molecular Cogs: Interplay between Circadian Clock and Cell Cycle,” *Trends Cell Biol.*, vol. 28, no. 5, pp. 368–379, May 2018.
- [65] K. Eckel-Mahan and P. Sassone-Corsi, “Metabolism and the circadian clock converge,” *Physiol. Rev.*, vol. 93, no. 1, pp. 107–35, Jan. 2013.
- [66] R. E. Mistlberger, “Neurobiology of food anticipatory circadian rhythms,” *Physiol. Behav.*, vol. 104, no. 4, pp. 535–545, Sep. 2011.
- [67] R. E. Mistlberger, “Circadian food-anticipatory activity: Formal models and physiological mechanisms,” *Neurosci. Biobehav. Rev.*, vol. 18, no. 2, pp. 171–195, Jun. 1994.
- [68] J. Richards and M. L. Gumz, “Advances in understanding the peripheral circadian clocks,” *FASEB J.*, vol. 26, no. 9, pp. 3602–13, Sep. 2012.
- [69] S. Yamazaki *et al.*, “Resetting central and peripheral circadian oscillators in transgenic rats,” *Science*, vol. 288, no. 5466, pp. 682–5, Apr. 2000.
- [70] C. Dibner, U. Schibler, and U. Albrecht, “The Mammalian Circadian Timing System: Organization and Coordination of Central and Peripheral Clocks,” *Annu. Rev. Physiol.*, vol. 72, no. 1, pp. 517–549, Mar. 2010.
- [71] U. Albrecht, “Timing to Perfection: The Biology of Central and Peripheral Circadian Clocks,” *Neuron*, vol. 74, no. 2, pp. 246–260, Apr. 2012.
- [72] K.-F. Storch *et al.*, “Extensive and divergent circadian gene expression in liver and heart,” *Nature*, vol. 417, no. 6884, pp. 78–83, May 2002.
- [73] H. R. Ueda *et al.*, “System-level identification of transcriptional circuits underlying mammalian circadian clocks,” *Nat. Genet.*, vol. 37, no. 2, pp. 187–192, Feb. 2005.

- [74] A. Korenčič, R. Košir, G. Bordyugov, R. Lehmann, D. Rozman, and H. Herzl, “Timing of circadian genes in mammalian tissues,” *Sci. Rep.*, vol. 4, no. 1, p. 5782, May 2015.
- [75] T. Matsuo, S. Yamaguchi, S. Mitsui, A. Emi, F. Shimoda, and H. Okamura, “Control Mechanism of the Circadian Clock for Timing of Cell Division in Vivo,” *Science (80-. )*, vol. 302, no. 5643, pp. 255–259, Oct. 2003.
- [76] T. K. Tamai, L. C. Young, C. A. Cox, and D. Whitmore, “Light acts on the zebrafish circadian clock to suppress rhythmic mitosis and cell proliferation.,” *J. Biol. Rhythms*, vol. 27, no. 3, pp. 226–36, Jun. 2012.
- [77] M. P. S. Dekens, C. Santoriello, D. Vallone, G. Grassi, D. Whitmore, and N. S. Foulkes, “Light regulates the cell cycle in zebrafish.,” *Curr. Biol.*, vol. 13, no. 23, pp. 2051–7, Dec. 2003.
- [78] P. Janich *et al.*, “The circadian molecular clock creates epidermal stem cell heterogeneity,” *Nature*, vol. 480, no. 7376, pp. 209–214, Dec. 2011.
- [79] M. Geyfman *et al.*, “Brain and muscle Arnt-like protein-1 (BMAL1) controls circadian cell proliferation and susceptibility to UVB-induced DNA damage in the epidermis,” *Proc. Natl. Acad. Sci.*, vol. 109, no. 29, pp. 11758–11763, Jul. 2012.
- [80] M. V. Plikus *et al.*, “Local circadian clock gates cell cycle progression of transient amplifying cells during regenerative hair cycling,” *Proc. Natl. Acad. Sci.*, vol. 110, no. 23, pp. E2106–E2115, Jun. 2013.
- [81] M. Weger, N. Diotel, A.-C. Dorsemans, T. Dickmeis, and B. D. Weger, “Stem cells and the circadian clock,” *Dev. Biol.*, vol. 431, no. 2, pp. 111–123, Nov. 2017.
- [82] E. Kowalska *et al.*, “NONO couples the circadian clock to the cell cycle,” *Proc. Natl. Acad. Sci.*, vol. 110, no. 5, pp. 1592–1599, Jan. 2013.
- [83] P. Karpowicz, Y. Zhang, J. B. Hogenesch, P. Emery, and N. Perrimon, “The circadian clock gates the intestinal stem cell regenerative state.,” *Cell Rep.*, vol. 3, no. 4, pp. 996–1004, Apr. 2013.
- [84] P. L. Lowrey and J. S. Takahashi, “Genetics of Circadian Rhythms in Mammalian Model Organisms,” in *Advances in genetics*, vol. 74, 2011, pp. 175–230.
- [85] G. A. Bjarnason *et al.*, “Circadian Expression of Clock Genes in Human Oral Mucosa and Skin: Association with Specific Cell-Cycle Phases,” *Am. J. Pathol.*, vol. 158, no. 5, pp. 1793–1801, May 2001.
- [86] G. A. Bjarnason, R. C. Jordan, and R. B. Sothorn, “Circadian variation in the expression of cell-cycle proteins in human oral epithelium.,” *Am. J. Pathol.*, vol. 154, no. 2, pp. 613–22, Feb. 1999.
- [87] J. Gaucher, E. Montellier, and P. Sassone-Corsi, “Molecular Cogs: Interplay between Circadian Clock and Cell Cycle,” *Trends Cell Biol.*, vol. 28, no. 5, pp. 368–379, May 2018.

- [88] A. Gréchez-Cassiau, B. Rayet, F. Guillaumond, M. Teboul, and F. Delaunay, “The circadian clock component BMAL1 is a critical regulator of p21WAF1/CIP1 expression and hepatocyte proliferation,” *J. Biol. Chem.*, vol. 283, no. 8, pp. 4535–42, Feb. 2008.
- [89] E. Nagoshi, C. Saini, C. Bauer, T. Laroche, F. Naef, and U. Schibler, “Circadian Gene Expression in Individual Fibroblasts: Cell-Autonomous and Self-Sustained Oscillators Pass Time to Daughter Cells,” *Cell*, vol. 119, no. 5, pp. 693–705, Nov. 2004.
- [90] C. Feillet, G. T. J. van der Horst, F. Levi, D. A. Rand, and F. Delaunay, “Coupling between the Circadian Clock and Cell Cycle Oscillators: Implication for Healthy Cells and Malignant Growth,” *Front. Neurol.*, vol. 6, p. 96, 2015.
- [91] J. Bieler, R. Cannavo, K. Gustafson, C. Gobet, D. Gatfield, and F. Naef, “Robust synchronization of coupled circadian and cell cycle oscillators in single mammalian cells,” *Mol. Syst. Biol.*, vol. 10, no. 7, p. 739, Jul. 2014.
- [92] L. Fu, H. Pelicano, J. Liu, P. Huang, and C. Lee, “The circadian gene *Period2* plays an important role in tumor suppression and DNA damage response in vivo,” *Cell*, vol. 111, no. 1, pp. 41–50, Oct. 2002.
- [93] A.-L. Huber *et al.*, “CRY2 and FBXL3 Cooperatively Degrade c-MYC,” *Mol. Cell*, vol. 64, no. 4, pp. 774–789, Nov. 2016.
- [94] J. Wang *et al.*, “Nuclear Proteomics Uncovers Diurnal Regulatory Landscapes in Mouse Liver,” *Cell Metab.*, vol. 25, no. 1, pp. 102–117, Jan. 2017.
- [95] K. J. Barnum and M. J. O’connell, “Cell Cycle Regulation by Checkpoints.”
- [96] A. Sancar, L. A. Lindsey-Boltz, T.-H. Kang, J. T. Reardon, J. H. Lee, and N. Ozturk, “Circadian clock control of the cellular response to DNA damage,” *FEBS Lett.*, vol. 584, no. 12, pp. 2618–2625, Jun. 2010.
- [97] N. Oztürk *et al.*, “Structure and function of animal cryptochromes,” *Cold Spring Harb. Symp. Quant. Biol.*, vol. 72, pp. 119–31, Jan. 2007.
- [98] S. J. Papp *et al.*, “DNA damage shifts circadian clock time via Hausp-dependent Cry1 stabilization.”
- [99] Y. Okamoto-Uchida, J. Izawa, and J. Hirayama, “A Molecular Link between the Circadian Clock, DNA Damage Responses, and Oncogene Activation,” in *Oncogenes and Carcinogenesis*, IntechOpen, 2019.
- [100] S. M. Reppert and D. R. Weaver, “Coordination of circadian timing in mammals,” *Nature*, vol. 418, no. 6901, pp. 935–941, Aug. 2002.
- [101] M. Hastings, J. S. O’Neill, and E. S. Maywood, “Circadian clocks: regulators of endocrine and metabolic rhythms,” *J. Endocrinol.*, vol. 195, no. 2, pp. 187–98, Nov. 2007.
- [102] U. Schibler *et al.*, “Clock-Talk: Interactions between Central and Peripheral Circadian Oscillators in Mammals,” *Cold Spring Harb. Symp. Quant. Biol.*, vol. 80, pp. 223–32, 2015.

- [103] T. K. Tamai, L. C. Young, and D. Whitmore, “Light signaling to the zebrafish circadian clock by Cryptochrome 1a,” *Proc. Natl. Acad. Sci.*, vol. 104, no. 37, pp. 14712–14717, 2007.
- [104] G. Vatine *et al.*, “Light Directs Zebrafish period2 Expression via Conserved D and E Boxes,” *PLoS Biol.*, vol. 7, no. 10, p. e1000223, Oct. 2009.
- [105] E. Isorna, N. de Pedro, A. I. Valenciano, Á. L. Alonso-Gómez, and M. J. Delgado, “Interplay between the endocrine and circadian systems in fishes,” *J. Endocrinol.*, vol. 232, no. 3, pp. R141–R159, 2017.
- [106] S. M. K. Glasauer and S. C. F. Neuhaus, “Whole-genome duplication in teleost fishes and its evolutionary consequences,” *Mol. Genet. Genomics*, vol. 289, no. 6, pp. 1045–1060, Dec. 2014.
- [107] J.-G. Park, Y.-J. Park, N. Sugama, S.-J. Kim, and A. Takemura, “Molecular cloning and daily variations of the Period gene in a reef fish *Siganus guttatus*,” *J. Comp. Physiol. A*, vol. 193, no. 4, pp. 403–411, Mar. 2007.
- [108] A. Davie, M. Minghetti, and H. Migaud, “Seasonal variations in clock-gene expression in Atlantic salmon (*Salmo salar*),” *Chronobiol. Int.*, vol. 26, no. 3, pp. 379–95, Apr. 2009.
- [109] A. Sánchez-Bretaño *et al.*, “Anatomical distribution and daily profile of *gper1b* gene expression in brain and peripheral structures of goldfish (*Carassius auratus*),” *Chronobiol. Int.*, vol. 32, no. 7, pp. 889–902, Aug. 2015.
- [110] A. Sánchez-Bretaño, Á. L. Alonso-Gómez, M. J. Delgado, and E. Isorna, “The liver of goldfish as a component of the circadian system: Integrating a network of signals,” *Gen. Comp. Endocrinol.*, vol. 221, pp. 213–6, Sep. 2015.
- [111] L. S. Costa, I. Serrano, F. J. Sánchez-Vázquez, and J. F. López-Olmeda, “Circadian rhythms of clock gene expression in Nile tilapia (*Oreochromis niloticus*) central and peripheral tissues: influence of different lighting and feeding conditions,” *J. Comp. Physiol. B*, vol. 186, no. 6, pp. 775–785, Aug. 2016.
- [112] E. Velarde, R. Haque, P. M. Iuvone, C. Azpeleta, A. L. Alonso-Gómez, and M. J. Delgado, “Circadian Clock Genes of Goldfish, *Carassius auratus* : cDNA Cloning and Rhythmic Expression of *Period* and *Cryptochrome* Transcripts in Retina, Liver, and Gut,” *J. Biol. Rhythms*, vol. 24, no. 2, pp. 104–113, Apr. 2009.
- [113] T.-S. Huang, P. Ruoff, and P. G. Fjelldal, “Effect of continuous light on daily levels of plasma melatonin and cortisol and expression of clock genes in pineal gland, brain, and liver in atlantic salmon postsmolts,” *Chronobiol. Int.*, vol. 27, no. 9–10, pp. 1715–34, Oct. 2010.
- [114] J. F. López-Olmeda, E. V. Tartaglione, H. O. De La Iglesia, and F. J. Sánchez-Vázquez, “Feeding entrainment of food-anticipatory activity and *per1* expression in the brain and liver of zebrafish under different lighting and feeding conditions,” *Chronobiol. Int.*, vol. 27, no. 7, pp. 1380–1400, 2010.
- [115] N. Cavallari *et al.*, “A blind circadian clock in cavefish reveals that opsins mediate peripheral clock photoreception,” *PLoS Biol.*, vol. 9, no. 9, 2011.

- [116] M. A. L. Patiño, A. Rodríguez-Illamola, M. Conde-Sieira, J. L. Soengas, and J. M. Míguez, “Daily Rhythmic Expression Patterns of *Clock1a*, *Bmal1*, and *Per1* Genes in Retina and Hypothalamus of the Rainbow Trout, *Oncorhynchus Mykiss*,” *Chronobiol. Int.*, vol. 28, no. 5, pp. 381–389, May 2011.
- [117] Á. J. Martín-Robles, D. Whitmore, F. J. Sánchez-Vázquez, C. Pendón, and J. A. Muñoz-Cueto, “Cloning, tissue expression pattern and daily rhythms of *Period1*, *Period2*, and *Clock* transcripts in the flatfish Senegalese sole, *Solea senegalensis*,” *J. Comp. Physiol. B*, vol. 182, no. 5, pp. 673–685, Jul. 2012.
- [118] L. G. Nisembaum *et al.*, “Light-dark cycle and feeding time differentially entrains the gut molecular clock of the goldfish (*Carassius auratus*).,” *Chronobiol. Int.*, vol. 29, no. 6, pp. 665–73, Jul. 2012.
- [119] L. M. Vera, P. Negrini, C. Zagatti, E. Frigato, F. J. Sánchez-Vázquez, and C. Bertolucci, “Light and feeding entrainment of the molecular circadian clock in a marine teleost (*Sparus aurata*),” *Chronobiol. Int.*, vol. 30, no. 5, pp. 649–661, Jun. 2013.
- [120] J. Hirayama, L. Cardone, M. Doi, and P. Sassone-Corsi, “Common pathways in circadian and cell cycle clocks: light-dependent activation of Fos/AP-1 in zebrafish controls *CRY-1a* and *WEE-1*,” *Proc. Natl. Acad. Sci. U. S. A.*, vol. 102, no. 29, pp. 10194–9, Jul. 2005.
- [121] J. Hirayama *et al.*, “Common light signaling pathways controlling DNA repair and circadian clock entrainment in zebrafish,” *Cell Cycle*, vol. 8, no. 17, pp. 2794–801, Sep. 2009.
- [122] N. Cermakian *et al.*, “Light induction of a vertebrate clock gene involves signaling through blue-light receptors and MAP kinases,” *Curr. Biol.*, vol. 12, no. 10, pp. 844–8, May 2002.
- [123] M. P. Pando, A. B. Pinchak, N. Cermakian, and P. Sassone-Corsi, “A cell-based system that recapitulates the dynamic light-dependent regulation of the vertebrate clock,” *Proc. Natl. Acad. Sci. U. S. A.*, vol. 98, no. 18, pp. 10178–83, Aug. 2001.
- [124] D. Vallone, S. B. Gondi, D. Whitmore, and N. S. Foulkes, “E-box function in a period gene repressed by light,” *Proc. Natl. Acad. Sci. U. S. A.*, vol. 101, no. 12, pp. 4106–11, Mar. 2004.
- [125] J. D. Plautz, M. Kaneko, J. C. Hall, S. A. Kay, and M. Menaker, “Independent photoreceptive circadian clocks throughout *Drosophila*,” *Science*, vol. 278, no. 5343, pp. 1632–5, Nov. 1997.
- [126] M. L. Idda, C. Bertolucci, D. Vallone, Y. Gothilf, F. J. Sánchez-Vázquez, and N. S. Foulkes, “Chapter 3 - Circadian clocks: Lessons from fish,” *Neurobiol. Circadian Timing*, vol. 199, pp. 41–57, 2012.
- [127] X. Li, J. Montgomery, W. Cheng, J. H. Noh, D. R. Hyde, and L. Li, “Pineal Photoreceptor Cells Are Required for Maintaining the Circadian Rhythms of Behavioral Visual Sensitivity in Zebrafish,” *PLoS One*, vol. 7, no. 7, p. e40508, Jul. 2012.
- [128] G. M. Cahill, “Clock mechanisms in zebrafish,” *Cell Tissue Res.*, vol. 309, no. 1, pp. 27–34, Jul. 2002.

- [129] G. M. Cahill, “Circadian regulation of melatonin production in cultured zebrafish pineal and retina.,” *Brain Res.*, vol. 708, no. 1–2, pp. 177–81, Feb. 1996.
- [130] Y. Gothilf, S. L. Coon, R. Toyama, A. Chitnis, M. A. A. Namboodiri, and D. C. Klein, “Zebrafish Serotonin *N*-Acetyltransferase-2: Marker for Development of Pineal Photoreceptors and Circadian Clock Function <sup>1</sup>,” *Endocrinology*, vol. 140, no. 10, pp. 4895–4903, Oct. 1999.
- [131] I. V Zhdanova, “Sleep and its regulation in zebrafish.,” *Rev. Neurosci.*, vol. 22, no. 1, pp. 27–36, 2011.
- [132] M. W. Hurd and G. M. Cahill, “Entraining Signals Initiate Behavioral Circadian Rhythmicity in Larval Zebrafish,” *J. Biol. Rhythms*, vol. 17, no. 4, pp. 307–314, Aug. 2002.
- [133] M. Southwell and S. McRobert, “Zebrafish as a Model Organism to Study Melatonin Mechanisms and Treatments,” *Curr. Psychopharmacol.*, vol. 5, no. 2, pp. 85–95, Jul. 2016.
- [134] D. Vallone, C. Santoriello, S. B. Gondi, and N. S. Foulkes, “Basic Protocols for Zebrafish Cell Lines,” in *Methods in molecular biology (Clifton, N.J.)*, vol. 362, 2007, pp. 429–441.
- [135] H. Zhao *et al.*, “Modulation of DNA Repair Systems in Blind Cavefish during Evolution in Constant Darkness,” *Curr. Biol.*, vol. 28, no. 20, p. 3229–3243.e4, 2018.
- [136] C. Pagano *et al.*, “Evolution shapes the responsiveness of the D-box enhancer element to light and reactive oxygen species in vertebrates,” *Sci. Rep.*, vol. 8, no. 1, pp. 1–17, 2018.
- [137] H. Mano, D. Kojima, and Y. Fukada, “Exo-rhodopsin: a novel rhodopsin expressed in the zebrafish pineal gland.,” *Brain Res. Mol. Brain Res.*, vol. 73, no. 1–2, pp. 110–8, Nov. 1999.
- [138] A. R. Philp, J. Bellingham, J. M. García-Fernández, and R. G. Foster, “A novel rod-like opsin isolated from the extra-retinal photoreceptors of teleost fish.,” *undefined*, 2000.
- [139] A. R. Philp, J. M. Garcia-Fernandez, B. G. Soni, R. J. Lucas, J. Bellingham, and R. G. Foster, “Vertebrate ancient (VA) opsin and extraretinal photoreception in the Atlantic salmon (*Salmo salar*).,” *J. Exp. Biol.*, vol. 203, no. Pt 12, pp. 1925–36, Jun. 2000.
- [140] S. Blackshaw and S. H. Snyder, “Parapinopsin, a Novel Catfish Opsin Localized to the Parapineal Organ, Defines a New Gene Family,” 1997.
- [141] J. Forsell, B. Holmqvist, and P. Ekström, “Molecular identification and developmental expression of UV and green opsin mRNAs in the pineal organ of the Atlantic halibut.,” *Brain Res. Dev. Brain Res.*, vol. 136, no. 1, pp. 51–62, May 2002.
- [142] D. Magnoli *et al.*, “Rhodopsin expression in the zebrafish pineal gland from larval to adult stage,” *Brain Res.*, vol. 1442, pp. 9–14, Mar. 2012.
- [143] R. Laurà *et al.*, “The photoreceptive cells of the pineal gland in adult zebrafish (*Danio rerio*).,” *Microsc. Res. Tech.*, vol. 75, no. 3, pp. 359–366, Mar. 2012.
- [144] V. Matos-Cruz, J. Blasic, B. Nickle, P. R. Robinson, S. Hattar, and M. E. Halpern,

“Unexpected Diversity and Photoperiod Dependence of the Zebrafish Melanopsin System,” *PLoS One*, vol. 6, no. 9, p. e25111, Sep. 2011.

- [145] B. C. R. Ramos, M. N. C. M. Moraes, M. O. Poletini, L. H. R. G. Lima, and A. M. L. Castrucci, “From Blue Light to Clock Genes in Zebrafish ZEM-2S Cells,” *PLoS One*, vol. 9, no. 9, p. e106252, Sep. 2014.
- [146] P. Moutsaki, D. Whitmore, J. Bellingham, K. Sakamoto, Z. K. David-Gray, and R. G. Foster, “Teleost multiple tissue (tmt) opsin: a candidate photopigment regulating the peripheral clocks of zebrafish?,” *Brain Res. Mol. Brain Res.*, vol. 112, no. 1–2, pp. 135–45, Apr. 2003.
- [147] Y. Kobayashi *et al.*, “Molecular analysis of zebrafish photolyase/cryptochrome family: two types of cryptochromes present in zebrafish.,” *Genes Cells*, vol. 5, no. 9, pp. 725–38, Sep. 2000.
- [148] J. Hirayama, S. Cho, and P. Sassone-Corsi, “Circadian control by the reduction/oxidation pathway: catalase represses light-dependent clock gene expression in the zebrafish.,” *Proc. Natl. Acad. Sci. U. S. A.*, vol. 104, no. 40, pp. 15747–52, Oct. 2007.
- [149] W. I. L. Davies *et al.*, “An extended family of novel vertebrate photopigments is widely expressed and displays a diversity of function,” *Genome Res.*, vol. 25, no. 11, pp. 1666–1679, Nov. 2015.
- [150] P. Mracek *et al.*, “Regulation of per and cry Genes Reveals a Central Role for the D-Box Enhancer in Light-Dependent Gene Expression,” *PLoS One*, vol. 7, no. 12, p. e51278, Dec. 2012.
- [151] T. K. Tamai, V. Vardhanabhuti, N. S. Foulkes, and D. Whitmore, “Early embryonic light detection improves survival.,” *Curr. Biol.*, vol. 14, no. 3, pp. R104-5, Feb. 2004.
- [152] S. Vanhauwaert *et al.*, “Expressed Repeat Elements Improve RT-qPCR Normalization across a Wide Range of Zebrafish Gene Expression Studies,” *PLoS One*, vol. 9, no. 10, p. e109091, Oct. 2014.
- [153] P. Mracek *et al.*, “Regulation of per and cry Genes Reveals a Central Role for the D-Box Enhancer in Light-Dependent Gene Expression,” *PLoS One*, vol. 7, no. 12, p. e51278, Dec. 2012.
- [154] J. F. Paredes, J. F. López-Olmeda, F. J. Martínez, and F. J. Sánchez-Vázquez, “Daily rhythms of lipid metabolic gene expression in zebra fish liver: Response to light/dark and feeding cycles.,” *Chronobiol. Int.*, vol. 32, no. 10, pp. 1438–48, Nov. 2015.
- [155] M. Von Schantz, A. Jenkins, and S. N. Archer, “Evolutionary History of the Vertebrate Period Genes.”
- [156] H. Wang, “Comparative Analysis of Period Genes in Teleost Fish Genomes,” *J. Mol. Evol.*, vol. 67, no. 1, pp. 29–40, Jul. 2008.
- [157] K. L. Toh *et al.*, “An hPer2 phosphorylation site mutation in familial advanced sleep phase syndrome.,” *Science*, vol. 291, no. 5506, pp. 1040–3, Feb. 2001.

- [158] K. Vanselow *et al.*, “Differential effects of PER2 phosphorylation: molecular basis for the human familial advanced sleep phase syndrome (FASPS).” *Genes Dev.*, vol. 20, no. 19, pp. 2660–72, Oct. 2006.
- [159] B. Grimaldi *et al.*, “PER2 controls lipid metabolism by direct regulation of PPAR $\gamma$ .” *Cell Metab.*, vol. 12, no. 5, pp. 509–20, Nov. 2010.
- [160] S. Gery, R. K. Virk, K. Chumakov, A. Yu, and H. P. Koeffler, “The clock gene *Per2* links the circadian system to the estrogen receptor,” *Oncogene*, vol. 26, no. 57, pp. 7916–7920, Dec. 2007.
- [161] X. Yang, X. He, Z. Yang, and E. Jabbari, “Mammalian PER2 regulates AKT activation and DNA damage response,” *Biochem. Cell Biol.*, vol. 90, no. 6, pp. 675–682, Dec. 2012.
- [162] T. Qin *et al.*, “Effect of Period 2 on the proliferation, apoptosis and migration of osteosarcoma cells, and the corresponding mechanisms,” *Oncol. Lett.*, vol. 16, no. 2, pp. 2668–2674, Jun. 2018.
- [163] W. W. Hwang-Verslues *et al.*, “Loss of corepressor PER2 under hypoxia up-regulates OCT1-mediated EMT gene expression and enhances tumor malignancy.”
- [164] Q. WANG, Y. AO, K. YANG, H. TANG, and D. CHEN, “Circadian clock gene *Per2* plays an important role in cell proliferation, apoptosis and cell cycle progression in human oral squamous cell carcinoma,” *Oncol. Rep.*, vol. 35, no. 6, pp. 3387–3394, Jun. 2016.
- [165] X. Gu *et al.*, “The circadian mutation PER2 S662G is linked to cell cycle progression and tumorigenesis,” *Cell Death Differ.*, vol. 19, no. 3, pp. 397–405, Mar. 2012.
- [166] L. Fu, H. Pelicano, J. Liu, P. Huang, and C. C. Lee, “The Circadian Gene *Period2* Plays an Important Role in Tumor Suppression and DNA Damage Response In Vivo,” *Cell*, vol. 111, no. 1, pp. 41–50, Oct. 2002.
- [167] U. Albrecht, A. Bordon, I. Schmutz, and J. Ripperger, “The Multiple Facets of *Per2*,” *Cold Spring Harb. Symp. Quant. Biol.*, vol. 72, no. 1, pp. 95–104, Jan. 2007.
- [168] Z. J. Huang, I. Edery, and M. Rosbash, “PAS is a dimerization domain common to *Drosophila* *Period* and several transcription factors,” *Nature*, vol. 364, no. 6434, pp. 259–262, Jul. 1993.
- [169] N. Gekakis *et al.*, “Isolation of *timeless* by PER protein interaction: defective interaction between *timeless* protein and long-period mutant PERL,” *Science*, vol. 270, no. 5237, pp. 811–5, Nov. 1995.
- [170] Ö. Yildiz *et al.*, “Crystal Structure and Interactions of the PAS Repeat Region of the *Drosophila* Clock Protein PERIOD,” *Mol. Cell*, vol. 17, no. 1, pp. 69–82, Jan. 2005.
- [171] C. Iitaka, K. Miyazaki, T. Akaike, and N. Ishida, “A Role for Glycogen Synthase Kinase-3 $\beta$  in the Mammalian Circadian Clock,” *J. Biol. Chem.*, vol. 280, no. 33, pp. 29397–29402, Aug. 2005.

- [172] C. P. Ponting and L. Aravind, "PAS: a multifunctional domain family comes to light.," *Curr. Biol.*, vol. 7, no. 11, pp. R674-7, Nov. 1997.
- [173] K. Kaasik and C. Chi Lee, "Reciprocal regulation of haem biosynthesis and the circadian clock in mammals," *Nature*, vol. 430, no. 6998, pp. 467-471, Jul. 2004.
- [174] S. Hill, S. Austin, T. Eydmann, T. Jones, and R. Dixon, "Azotobacter vinelandii NIFL is a flavoprotein that modulates transcriptional activation of nitrogen-fixation genes via a redox-sensitive switch.," *Proc. Natl. Acad. Sci. U. S. A.*, vol. 93, no. 5, pp. 2143-8, Mar. 1996.
- [175] S. I. Bibikov, R. Biran, K. E. Rudd, and J. S. Parkinson, "A signal transducer for aerotaxis in Escherichia coli.," *J. Bacteriol.*, vol. 179, no. 12, pp. 4075-9, Jun. 1997.
- [176] K. Miyazaki, M. Mesaki, and N. Ishida, "Nuclear entry mechanism of rat PER2 (rPER2): role of rPER2 in nuclear localization of CRY protein.," *Mol. Cell. Biol.*, vol. 21, no. 19, pp. 6651-9, Oct. 2001.
- [177] T. Ohno, Y. Onishi, and N. Ishida, "The negative transcription factor E4BP4 is associated with circadian clock protein PERIOD2," *Biochem. Biophys. Res. Commun.*, vol. 354, no. 4, pp. 1010-1015, Mar. 2007.
- [178] S. A. Oñate, S. Y. Tsai, M. J. Tsai, and B. W. O'Malley, "Sequence and characterization of a coactivator for the steroid hormone receptor superfamily.," *Science*, vol. 270, no. 5240, pp. 1354-7, Nov. 1995.
- [179] U. Albrecht, Z. S. Sun, G. Eichele, and C. C. Lee, "A differential response of two putative mammalian circadian regulators, mper1 and mper2, to light.," *Cell*, vol. 91, no. 7, pp. 1055-64, Dec. 1997.
- [180] L. Yan and R. Silver, "Differential induction and localization of mPer1 and mPer2 during advancing and delaying phase shifts.," *Eur. J. Neurosci.*, vol. 16, no. 8, pp. 1531-40, Oct. 2002.
- [181] C. Fukuhara, J. M. Brewer, J. C. Dirden, E. L. Bittman, G. Tosini, and M. E. Harrington, "Neuropeptide Y rapidly reduces Period 1 and Period 2 mRNA levels in the hamster suprachiasmatic nucleus.," *Neurosci. Lett.*, vol. 314, no. 3, pp. 119-22, Nov. 2001.
- [182] H. S. Nielsen, J. Hannibal, and J. Fahrenkrug, "Vasoactive intestinal polypeptide induces per1 and per2 gene expression in the rat suprachiasmatic nucleus late at night.," *Eur. J. Neurosci.*, vol. 15, no. 3, pp. 570-4, Feb. 2002.
- [183] L. A. Segall, J. S. Perrin, C.-D. Walker, J. Stewart, and S. Amir, "Glucocorticoid rhythms control the rhythm of expression of the clock protein, Period2, in oval nucleus of the bed nucleus of the stria terminalis and central nucleus of the amygdala in rats," *Neuroscience*, vol. 140, no. 3, pp. 753-757, Jan. 2006.
- [184] P. C. Yannielli, P. C. Molyneux, M. E. Harrington, and D. A. Golombek, "Ghrelin Effects on the Circadian System of Mice," *J. Neurosci.*, vol. 27, no. 11, pp. 2890-2895, Mar. 2007.
- [185] S.-H. Yoo *et al.*, "A noncanonical E-box enhancer drives mouse Period2 circadian

- oscillations in vivo,” *Proc. Natl. Acad. Sci.*, vol. 102, no. 7, pp. 2608–2613, Feb. 2005.
- [186] M. Akashi, T. Ichise, T. Mamine, and T. Takumi, “Molecular mechanism of cell-autonomous circadian gene expression of *Period2*, a crucial regulator of the mammalian circadian clock,” *Mol. Biol. Cell*, vol. 17, no. 2, pp. 555–65, Feb. 2006.
- [187] E. L. McDearmon *et al.*, “Dissecting the Functions of the Mammalian Clock Protein BMAL1 by Tissue-Specific Rescue in Mice,” *Science (80-. )*, vol. 314, no. 5803, pp. 1304–1308, Nov. 2006.
- [188] D. Yamajuku *et al.*, “Cellular DBP and E4BP4 proteins are critical for determining the period length of the circadian oscillator,” *FEBS Lett.*, vol. 585, no. 14, pp. 2217–2222, Jul. 2011.
- [189] B. D. Weger *et al.*, “The Light Responsive Transcriptome of the Zebrafish: Function and Regulation,” *PLoS One*, vol. 6, no. 2, p. e17080, Feb. 2011.
- [190] C. von Gall *et al.*, “CREB in the mouse SCN: a molecular interface coding the phase-adjusting stimuli light, glutamate, PACAP, and melatonin for clockwork access,” *J. Neurosci.*, vol. 18, no. 24, pp. 10389–97, Dec. 1998.
- [191] K. Obrietan, S. Impey, D. Smith, J. Athos, and D. R. Storm, “Circadian regulation of cAMP response element-mediated gene expression in the suprachiasmatic nuclei,” *J. Biol. Chem.*, vol. 274, no. 25, pp. 17748–56, Jun. 1999.
- [192] Z. Travnickova-Bendova, N. Cermakian, S. M. Reppert, and P. Sassone-Corsi, “Bimodal regulation of *mPeriod* promoters by CREB-dependent signaling and CLOCK/BMAL1 activity,” *Proc. Natl. Acad. Sci. U. S. A.*, vol. 99, no. 11, pp. 7728–33, May 2002.
- [193] B. Kornmann, O. Schaad, H. Bujard, J. S. Takahashi, and U. Schibler, “System-Driven and Oscillator-Dependent Circadian Transcription in Mice with a Conditionally Active Liver Clock,” *PLoS Biol.*, vol. 5, no. 2, p. e34, Jan. 2007.
- [194] Z. Li *et al.*, “Sex-related difference in food-anticipatory activity of mice,” *Horm. Behav.*, vol. 70, pp. 38–46, Apr. 2015.
- [195] R. Chavan *et al.*, “Liver-derived ketone bodies are necessary for food anticipation,” *Nat. Commun.*, vol. 7, no. 1, p. 10580, Dec. 2016.
- [196] J. S. Pendergast, R. H. Wendroth, R. C. Stenner, C. D. Keil, and S. Yamazaki, “*MPeriod2Brdm1* and other single *Period* mutant mice have normal food anticipatory activity,” *Sci. Rep.*, vol. 7, no. 1, pp. 1–8, 2017.
- [197] G. A. Bjarnason, R. C. Jordan, and R. B. Sothorn, “Circadian variation in the expression of cell-cycle proteins in human oral epithelium,” *Am. J. Pathol.*, vol. 154, no. 2, pp. 613–22, Feb. 1999.
- [198] Y.-M. Lin *et al.*, “Disturbance of circadian gene expression in hepatocellular carcinoma,” *Mol. Carcinog.*, vol. 47, no. 12, pp. 925–933, Dec. 2008.

- [199] H. Hua *et al.*, “Circadian gene mPer2 overexpression induces cancer cell apoptosis,” *Cancer Sci.*, vol. 97, no. 7, pp. 589–596, Jul. 2006.
- [200] X.-M. Tan *et al.*, “Circadian variations of clock gene Per2 and cell cycle genes in different stages of carcinogenesis in golden hamster buccal mucosa,” *Sci. Rep.*, vol. 5, no. 1, p. 9997, Sep. 2015.
- [201] C.-M. Hsu, S.-F. Lin, C.-T. Lu, P.-M. Lin, and M.-Y. Yang, “Altered expression of circadian clock genes in head and neck squamous cell carcinoma,” *Tumor Biol.*, vol. 33, no. 1, pp. 149–155, Feb. 2012.
- [202] Z. Lengyel *et al.*, “Altered expression patterns of clock gene mRNAs and clock proteins in human skin tumors,” *Tumor Biol.*, vol. 34, no. 2, pp. 811–819, Apr. 2013.
- [203] S.-J. Kuo *et al.*, “Disturbance of circadian gene expression in breast cancer,” *Virchows Arch.*, vol. 454, no. 4, pp. 467–474, Apr. 2009.
- [204] M. Soták, L. Polidarová, P. Ergang, A. Sumová, and J. Pácha, “An association between clock genes and clock-controlled cell cycle genes in murine colorectal tumors,” *Int. J. Cancer*, vol. 132, no. 5, pp. 1032–1041, Mar. 2013.
- [205] M. P. Antoch, I. Toshkov, K. K. Kuropatwinski, and M. Jackson, “Deficiency in PER proteins has no effect on the rate of spontaneous and radiation-induced carcinogenesis,” *Cell Cycle*, vol. 12, no. 23, pp. 3673–3680, Dec. 2013.
- [206] M. Oklejewicz, E. Destici, F. Tamanini, R. A. Hut, R. Janssens, and G. T. J. van der Horst, “Phase Resetting of the Mammalian Circadian Clock by DNA Damage,” *Curr. Biol.*, vol. 18, no. 4, pp. 286–291, Feb. 2008.
- [207] T. Miki, T. Matsumoto, Z. Zhao, and C. C. Lee, “p53 regulates Period2 expression and the circadian clock,” *Nat. Commun.*, vol. 4, p. 2444, 2013.
- [208] R. Laranjeiro, T. K. Tamai, W. Letton, N. Hamilton, and D. Whitmore, “Circadian Clock Synchronization of the Cell Cycle in Zebrafish Occurs through a Gating Mechanism Rather Than a Period-phase Locking Process,” *J. Biol. Rhythms*, vol. 33, no. 2, pp. 137–150, Apr. 2018.
- [209] R. Laranjeiro, T. K. Tamai, E. Peyric, P. Krusche, S. Ott, and D. Whitmore, “Cyclin-dependent kinase inhibitor p20 controls circadian cell-cycle timing,” *Proc. Natl. Acad. Sci. U. S. A.*, vol. 110, no. 17, pp. 6835–40, Apr. 2013.
- [210] M. L. Idda, E. Kage, J. F. Lopez-Olmeda, P. Mracek, N. S. Foulkes, and D. Vallone, “Circadian Timing of Injury-Induced Cell Proliferation in Zebrafish,” *PLoS One*, vol. 7, no. 3, p. e34203, Mar. 2012.
- [211] P. A. Wood, X. Xiaoming Yang, and W. J. M. Hrushesky, “Clock Genes and Cancer,” *Integr. Cancer Ther.*, vol. 8, no. 4, pp. 303–308, Dec. 2009.
- [212] C. Savvidis and M. Koutsilieris, “<Title/>,” *Mol. Med.*, vol. 18, no. 9, p. 1, 2012.

- [213] F. W. Turek *et al.*, “Obesity and Metabolic Syndrome in Circadian Clock Mutant Mice,” *Science* (80-. ), vol. 308, no. 5724, pp. 1043–1045, May 2005.
- [214] E. S. Musiek, “Circadian clock disruption in neurodegenerative diseases: cause and effect?,” *Front. Pharmacol.*, vol. 6, p. 29, Feb. 2015.
- [215] A. A. Kondratova and R. V. Kondratov, “The circadian clock and pathology of the ageing brain,” *Nat. Rev. Neurosci.*, vol. 13, no. 5, pp. 325–335, May 2012.
- [216] M. de Caestecker, “The transforming growth factor-beta superfamily of receptors.,” *Cytokine Growth Factor Rev.*, vol. 15, no. 1, pp. 1–11, Feb. 2004.
- [217] J. Massagué, “How cells read TGF- $\beta$  signals,” *Nat. Rev. Mol. Cell Biol.*, vol. 1, no. 3, pp. 169–178, Dec. 2000.
- [218] E. J. Bategay, E. W. Raines, R. A. Seifert, D. F. Bowen-Pope, and R. Ross, “TGF-beta induces bimodal proliferation of connective tissue cells via complex control of an autocrine PDGF loop.,” *Cell*, vol. 63, no. 3, pp. 515–24, Nov. 1990.
- [219] P. M. Siegel and J. Massagué, “Cytostatic and apoptotic actions of TGF- $\beta$  in homeostasis and cancer,” *Nat. Rev. Cancer*, vol. 3, no. 11, pp. 807–820, Nov. 2003.
- [220] J. Massagué and R. R. Gomis, “The logic of TGF $\beta$  signaling,” *FEBS Lett.*, vol. 580, no. 12, pp. 2811–2820, May 2006.
- [221] J. W. Penn, A. O. Grobbelaar, and K. J. Rolfe, “The role of the TGF- $\beta$  family in wound healing, burns and scarring: a review.,” *Int. J. Burns Trauma*, vol. 2, no. 1, pp. 18–28, 2012.
- [222] G. Ferrari, B. D. Cook, V. Terushkin, G. Pintucci, and P. Mignatti, “Transforming growth factor-beta 1 (TGF- $\beta$ 1) induces angiogenesis through vascular endothelial growth factor (VEGF)-mediated apoptosis,” *J. Cell. Physiol.*, vol. 219, no. 2, pp. 449–458, May 2009.
- [223] L. A. van Meeteren, M.-J. Goumans, and P. ten Dijke, “TGF- $\beta$  receptor signaling pathways in angiogenesis; emerging targets for anti-angiogenesis therapy.,” *Curr. Pharm. Biotechnol.*, vol. 12, no. 12, pp. 2108–20, Dec. 2011.
- [224] K. Kitisin *et al.*, “TGF-beta Signaling in Development,” *Sci. STKE*, vol. 2007, no. 399, pp. cm1-cm1, Aug. 2007.
- [225] M. Y. Wu and C. S. Hill, “TGF- $\beta$  Superfamily Signaling in Embryonic Development and Homeostasis,” *Dev. Cell*, vol. 16, no. 3, pp. 329–343, Mar. 2009.
- [226] G. C. Blobe, W. P. Schiemann, and H. F. Lodish, “Role of Transforming Growth Factor  $\beta$  in Human Disease,” *N. Engl. J. Med.*, vol. 342, no. 18, pp. 1350–1358, May 2000.
- [227] N. S. Nagaraj and P. K. Datta, “Targeting the transforming growth factor- $\beta$  signaling pathway in human cancer,” *Expert Opin. Investig. Drugs*, vol. 19, no. 1, pp. 77–91, Jan. 2010.
- [228] J. Massagué, “How cells read TGF- $\beta$  signals,” *Nat. Rev. Mol. Cell Biol.*, vol. 1, no. 3, pp.

169–178, Dec. 2000.

- [229] J. Massagué, “TGF $\beta$  signalling in context.,” *Nat. Rev. Mol. Cell Biol.*, vol. 13, no. 10, pp. 616–30, Oct. 2012.
- [230] J. F. Santibañez, M. Quintanilla, and C. Bernabeu, “TGF- $\beta$ /TGF- $\beta$  receptor system and its role in physiological and pathological conditions,” *Clin. Sci.*, vol. 121, no. 6, pp. 233–251, Sep. 2011.
- [231] R. A. Rahimi and E. B. Leof, “TGF-beta signaling: a tale of two responses.,” *J. Cell. Biochem.*, vol. 102, no. 3, pp. 593–608, Oct. 2007.
- [232] D. Wotton, R. S. Lo, L.-A. C. Swaby, and J. Massagué, “Multiple Modes of Repression by the Smad Transcriptional Corepressor TGIF,” *J. Biol. Chem.*, vol. 274, no. 52, pp. 37105–37110, Dec. 1999.
- [233] R. G. Wells, “V. TGF- $\beta$  signaling pathways,” *Am. J. Physiol. Liver Physiol.*, vol. 279, no. 5, pp. G845–G850, Nov. 2000.
- [234] N. Kon, T. Hirota, T. Kawamoto, Y. Kato, T. Tsubota, and Y. Fukada, “Activation of TGF-beta/activin signalling resets the circadian clock through rapid induction of Dec1 transcripts.,” *Nat. Cell Biol.*, vol. 10, no. 12, pp. 1463–9, Dec. 2008.
- [235] H. Gast *et al.*, “Transforming growth factor-beta inhibits the expression of clock genes,” *Ann. N. Y. Acad. Sci.*, vol. 1261, no. 1, pp. 79–87, Jul. 2012.
- [236] F. Sato *et al.*, “Smad3 and Snail show circadian expression in human gingival fibroblasts, human mesenchymal stem cell, and in mouse liver,” *Biochem. Biophys. Res. Commun.*, vol. 419, no. 2, pp. 441–446, Mar. 2012.
- [237] A. L. Beynon, J. Thome, and A. N. Coogan, “Age and time of day influences on the expression of transforming growth factor-beta and phosphorylated SMAD3 in the mouse suprachiasmatic and paraventricular nuclei.,” *Neuroimmunomodulation*, vol. 16, no. 6, pp. 392–9, 2009.
- [238] Y. Li, G. Li, H. Wang, J. Du, and J. Yan, “Analysis of a Gene Regulatory Cascade Mediating Circadian Rhythm in Zebrafish,” *PLoS Comput. Biol.*, vol. 9, no. 2, p. e1002940, Feb. 2013.
- [239] Y. Li, G. Li, B. Görling, B. Luy, J. Du, and J. Yan, “Integrative Analysis of Circadian Transcriptome and Metabolic Network Reveals the Role of De Novo Purine Synthesis in Circadian Control of Cell Cycle,” *PLOS Comput. Biol.*, vol. 11, no. 2, p. e1004086, Feb. 2015.
- [240] H. E. Sloin, G. Ruggiero, A. Rubinstein, S. S. Storz, N. S. Foulkes, and Y. Gothilf, “Interactions between the circadian clock and TGF- $\beta$  signaling pathway in zebrafish,” *PLoS One*, vol. 13, no. 6, pp. 1–23, 2018.
- [241] B. Schmid, C. Helfrich-Förster, and T. Yoshii, “A New ImageJ Plug-in ‘ActogramJ’ for Chronobiological Analyses,” *J. Biol. Rhythms*, vol. 26, no. 5, pp. 464–467, Oct. 2011.

- [242] A. Tovin *et al.*, “Systematic Identification of Rhythmic Genes Reveals *camk1gb* as a New Element in the Circadian Clockwork,” *PLoS Genet.*, vol. 8, no. 12, p. e1003116, Dec. 2012.
- [243] Z. Ben-Moshe *et al.*, “The light-induced transcriptome of the zebrafish pineal gland reveals complex regulation of the circadian clockwork by light,” *Nucleic Acids Res.*, vol. 42, no. 6, pp. 3750–3767, Apr. 2014.
- [244] Z. Ben-Moshe Livne *et al.*, “Genetically Blocking the Zebrafish Pineal Clock Affects Circadian Behavior,” *PLOS Genet.*, vol. 12, no. 11, p. e1006445, Nov. 2016.
- [245] S. Smadja Storz, A. Tovin, P. Mracek, S. Alon, N. S. Foulkes, and Y. Gothilf, “Casein Kinase 1 $\delta$  Activity: A Key Element in the Zebrafish Circadian Timing System,” *PLoS One*, vol. 8, no. 1, p. e54189, Jan. 2013.
- [246] L. Ziv, S. Levkovitz, R. Toyama, J. Falcon, and Y. Gothilf, “Functional Development of the Zebrafish Pineal Gland: Light-Induced Expression of *Period2* is Required for Onset of the Circadian Clock,” *J. Neuroendocrinol.*, vol. 17, no. 5, pp. 314–320, May 2005.
- [247] A. Casari *et al.*, “A *Smad3* transgenic reporter reveals TGF- $\beta$  control of zebrafish spinal cord development,” *Dev. Biol.*, vol. 396, no. 1, pp. 81–93, Dec. 2014.
- [248] S.-B. Peng *et al.*, “Kinetic Characterization of Novel Pyrazole TGF- $\beta$  Receptor I Kinase Inhibitors and Their Blockade of the Epithelial–Mesenchymal Transition,” *Biochemistry*, vol. 44, no. 7, pp. 2293–2304, Feb. 2005.
- [249] H. Li *et al.*, “Dihydropyrrolopyrazole Transforming Growth Factor- $\beta$  Type I Receptor Kinase Domain Inhibitors: A Novel Benzimidazole Series with Selectivity versus Transforming Growth Factor- $\beta$  Type II Receptor Kinase and Mixed Lineage Kinase-7,” *J. Med. Chem.*, vol. 49, no. 6, pp. 2138–2142, Mar. 2006.
- [250] J. Singh *et al.*, “Successful shape-based virtual screening: the discovery of a potent inhibitor of the type I TGF $\beta$  receptor kinase (T $\beta$ RI),” *Bioorg. Med. Chem. Lett.*, vol. 13, no. 24, pp. 4355–9, Dec. 2003.
- [251] J. Scott Sawyer *et al.*, “Synthesis and activity of new aryl- and heteroaryl-substituted 5,6-dihydro-4H-pyrrolo[1,2-b]pyrazole inhibitors of the transforming growth factor- $\beta$  type I receptor kinase domain,” *Bioorg. Med. Chem. Lett.*, vol. 14, no. 13, pp. 3581–3584, Jul. 2004.
- [252] P. Bragado *et al.*, “TGF- $\beta$ 2 dictates disseminated tumour cell fate in target organs through TGF- $\beta$ -RIII and p38 $\alpha$ / $\beta$  signalling,” *Nat. Cell Biol.*, vol. 15, no. 11, pp. 1351–1361, Nov. 2013.
- [253] T. Hayashida *et al.*, “HOXB9, a gene overexpressed in breast cancer, promotes tumorigenicity and lung metastasis,” *Proc. Natl. Acad. Sci.*, vol. 107, no. 3, pp. 1100–1105, Jan. 2010.
- [254] L. Maddaluno *et al.*, “EndMT contributes to the onset and progression of cerebral cavernous malformations,” *Nature*, vol. 498, no. 7455, pp. 492–496, Jun. 2013.

- [255] Y. Zhou *et al.*, “Latent TGF- $\beta$  binding protein 3 identifies a second heart field in zebrafish,” *Nature*, vol. 474, no. 7353, pp. 645–648, May 2011.
- [256] A. Willaert *et al.*, “GLUT10 is required for the development of the cardiovascular system and the notochord and connects mitochondrial function to TGF $\beta$  signaling,” *Hum. Mol. Genet.*, vol. 21, no. 6, pp. 1248–1259, Mar. 2012.
- [257] M. Abrial *et al.*, “TGF- $\beta$  Signaling Is Necessary and Sufficient for Pharyngeal Arch Artery Angioblast Formation,” *Cell Rep.*, vol. 20, no. 4, pp. 973–983, Jul. 2017.
- [258] D. Gays *et al.*, “An exclusive cellular and molecular network governs intestinal smooth muscle cell differentiation in vertebrates,” *Development*, vol. 144, no. 3, pp. 464–478, Feb. 2017.
- [259] Y. Shi *et al.*, “Alantolactone Inhibits Cell Proliferation by Interrupting the Interaction between Cripto-1 and Activin Receptor Type II A in Activin Signaling Pathway,” *J. Biomol. Screen.*, vol. 16, no. 5, pp. 525–535, Jun. 2011.
- [260] S. Lin *et al.*, “Integration and germ-line transmission of a pseudotyped retroviral vector in zebrafish,” *Science*, vol. 265, no. 5172, pp. 666–9, Jul. 1994.
- [261] Y. WANG *et al.*, “Bone morphogenetic protein-2 acts upstream of myocyte-specific enhancer factor 2a to control embryonic cardiac contractility☆,” *Cardiovasc. Res.*, vol. 74, no. 2, pp. 290–303, May 2007.
- [262] Y.-X. Wang *et al.*, “Requirements of myocyte-specific enhancer factor 2A in zebrafish cardiac contractility,” *FEBS Lett.*, vol. 579, no. 21, pp. 4843–4850, Aug. 2005.
- [263] D. J. Durgan and M. E. Young, “The Cardiomyocyte Circadian Clock,” *Circ. Res.*, vol. 106, no. 4, pp. 647–658, Mar. 2010.
- [264] T. Martino *et al.*, “Day/night rhythms in gene expression of the normal murine heart,” *J. Mol. Med.*, vol. 82, no. 4, pp. 256–264, Apr. 2004.
- [265] F. Sato *et al.*, “Smad3 and Snail show circadian expression in human gingival fibroblasts, human mesenchymal stem cell, and in mouse liver,” *Biochem. Biophys. Res. Commun.*, vol. 419, no. 2, pp. 441–446, Mar. 2012.
- [266] G. Carmona-Antoñanzas, M. Santi, H. Migaud, and L. M. Vera, “Light- and clock-control of genes involved in detoxification,” *Chronobiol. Int.*, vol. 34, no. 8, pp. 1026–1041, Sep. 2017.
- [267] J. Lin *et al.*, “PGC-1 $\beta$  in the Regulation of Hepatic Glucose and Energy Metabolism,” *J. Biol. Chem.*, vol. 278, no. 33, pp. 30843–30848, Aug. 2003.
- [268] G. Courtois, J. G. Morgan, L. A. Campbell, G. Fourel, and G. R. Crabtree, “Interaction of a liver-specific nuclear factor with the fibrinogen and alpha 1-antitrypsin promoters.,” *Science*, vol. 238, no. 4827, pp. 688–92, Oct. 1987.
- [269] C. Faculties and N. Sciences, “Ying Li M.Sc. Born in Hebei, China Oral examination: .07.2017,” 2017.

- [270] M. Hatori *et al.*, “Light-dependent and circadian clock-regulated activation of sterol regulatory element-binding protein, X-box-binding protein 1, and heat shock factor pathways,” *Proc. Natl. Acad. Sci.*, vol. 108, no. 12, pp. 4864–4869, Mar. 2011.
- [271] I. P. G. Amaral and I. A. Johnston, “Circadian expression of clock and putative clock-controlled genes in skeletal muscle of the zebrafish,” *AJP Regul. Integr. Comp. Physiol.*, vol. 302, no. 1, pp. R193–R206, 2012.
- [272] S.-W. Chong, V. Korzh, and Y.-J. Jiang, “Myogenesis and molecules- insights from zebrafish *Danio rerio*,” *J. Fish Biol.*, vol. 74, no. 8, pp. 1693–1755, May 2009.
- [273] Y. Hinitz, D. P. S. Osborn, J. J. Carvajal, P. W. J. Rigby, and S. M. Hughes, “Mrf4 (myf6) is dynamically expressed in differentiated zebrafish skeletal muscle,” *Gene Expr. Patterns*, vol. 7, no. 7, pp. 738–745, Aug. 2007.
- [274] Y.-H. Wang, C.-K. Li, G.-H. Lee, H.-J. Tsay, H.-J. Tsai, and Y.-H. Chen, “Inactivation of zebrafish *mrf4* leads to myofibril misalignment and motor axon growth disorganization,” *Dev. Dyn.*, vol. 237, no. 4, pp. 1043–1050, Apr. 2008.
- [275] H. Gast *et al.*, “Transforming growth factor-beta inhibits the expression of clock genes,” *Ann. N. Y. Acad. Sci.*, vol. 1261, no. 1, pp. 79–87, Jul. 2012.
- [276] M. W. Hurd, J. Debruyne, M. Straume, and G. M. Cahill, “Circadian rhythms of locomotor activity in zebrafish,” *Physiol. Behav.*, vol. 65, no. 3, pp. 465–72, Dec. 1998.
- [277] O. Levy *et al.*, “Complex Diel Cycles of Gene Expression in Coral-Algal Symbiosis,” *Science (80-. )*, vol. 331, no. 6014, pp. 175–175, Jan. 2011.
- [278] H. A. Burgess and M. Granato, “Modulation of locomotor activity in larval zebrafish during light adaptation,” *J. Exp. Biol.*, vol. 210, no. Pt 14, pp. 2526–39, Jul. 2007.
- [279] X. Hu and M. A. Lazar, “The CoRNR motif controls the recruitment of corepressors by nuclear hormone receptors,” *Nature*, vol. 402, no. 6757, pp. 93–96, Nov. 1999.
- [280] M. Wang, Z. Zhong, Y. Zhong, W. Zhang, and H. Wang, “The zebrafish period2 protein positively regulates the circadian clock through mediation of retinoic acid receptor (RAR)-related orphan receptor  $\alpha$  (Rora),” *J. Biol. Chem.*, vol. 290, no. 7, pp. 4367–4382, 2015.
- [281] I. Schmutz, J. A. Ripperger, S. Baeriswyl-Aebischer, and U. Albrecht, “The mammalian clock component PERIOD2 coordinates circadian output by interaction with nuclear receptors,” *Genes Dev.*, vol. 24, no. 4, pp. 345–357, 2010.
- [282] M. Peckova, C. E. Fahrenbruch, L. A. Cobb, and A. P. Hallstrom, “Circadian variations in the occurrence of cardiac arrests: initial and repeat episodes,” *Circulation*, vol. 98, no. 1, pp. 31–9, Jul. 1998.
- [283] D. J. Durgan and M. E. Young, “The Cardiomyocyte Circadian Clock,” *Circ. Res.*, vol. 106, no. 4, pp. 647–658, Mar. 2010.
- [284] B. Grimaldi *et al.*, “PER2 Controls Lipid Metabolism by Direct Regulation of PPAR $\gamma$ ,” *Cell*

*Metab.*, vol. 12, no. 5, pp. 509–520, Nov. 2010.

- [285] T. Gotoh, M. Vila-Caballer, C. S. Santos, J. Liu, J. Yang, and C. V Finkielstein, “The circadian factor Period 2 modulates p53 stability and transcriptional activity in unstressed cells.,” *Mol. Biol. Cell*, vol. 25, no. 19, pp. 3081–93, Oct. 2014.
- [286] N. Kon, T. Hirota, T. Kawamoto, Y. Kato, T. Tsubota, and Y. Fukada, “Activation of TGF- $\beta$ /activin signalling resets the circadian clock through rapid induction of Dec1 transcripts,” *Nat. Cell Biol.*, vol. 10, no. 12, pp. 1463–1469, Dec. 2008.
- [287] E. D. Buhr and J. S. Takahashi, “Molecular components of the Mammalian circadian clock.,” *Handb. Exp. Pharmacol.*, no. 217, pp. 3–27, 2013.